View metadata, citation and similar papers at core.ac.uk
brought to you by CORE
provided by OpenGrey Repository

CRANFIELD UNIVERSITY

INSTITUTE OF BIOSCIENCE AND TECHNOLOGY

PhD THESIS

Academic Year 2003-2004

Reinhard Fend

Development of medical point-of-care applications for renal medicine and tuberculosis based on electronic nose technology

Supervisors

Dr. Anthony C Woodman (Cranfield University)
Dr. Conrad Bessant (Cranfield University)

Dr. Anthony J Williams (Gloucestershire Royal Hospital)

Dr. Arend JH Kolk (KIT, Royal Tropical Institute, The Netherlands)
Dr. Paul R Klatser (KIT, Royal Tropical Institute, The Netherlands)

2004

This thesis is submitted for the degree of Doctor of Philosophy

PhD THESIS

ACADEMIC YEAR 2003-2004

Reinhard Fend

Development of medical point-of-care applications for renal medicine and tuberculosis based on electronic nose technology

"This thesis is submitted in partial fulfilment of the requirements for the degree of Doctor of Philosophy"

© Cranfield University, 2004. All rights reserved. No part of this publication may be reproduced without the written permission of the copyright holder.

ABSTRACT

INTRODUCTION: Current clinical diagnostics are based on biochemical, immunological or microbiological methods. However, these methods are operator dependent, time consuming, expensive and require special skills, and are therefore not suitable for point-of-care testing. Recent developments in gas-sensing technology and pattern recognition methods make electronic nose technology an interesting alternative for medical point-of-care devices. **METHODS:** We applied a gas sensor array based on 14 conducting polymers to monitor haemodialysis *in vitro* and to detect pulmonary tuberculosis in both culture and sputum. **RESULTS and DISCUSSION:** The electronic nose is able to distinguish between control blood and "uraemic" blood. Furthermore, the gas sensor array is not only capable of discriminating pre- from post-dialysis blood (97% accuracy) but also can follow the volatile shift occurring during a single haemodialysis session. The electronic nose can be used for both dialysate side and blood-side monitoring of haemodialysis. The pattern observed for post- and pre-dialysis blood might reflect the health status of the patients and can therefore be related to the long-term outcome. Furthermore, the gas sensor array was also able to discriminate between *Mycobacterium spp*. and other lung pathogens such as *Pseudomonas aeruginosa*. More importantly the gas sensor array was capable of resolving different *Mycobacterium spp*. such as *Mycobacterium tuberculosis*, *M. scrofulaceum*, and *M. avium* in both liquid culture and spiked sputum samples. The detection limit for *M. tuberculosis* in both sputum and liquid culture is 1 x 10^4 mycobacteria ml^{-1} and therefore partially fulfils the requirement set by the WHO. The gas sensor array was able to detect culture proven TB with a sensitivity of 89% and a specificity of 91%. **CONCLUSIONS**: In conclusion, this study has shown the ability of an electronic nose as a point-of-care device in these areas.

ACKNOWLEDGEMENT

I would like to thank my principal supervisors Dr. Anthony Woodman and Dr. Conrad Bessant at Cranfield University for their help and support throughout the thesis.

The help and support of Dr Arend Kolk, Dr. Paul Klatser and Sjoukje Kuijper at the Royal Tropical Institute (Amsterdam, The Netherlands) is very much appreciated.

I gratefully acknowledge the help and guidance of Dr. Anthony Williams at the Cotswold Dialysis Unit (Gloucestershire Royal Hospital, Gloucester, UK).

I also wish to thank Sharon King, and the nursing staff at Gloucestershire Royal Hospital (Gloucester, UK) and Academic Medical Centre (Amsterdam, The Netherlands) for taking the samples and all patients and volunteers for participating in this study.

The funding for this research project was provided by the Gloucester Kidney Patients Association (Gloucester, UK), Fresenius AG (Bad Homburg v.d.H., Germany) and from the World Health Organisation (TDR grant A20565).

TABLE OF CONTENTS

Chapter 2: General Materials and Methods

Chapter 3: Electronic nose in renal medicine

Appendices

LIST OF FIGURES AND TABLES

LIST OF ABBREVIATIONS

AFB	Acid fast bacilli
AGEP	Advanced glycosylated end products
AIDS	Acquired immunodeficiency syndrome
AMC	Academic Medical Centre
ANN	Artificial neural network
ARF	Acute renal failure
AV	Arteriovenous
BAW	Bulk acoustic wave
BCG	Bacillus Calmette-Guerin
BUN	Blood urea nitrogen
BV	Bacterial vaginosis
CAPD	Continuous ambulatory peritoneal dialysis
CFU	Colony forming units
CP	Conducting polymers
CRF	Chronic renal failure
CSF	Cerebrospinal fluid
Da	Dalton
DFA	Discriminant function analysis
DMA	Dimethylamine
D_{opt}	Optimal dilution
DUN	Dialysate urea nitrogen
EDTA	Ethylendiaminetetracetic acid
ELISA	Enzyme linked immunosorbent assay

EN	Electronic nose
Equ	Equation
ESRD	End stage renal disease
FIA	Flow injection analysis
FTIR	Fourier transform infrared
GC	Gas chromatography
GC-MS	Gas chromatography – mass spectroscopy
GS	Genetic supervisor
HCA	Hierarchical Cluster Analysis
HD	Haemodialysis
HF	Haemofiltration
HIV	Human immunodeficiancy virus
HLA	Human leukocyte antigen
HPLC	High performance liquid chromatography
HSA	Head space analysis
IFN	Interferon
IL	Interleukin
IUATLD	International Union against Tuberculosis and Lung Disease
LAM	Lipoarabinomannan
MO	Metal oxide
MW	Molecular weight
NCDS	National cooperative dialysis study
Neg	Negative
NPV	Negative predictive value
nPCR	Normalised protein catabolic rate

PARC	Pattern Recognition
PC	Principal component
PCA	Principal component analysis
PCR	Polymerase chain reaction (chapter 4)
PCR	Protein catabolic rate (chapter 3)
PI	Photo ionisation
Pos	Positive
PPD	Purified protein derivative
ppb	parts per billion
ppm	parts per million
PPV	Positive predictive value
RIVM	National Institute of Public Health and the Environment
RO	Reverse osmosis
RRT	Renal replacement therapy
RT	Room temperature
SAW	Sound acoustic wave
SDA	Strand displacement amplification
SRI	Solute removal index
TB	Tuberculosis
TMA	Trimethylamine
T_{opt}	Optimal temperature
t_{opt}	Optimal time
TBSA	Tuberculostearic acid
TMA	Transcription-mediated amplification
TNF	Tumour necrosis factor

UKM	Urea kinetic modelling
URR	Urea reduction ratio
UTI	Urinary tract infections
VOCs	Volatile organic compounds
V_{opt}	Optimal volume
WHO	World Health Organisation
ZN	Ziehl-Neelsen

Chapter 1

Introduction

and

Literature Review

1.1 INTRODUCTION

The increased knowledge in bionics and artificial intelligence has revolutionised many areas of human activity. The employment of these approaches in medicine will be no exception. New socio-economic factors and general globalisation of the world requires the development and application of new intelligent diagnostic devices (Armoni, 1998; Moret-Bonillo, 1998).

Advances in information technology and satellite communications combined with novel intelligent sensors could result in the better management of epidemic diseases such as tuberculosis or AIDS by central organisations such as the World Health Organisation (WHO). Applying this information could lead to a better global control and thus, could reduce the risk of spreading the disease around the world.

On the other hand, effective clinical care requires decision making based on multiple data inputs, e.g. symptoms, history, biochemical or physical tests. Such a general approach has not been implemented in current development strategies of diagnostic devices, which rely on a "one target – one result" approach (Woodman and Fend, 2004).

In the past, nature often served as a provider of principles leading to astonishing innovations and hence, applications. One of the most incredible natural systems is the mammalian olfactory system. Today, the same principle is applied in machine olfaction and in "olfactory diagnosis" (Woodman and Fend, 2004)

1.2 DIAGNOSTIC POWER OF SMELL

The origins of "odours as diagnostic indicators" go back to around 400BC and the father of medicine – Hippocrates (Adams, 1994). Descriptions at that time of the

pouring of human sputum on hot coal to thermally generate a smell could very well be considered a primitive pyrolysis of long chain fatty acids, release of volatile hydrocarbons or possibly lipid peroxidation, bacterial or infected tissue products. Similarly, traditional Chinese medicine also exploited the power of olfactory diagnosis (Porter, 1997). Whilst early medical practitioners had not discovered bacterial pathogenicity, they clearly recognised that a disease-host interaction could change the odour of body excretions such as sweat, urine, vaginal fluid and sputum (Porter 1997). Diagnosis using the human sense of smell remained one of the most reliable methods in bedside medicine. For many years, paediatricians associated phenylkentouria with a mousy/honey smell of urine. Other disease like liver failure, chronic congestive heart failure of portcaval shunts are associated with characteristic odour of dimethyl sulphide (Smith, 1982). Certain conditions are associated with a malodour emerging form the skin. Among them are, squamous cell carcinoma, which is linked to a full-offensive skin aroma (Lidell *et al*, 1975), or Yellow fever, which is often related to the smell of a butchers shop (Lidell *et al*, 1976; Hayden 1980).

A collection of recorded diseases and infections liberating specific odours is presented in Table 1.1.

1.2.1 EARLY DIAGNOSIS OF VOLATILE BIOMARKERS

During the 1950's and early 1960's, gas chromatography (GC) and GC-linked with mass spectrometry (GC-MS) provided the instrumentation with which to separate and identify volatile biomarkers.

Table 1.1: Diseases and their recorded liberated odours (adapted from Pavlou and Turner, 2000).

Odour	Site/Source	Disease
Baked brown bread	Skin	Typhoid
Stale beer	Skin	Tuberculosis lymphadenitis
Butchers shop	Skin	Yellow fever
Grape	Skin/sweat	*Pseudomonas* infection
Rotten apples	Skin/sweat	Anaerobic infection
Over-ripe Camembert	Skin	Bacterial proteolysis
Ammoniacal	Urine	Bladder infection
Amine-like	Vaginal discharge	Bacterial vaginosis
Rancid	Stool	Shigellosis
Full	Stool	*Rotavirus* gastroenteritis
Freshly plucked feathers	Sweat	Rubella
Sweet	Sweat	Diphtheria
Full	Sputum	Bacterial infection
Putrid	Breath	Lung abscess, anaerobic infection, necrotising pneumonia
Full-offensive	Skin	Squamous cell carcinoma
Acetone-like	Breath	Diabetes mellitus
Musty/horsey	Infant skin	Phenylketonuria
Foul	Infant stool	Cystic fibrosis
Sweaty feet	Skin/sweat	Isovaleric academia
Burnt sugar	Urine	Maple syrup urine disease
Sweet/fruity or boiled cabbage	Infant breath	Hypermethionemia
Fishy	Skin/urine	Trimethylaminouria

One of the most obvious sources where volatile disease markers can be found is breath. Breath tests date from the earliest history of medicine because physicians in ancient times knew that the odour of the breath is altered in some diseases (Philips, 1997). Some breath aromas are highly characteristic of disease: e.g. patients with diabetic ketoacidosis smell like rotten apples, mainly due to acetonemia. Chronic renal failure causes the breath to smell like stale urine (Phillips, 2002).

However, the modern era of breath testing did not commence until 1971, when Linus Pauling used dry ice to freeze out breath volatile organic compounds (VOCs).

To date more than 3000 volatile organic compounds in human breath have been identified, but the biochemical significance of most of these compounds is still unknown (Phillips *et al*, 1995; Phillips *et al*, 1999). A collection of GC-MS applications in clinical diagnosis is presented in Table 1.2

Table 1.2: The application of GC-MS analysis of volatiles in clinical samples (adapted from Pavlou and Turner, 2000).

Method	Source/Disease	Volatile
GC	Breath, urine	VOCs
GC	Aerobic Gram(-) bacteria	VOCs
HSA-GC	Intraperitoneal fluid	VOCs
GC	Anaerobic bacteria	Acetic, butyric acid
GC	Human pus, purulent fluid	Isobutyric, isovaleric acid
HSA-GC	Urine/ metabolic disorder	Isovaleric acid
GC-MS	Blood plasma, CSF/ liver disorder	3-methylbutanal
FI-GC	Breath/ liver disorder	Methyl-mercaptan
GC-MS	Breath/ schizophrenia	Pentane
GC-MS	Breath/ketosis	Acetone
GC-PI	Breath/ Cardiopulmonary disease	Acetone, ethanol

Abbreviations: GC – gas chromatography, GC-MS – gas chromatography-mass spectroscopy, HSA – head space analysis, CSF – cerebrospinal fluid, PI – photo ionisation, VOCs – volatile organic compounds

Recently, Phillips *et al* presented two studies, where volatile organic compounds (VOCs) were related to cancer. In the first study, the presence of VOCs, mainly alkanes and monomethylated alkanes were investigated in breath as tumour markers for lung cancer (Phillips *et al*, 2003a). The second study investigated the presence of VOCs as markers for breast cancer (Phillips *et al*, 2003b). The results of both studies

are promising, but will require validation in larger trials. Even inflammatory lung diseases such as asthma, chronic obstructive pulmonary disease, or cystic fibrosis have been associated with specific volatile markers in exhaled breath including nitric oxide or hydrocarbons (Kharitonov and Barnes, 1997; Kharitonov, 2004).

The production of volatiles is not limited to humans. At the beginning of the 19th century, Liebig and Woehler (1837) described the production of benzaldehyde by microorganisms. Since then many reports have been published. Among the first was Omelianski (1923) who reviewed naturally liberated microbial odours. He reported the accumulation of organic acids and alcohols in cultures of *Mycobacterium tuberculosis* and *Pseudomonas aeruginosa*.

Since the development of GC instruments, the characterisation of bacterial volatiles of pathogenic origin has been of interest. Davies & Hayward (1984) identified acetylcholine and suggested that it could act as a precursor of trimethylamine, a possible early biochemical marker of urinary tract infections (UTI) caused by *Proteus spp.* and *Klebsiella spp*. Grametbauer *et al* (1988) reported the production of a number of volatile compounds derived from 189 strains of 33 bacterial species. They concluded that even when the volatile profiles (chromatograms) showed distinct peaks, it was not always possible to completely differentiate between strains of the same species. The GC-MS analysis of pathogenic bacteria such as *Pseudomonas aeruginosa, Proteus mirabilis, Klebsiella pneumoniae, Staphylococcus aureus, and Clostridium septicum* revealed that all of them produced complex odours pattern (Larsson *et al*, 1978). Similarly, species of the lactic acid family, important industrial bacteria were extensively studied using gas chromatographic techniques allowing a discrimination between *Leuconostoc spp,*

Pediococcus spp, and *Lactobacillus spp* (Radler and Gerwarth, 1971). Mayakova *et al* (1989) proposed a rapid method for detecting post-operative infections in abdominal and gynaecological surgery caused by non-clostridial anaerobes via GC-MS analysis of volatile fatty acids.

Although the introduction of GC-MS enabled the comprehensive study of possible diseases markers, it has never emerged as a fully evaluated routine instrument for clinical diagnosis. Factors such as high capital costs, laborious and time-consuming methods requiring significant expertise and the shear complexity of volatiles detected using GC-MS have all conspired to limit the application of this technology (Manolis, 1983; Phillips, 1997). However, the wealth of knowledge generated by GC-MS has significantly enriched the understanding of the way the human body responds to disease and in particular the potential role of volatile organic compounds (VOC) as diagnostic markers. The drive to develop instruments for routine clinical application without the drawbacks of GC-MS was on.

1.3 PRINCIPLES OF OLFACTION

The basic idea of electronic noses is to mimic the human olfactory system. This section describes the similarities and differences between human olfaction and machine olfaction.

The human olfactory system comprises three basic elements, namely the olfactory receptor cells, the olfactory bulb and finally the brain (Pearce, 1997a). These three elements formed the basis for the development of the artificial olfaction devices (electronic noses). The main components of an electronic nose are an array of

chemical sensors, a data pre-processing unit and a pattern recognition engine (PARC) (Pearce, 1997b). The basic elements of both olfactory systems are as illustrated in Figure 1.1.

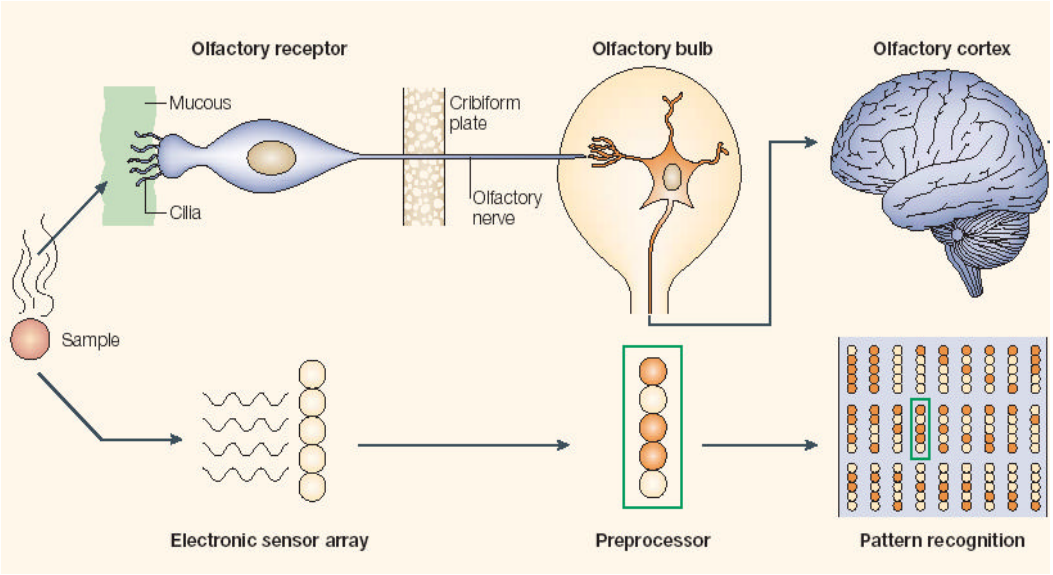

***Figure 1.1**:* Comparison of the human olfaction with artificial olfaction (adapted from Turner and Magan, 2004).

1.3.1 HUMAN OLFACTORY SYSTEM

The sensation of smell is caused by the interaction of odorant molecules with a group of specialised nerve cells called olfactory receptors. The olfactory cells are situated in the olfactory epithelium, a specialised tissue in the nose (Craven *et al*, 1996; Bartlett *et al*, 1997; Pearce 1997a). Odorant molecules are typically small, polar, and hydrophobic molecules with a molecular weight between 30 and 300 Da, with one or more functional groups (Gardner and Bartlett, 1999). The hydrophobicity

of the molecules is important, as the initial step in olfactory recognition is the dissolution of the molecules in an aqueous mucous layer, which covers the olfactory receptor cells and the epithelium (Craven *et al*, 1996; Bartlett *et al*, 1997a; Pearce 1997a). The receptor surface area is increased by a number of cilia, which lie in the mucous layer (Pearce, 1997a). On the surface of the cilia are G-receptor binding proteins. The interaction of the odorant molecules with the G-receptor binding proteins stimulates the neurons (Craven *et al*, 1996). It is unknown how many different types of G-receptor proteins exist, but presumably between 100 and 1000 (Craven *et al*, 1996). It is believed that olfactory cells (ca. 100 millions) are involved in both amplifying the signal and generating second messenger (Gardner and Bartlett, 1994). Hence, many olfactory neurons appear to express only one of the many possible G-binding proteins, explaining the large number of olfactory cells (Pearce, 1997a). The second messenger controls ion channels and thus generates signals, which travel from the neuron via axons to the glomeruli nodes in the olfactory bulb (Gardner and Bartlett, 1994; Pearce, 1997a). These signals are pre-processed by mitral cells and subsequently sent to the brain via a granular cell layer (Gardner and Bartlett, 1994; Pearce, 1997a). The different G-binding proteins have an overlapping sensitivity to different odorant molecules (Gardner and Bartlett, 1994; Gibson *et al*, 1997).

The human nose can discriminate complex aromas without separating the mixture into individual components (Pearce, 1997a). Due to the high sensitivity of the human nose, it is possible to detect odorant molecules in very low concentrations (ppm, ppb) (Pearce, 1997a).

1.3.2 ARTIFICIAL OLFACTORY SYSTEM

In the artificial olfactory system, the olfactory receptor cells are replaced by a chemical sensor array. The sensors generate a time-dependent electrical signal in response to the interaction of an odour with the sensor itself (Gardner and Bartlett, 1994, Pearce, 1997b; Gardner and Bartlett, 1999). The olfactory bulb is represented by a data pre-processing unit, which compensates for sensor drift and noise (Pearce, 1997b; Gardner and Bartlett, 1999). The final stage in artificial olfaction is the PARC engine, which is equivalent to the human brain (Pearce, 1997b). In summary, it can be said that electronic noses mimic the mammalian olfactory system by combining non-specific gas sensors with a PARC software to analyse and characterise complex odours without prior separation of the mixture into individual components (Bartlett *et al*, 1997)

1.4 DEFINITION OF ELECTRONIC NOSES

Electronic nose is the informal name for an instrument made up of chemical sensors combined with some sort of pattern recognition system, enabling discrimination between, or recognition of, simple or complex odours (Gibson *et al*, 2000). The term "electronic nose" was introduced by Julian Gardner in 1988 (Gardner and Bartlett, 1999). In 1964, Wilkins and Hatman built the first devices aimed at mimicking the human nose (Gardner and Bartlett, 1994). However, the first electronic nose, as an intelligent sensor system, was introduced by Persaud and Dodd (1982) at Warwick University. The first commercial electronic noses were launched in the earlier 1990s (Gibson *et al,* 2000). Among the first systems were devices from Alpha MOS in 1993, Neotronics and Aromascan in 1994 and Bloodhound Sensors and HKR

Sensorsysteme in 1995 (Gibson *et al*, 2000). A list of commercially available electronic noses is shown in Table 1.3.

1.5 GAS SENSORS FORMATS

The central part of an electronic nose is the chemical gas sensor array. Sensors used in electronic noses are non-specific gas sensors (Gardner and Bartlett, 1999). Hence, they should possess good stability and a high sensitivity coupled with a short response time (Bartlett *et al*, 1997).

Currently the following types of sensors are used in electronic noses (Craven *et al*, 1996; Dickinson *et al*, 1998; Chang *et al*, 2000):

- Metal Oxide Sensor (MO)
- Conducting Polymers (CP)
- Piezoelectric based Sensors
  - Sound Acoustic Wave Sensors (SAW)
  - Bulk Acoustic Wave Sensors (BAW)

Table 1.3: Commercially available electronic noses (adapted from Gibson *et al*, 2000).

Company	Location	Model
Alpha MOS	France	Fox 2000, 3000, 4000, 5000 Alpha Kronos, Alpha Gemini
Bloodhound Sensors	UK	Bloodhound BH114
Cyrano Science	USA	Cyranose 320
Etherdata	Iceland	FreshSense
Environics Industry Oy	Finland	MGD-1
Electronic Sensor Technology	USA	GC/SAW System
Hewlett Packard	USA	HP4440A
Lennartz Electronic	Germany	MOSES II
Marconi Applied Technology	UK	e-nose 5000
Mo Tech Sensoric	Germany	VOCmeter, VOCcheck, OEM modules
Osmetech (formerly Aromascan)	UK and USA	Multi-Sampler SP, CP sensors
RST Rostock	Germany	Sam
Smart Nose	Switzerland	Smart Nose – 300
WMA Airsense	Germany	PEN

1.5.1 METAL OXIDE SENSORS

These devices consist of an electrically heated ceramic pellet, onto which a thin porous film of SnO_2 doped with metal ions has been deposited (Persaud and Travers, 1997). The doped SnO_2-film behaves as an n-type semiconductor and the chemisorption of oxygen at the sensor surface results in the removal of electrons from the conducting band. Gases in a sample interact with the absorbed oxygen and thereby affect the conductivity of the SnO_2 film (Persaud and Travers, 1997; Dickinson *et al*, 1998). The change in conductivity is typically used as the output signal (Dickinson *et al*, 1998).

The devices are run at elevated temperatures (typically at 300 – 400 ^{o}C) to achieve a fast response time and to avoid interferences from water. The response characteristics can be tailored by varying the operating temperatures and the doping agent (Gardner and Bartlett, 1994; Dickinson *et al*, 1998).

The sensor is characterised by a short recovery time, insensitivity to moisture and little drift over time, and the electrical output signal is proportional to the odour concentration (Harper, 2001). On the other hand, it must be mentioned, that the devices are typified by high power consumption and a poor selectivity (Harper, 2001).

1.5.2 CONDUCTING POLYMERS

The use of Conducting Polymers (CP) as sensors dates back to 1979, when Diaz and co-workers first electropolymerised a thin film of polypyrrole (Dickinson *et al*, 1998). Since then, much attention has been paid to these materials and their unique properties (Dickinson *et al*, 1998).

Sensors are fabricated by electropolymerising thin polymer films across a narrow electrode gap (Bartlett *et al*, 1989; Dickinson *et al*, 1998). The reversible absorption of molecules onto the film induces a temporary change in the electrical conductivity of the film by altering the amount of active charge carriers in the polymer structure (Bartlett *et al*, 1989; Shurmer and Gardner, 1992; Dickinson *et al*, 1998). CPs in an electronic nose are typically based on either poly(pyrolle) or poly(aniline) (Bartlett *et al*, 1989; Dickinson *et al*, 1998). In both cases, it is easy to obtain a thin polymer film, and therefore reproducible sensors can be produced (Gardner and Bartlett, 1999). In CP-sensors, the molecular-interaction capabilities of the polymer can be selectively modified by incorporating different counterions during polymer preparation or by attaching functional groups to the polymer backbone (Dickinson *et al*, 1998),

The advantages of CP include the low power consumption and the high selectivity of the sensors. The shortcomings are long response times, inherent time- and temperature drift, the sensitivity to water and the high cost of sensor fabrication (Dickinson *et al*, 1998; Harper, 2001).

1.5.3 PIEZOELECTRIC BASED SENSORS

The use of piezoelectric crystals as transducers for chemical analysis was first suggested by Sauerbrey in 1959 and demonstrated by King in 1964 (Dickinson *et al*, 1998). The two most commonly used piezoelectric based sensors are the Surface Acoustic Wave sensor and the Bulk Acoustic Wave sensor (Gardner and Bartlett, 1999).

Surface Acoustic Wave (SAW) sensor:

SAW devices consist of interdigitated electrodes fabricated onto a piezoelectric substrate (e.g. quartz) onto which a thin film coating of a selective material is deposited (Persaud and Travers, 1997; Dickinson *et al*, 1998). An applied radio frequency produces an acoustic wave on the sensor surface (surface oscillation). The adsorption of odour molecules onto the thin film coating leads to an increase in mass and elastic module of the coating. This change in mass and elastic module perturbs the wave leading to a frequency shift (Persaud and Travers, 1997; Dickinson *et al*, 1998). To compensate for pressure and temperature effects the sample sensor is usually connected to a reference SAW device and the frequency difference is detected (Gardner and Bartlett, 1999).

Bulk Acoustic Wave (BAW) sensor:

BAW devices consist of a piezoelectric resonator with one or both surfaces covered by a membrane such as acetyl cellulose or lecithin (Bartlett *et al*, 1997; D'Amico *et al*, 1997). The BAW structure is connected to a suitable amplifier to form an oscillator. The resonant frequency of the oscillator is determined by the physical and geometrical properties of the device (D'Amico *et al*, 1997). Any changes in the physical properties of the membrane due to absorption of molecules affects the resonant frequency of the BAW device (Bartlett *et al*, 1997; D'Amico *et al*, 1997). This frequency shift is detected (Dickinson *et al*, 1998).

1.5.4 OTHER TECHNOLOGIES

Other sensor formats are in development, but none of these alternative technologies are currently applied in commercial electronic noses. Among these are optical transducers (Sutter *et al*, 1997, Walt, 2002), surface plasmon resonance (Magan and Turner, 2004), electrochemical sensors (Baltruschat *et al*, 1997), or discotic liquid crystals (Magan and Turner, 2004).

1.6 APPLICATION OF ELECTRONIC NOSES

Since the introduction of the electronic nose, there is an increasing awareness of the potential of this technology and with it a broad range of possible applications. Electronic noses were designed to be used in numerous areas, ranging from food to modern medicine.

1.6.1 MEDICAL APPLICATIONS

When attempting to navigate through applications of this technology in medicine, it soon becomes apparent that there is one clear delineator: Application of electronic-nose in *infectious* diseases or *non-infectious* diseases. Using these two very broad subject headings, this section attempts to highlight both current and future applications of electronic-nose technology.

Infectious Diseases

The analysis of infectious diseases represents by far the largest clinical research area for electronic nose technology attracting both academic and commercial interest.

As a result it is safe to speculate that this area will be the first to deliver a routine medical application for the technology.

The reasons for such widespread interest are many fold. Using conventional culture methods, diagnosis of infection can take 24-48 hours for bacterial infections (identification of *Mycobacterium tuberculosis* can require 4-8 weeks) and often around 7 days for fungal diseases. For appropriate early treatment including screening for therapeutic sensitivity, it is essential to obtain relevant rapid results in easily interpretable formats. Ideally such analysis should be amenable to use at "point-of-care" and being the first step in rapid, responsive and appropriate anti-infectious therapy, reducing the incidence of unchecked infection and/or poorly targeted antibiotics.

Diagnosis and management of sepsis in wound healing

The "point-of-care" analysis of the odours over the headspace of 24 low adherent contact dressing collected from 21 patients with leg ulcers was in fact one of first clinical applications of electronic-nose technology (Parry and Oppenheim, 1995). Using 20 conducting polymer sensors, a two-dimensional odour map demonstrated clear differences between ulcers of differing bacterial aetiology. Ulcers infected with beta-haemolytic S*treptococci* formed a distinctive cluster away from the other three categories (mixed infection, *Staphylococcus aureus* and control), which could not be resolved from each other. Despite this, the unambiguous separation of at least one bacterial species provided proof that host-pathogen interactions are identifiable by an electronic nose (Pavlou and Turner, 2000).

Today the analysis of wound healing remains at the forefront of clinical electronic-nose application. A recent European Union funded project "WUNSENS"

has integrated image capture technology with the electronic-nose technology of AlphaMOS to develop a portable integrated wound assessment system for use at "point-of-care" (IST-2001-52058).

Diagnosis and management of urogenital infections

One of the areas where appropriate and effective therapy is most dependant upon early diagnosis is that of urogenital infections. Urinary tract infections (UTI) are a significant cause of morbidity, with 3 million cases each year in the USA alone (Schaechter *et al*, 1993; Pavlou *et al*, 2002). Estimates suggest that 20% of females between the ages of 20 and 65 years suffer at least one episode per year, which in turn increase the risk of contracting complicated or chronic urological disorders such as pyelonephritis, urethritis and prostatitis (Orenstein and Wong, 1999; Lipsky, 1999). Approximately 80% of uncomplicated UTIs are caused by *Escherichia coli* and the remaining 20% by enteric pathogens such as *Enterocci*, *Klebsiella*, *Proteus*, and fungal opportunistic pathogens such as *Candida albicans* (Krcmery *et al*, 1983; Honiken *et al*, 1999; Pavlou *et al*, 2002). Current diagnostics and antibiotic sensitivity tests require 24-48 hours to identify pathological species in a midstream specimen containing at least 10^5 CFU ml^{-1}.

A similar story is true for bacterial vaginosis; in the US alone there are an estimated 10 million doctor visits for vaginal infections. Bacterial vaginosis (BV) is one of the most common causes of vaginal infection with high prevalence in women of childbearing age. Vaginal infection during pregnancy has been linked to pre-term delivery (McGregor and French, 1997), and spontaneous abortion in the third trimester and upper genital tract infections including histologic chorioamnionitis (Hillier *et al*, 1988).

With a requirement for simple, accurate and ideally "point-of-care" analysis, the application of electronic-nose technology in managing urogenital infection has received considerable academic and commercial interest. The premise that analysis of volatiles generated from urine is clinically relevant stems from several gas-chromatographic studies during the 1970's (Pavlou *et al*, 2002). Whilst these early studies lacked advanced computation to resolve data, they did demonstrate discrimination between *E. coli* and *Proteus spp* (Haywood *et al*, 1977).

Almost 25 years later, electronic-nose technology replicated these studies both in "spiked" urine samples where discrimination between *E. coli* and *P. mirabilis* was obtained after just 4 hours in culture (Saini *et al*, 2001) and clinical specimens (Aathithan *et al*, 2001; Pavlou *et al*, 2002). Pavlou *et al* (2002) using an array of 14 conducting polymer sensors (Bloodhound BH114) discriminated between *E. coli*, *Proteus spp*, *Staphylococcus spp* and no infection in a total of 70 patients with a combined positive predictive outcome of 99%, following 4.5 hour liquid culture incubation (Pavlou *et al*, 2002). Aathithan *et al* (2001) used an Osmetech Microbial Analyser (Osmetech plc, Manchester, UK), to diagnoses bacteriuria. Analysing 534 clinical urine specimens, the sensitivity and specificity of this device were 83.5 and 87.6 %, respectively compared to traditional culture, when the cut-off was defined as 10^5 CFU ml^{-1}. Whilst this data again shows the potential for electronic-nose technology, it is the Osmetech Microbial Analyser (OMA), which warrants further discussion. Osmetech has received 510(k) approval from the FDA for the use of its microbial analyser as a UTI sensor device.

The OMA is also marketed for the diagnosis of bacterial vaginosis. A case study on bacterial vaginosis in the United Kingdom has shown that conducting-polymer-

based sensor arrays similar to that in the microbial analyser could be used to successfully diagnose 89% of test subjects as being positive or negative for both bacterial and yeast infections (Persaud *et al*, 2002; Turner and Magan, 2004). Following the evaluation of over 1000 patients, the Osmetech device was given 501(k) approval by the FDA in January 2003, citing that the instrument had a sensitivity and specificity of 81.5% and 76.1% as compared to the current "gold-standard" of the Amsel criteria but with significant improvements in speed and expertise required (Hay *et al*, 2003).

Disease and management of tuberculosis and respiratory disease

Pavlou and Turner (2000) investigated the possibility of applying electronic nose technology to diagnose tuberculosis (TB). Using a Bloodhound BH114 system comprising 14 conducting polymers, this group demonstrated the ability of this system to discriminate between different *Mycobacterium spp*. and other lung pathogens (*Pseudomonas aeruginosa*) with an accuracy of 99 %. The system performed equally well in spiked sputum and culture (Pavlou and Turner, 2000, Pavlou *et al*, 2004).

Gardner and co-workers have applied an AlphaMos Fox 2000 to identify bacteria that cause infections of the ears, nose and throat. These diseases are often associated with microorganisms such as *Staphylococcus aureus*, *Legionalla pneumphilia*, and *Escherichia coli*. Currently, the diagnosis is based on taking a swab specimen of the infected area with subsequent culturing, assaying and staining for classification. The entire procedure can take many days causing a delay in treatment. In contrast, the electronic nose is not only able to detect the type of bacteria but also the growth phase in a relatively short period of time (≈ hours). Gardner and his group analysed 180

unknown samples using a neural network. 100 % of the *Staphylococcus aureus* and 92 % of the *Escherichia coli* were correctly identified independent of the growth phase. These are remarkable findings since all *Staphylococcus* samples collected during the initial lag phase were correctly predicted and this after an incubation period of only 10 min (Gardner *et al*, 2000)

Whilst we have highlighted a few of the infectious diseases where electronic-nose technology has received considerable attention, it is by no means an exhaustive review, but it is an insight into which infectious areas may well see "point-of-care" applications. From "point-of-care" diagnosis of eye infections (Dutta *et al*, 2002) to detection of *Helicobacter pylori* in gastroesophageal isolates (Pavlou *et al*, 2000) and general clinical microbiology (Turner and Magan, 2004) new potential applications are being explored.

Non-infectious Diseases

The application of electronic-nose technology for the investigation of non-infectious disease has not as yet received such detailed evaluation. The main specimens for these studies are blood, breath and sweat. These body fluids are very complex which combined with complex disease pathology, makes non-infectious analysis much more difficult, but as will be briefly reviewed not impossible.

Application of electronic-nose technology in renal medicine

One non-infectious area, which has received significant interest, is renal medicine. The motivation for this most probably lies in the fact that well characterised

markers of renal disease are available. The first of these is microscopic haematuria. Di Natale and co-workers applied an electronic nose based on eight quartz microbalance sensors to analyse urine samples. Not only were they able to discriminate between urine containing blood compared to normal "healthy" urine, they were also able to correlate the sensor response to the amount of blood present in urine (Di Natale *et al*, 1999). However, this correlation was of a qualitative nature and no further attempts were made to find a quantitative correlation.

Patients suffering form kidney failure generally have a characteristic breath odour mainly caused by dimethylamine (DMA) and trimethylamine (TMA). Lin *et al* using these two marker substances to investigate the potential of an electronic nose (6 piezoelectric quartz-crystals) as a diagnostic tool for uraemia based on breath analysis, successfully distinguished between healthy individuals and chronic renal failure patients (Lin *et al*, 2001). There was, however, an overlap between patients suffering form renal insufficiency and haemodialysis patients. Nevertheless, the breath of kidney patients "smelt" significantly different to the breath of the healthy controls, indicating the potential of an electronic nose as an early, non-invasive diagnosis system for uraemia.

Other non-infectious applications

Two further interesting applications for electronic-nose technology are in the non-invasive diagnosis and management of diabetes (Ping *et al*, 1997; Mohamed *et al* 2002) and in the diagnosis of lung cancer (Di Natale *et al*, 2003).

Ping *et al* used electronic nose technology to directly analyse exhaled breath from 18 patients with type I diabetes and 14 healthy volunteers before and after eating, and

demonstrated that such non-invasive monitoring could be a reliable method for monitoring diabetics (Ping *et al*, 1997). Mohamed *et al* used an electronic-nose and artificial neural network analysis to demonstrate that type II diabetes could be detected via urine analysis with a 92% success rate (Mohamed *et al*, 2002).

Di Natale *et al* have extended previous GC-MS studies (Phillips *et al*, 1999) and demonstrated the utility of electronic-nose technology in detecting lung cancer (Di Natale *et al*, 2003). All patients with lung cancer and 94% of patients free from the disease were correctly classified following the analysis of alkenes and aromatic compounds in expired breath. Whilst the sample size (42 patients) was relatively small, this study demonstrated just how broad the application of electronic-nose in clinical practice potentially is.

1.6.2 NON-MEDICAL APPLICATIONS

Non-medical applications possess the biggest share in the global electronic nose market, with the food industry being the largest customer. Applications reach from monitoring the quality of food packaging (Forgren *et al*, 1999) and dairy products (Schaller *et al*, 1999; Magan *et al*, 2001; Ampuero and Bosset, 2003; Brudzewski *et al*, 2004), classification of vegetable oils (Martin *et al*, 1999) and olive oil (Guadarrama *et al*, 2001), wines (Baldacci *et al*, 1998), cheese (Schaller *et al*, 1998) and to monitoring sausage fermentation (Eklov *et al*, 1998).

Aroma is not only essential in the food industry and therefore, electronic noses have been applied by different industries, where the smell of a product is as important. The car manufacturer Renault used electronic nose technology to analyse the emission

of plastic constituents into the passenger cabin (Guadarrama *et al*, 2002). Schiffman *et al* (1997) applied an AromaScan system to analyse off-odours in pharmaceutical products caused by inappropriate packaging materials.

1.7 PATTERN RECOGNITION

Modern analytical instruments generate a vast amount of data. A modern electronic nose for example comprises up to 32 individual sensors, whereby each sensor provides several parameters with which the sample is described. This non-specific description due to the nature of the electronic nose gives an overview of the sample (pattern) and not the chemical composition of it. The interpretation of such a vast data set is difficult and cannot be done by simply looking at the data.

Analysing such multivariate data sets is a multi-step process including data preprocessing, visualising relevant information, and finally classification of samples. This multi-step process is collectively known as pattern recognition.

1.7.1 DATA PREPROCESSING

Electronic nose raw data might not be the most useful input variables for statistical analysis due to noise, sensor drift or inconsistency (Dickinson *et al*, 1998; Otto, 1999). Good results are only obtained from quality raw data. Data preprocessing is aimed to modify existing raw data with the hope to obtain more quality input variable (Bartlett *et al*, 1997).

The most commonly used data preprocessing techniques are normalisation, mean centering and scaling.

Normalisation

Normalisation is a procedure to eliminate quantitative information (concentration) from a data set. The concentration of a variable is represented by the magnitude (vector length) (Massart *et al*, 1988; Otto, 1999). Therefore, for qualitative assessment of the original data set, each sensor response is normalised according to:

$$x'_{ij} = \frac{x_{ij}}{\sqrt{\sum_{k=1}^{m} x_{ik}^2}} \tag{1.1}$$

where x'_{ij} is the normalised sensor response, x_{ij} is the raw sensor response and x_{ik} are the individual sensor responses.

Mean-centering

This method is aimed to eliminate a constant offset (drift) from a data set. Thereby, each variable, x_{ik}, is centred by subtracting the column mean, $\overline{x_k}$, according to:

$$x'_{ik} = x_{ik} - \overline{x_k} \tag{1.2}$$

where i is the row index, k the column index, x'_{ik} is the mean-centered variable and $\overline{x_k}$ is the column mean (Massart *et al*, 1988; Otto, 1999).

Scaling

Often sensors with small signal changes are equally important as sensors showing large changes. To overcome this problem, the input variable can be scaled either to similar ranges (range scaling) or to similar variances (autoscaling).

Range scaling is a procedure to eliminate the influence of absolute values by scaling them to values between zero and one according to:

$$x'_{ik} = \frac{x_{ik} - x_{k(\min)}}{x_{k(\max)} - x_{k(\min)}} \qquad 0 \le x'_{ik} \le 1 \tag{1.3}$$

where i is the row index, k the column index, x'_{ik} is the range-scaled variable, $x_{k(\min)}$ is the minimal value in column k, and $x_{k(\max)}$ is the maximal value in column k (Massart *et al*, 1988; Otto, 1999).

Autoscaling is a technique to scale the variables to similar standard deviations and thereby reduce the effect of signal changes (variance) according to:

$$x'_{ik} = \frac{x_{ik} - \overline{x_k}}{s_k} \tag{1.4}$$

where i is the row index, k the column index, x'_{ik} is the autoscaled variable, $\overline{x_k}$ is the column mean, and s_k is the standard deviation of column k (Massart *et al*, 1988; Otto, 1999).

Unfortunately, no general guidelines exist to determine the appropriate preprocessing technique and thus the different techniques are controversially discussed in the literature (Despagne and Massart, 1998; Jurs *et al*, 2000). In many cases, normalisation can improve the quality of the input variables but in some case valuable quantitative information will be removed. Autoscaling for example, can enhance noise by treating sensors delivering little information equal to important sensors (Dieterle and Strathmann, 2000). The choice of pre-processing is also dependent on the application, i.e. the nature of the data obtained from the electronic nose.

1.7.2 MULTIVARIATE DATA ANALYSIS

Understanding and interpreting multivariate data is the key to success. The list of available multivariate methods is long, but only a limited number are frequently used in gas sensing.

Multivariate methods are generally described by terms such as parametric or non-parametric, supervised or unsupervised, or linear and non-linear. A schematic representation of some of the most popular pattern recognition techniques employed in gas sensing is given in Figure 1.2.

Parametric techniques model the probability density function of the parameters used to describe the sensor response and are based on the assumption that the data are normal (gaussian) distributed. In contrast, non-parametric do not require a defined statistical distribution of the data to model the sensor response (Massart *et al*, 1988).

Unsupervised learning methods are generally used in exploratory data analysis because they show the relationship between samples and variables without prior

information on the nature of the sample (Schaller *et al*, 1998). Conversely, supervised learning techniques classify an odour by developing a mathematical model relating training data, i.e. samples with known properties, to a set of given descriptors. Test samples are then used to evaluate the model (Gardner and Bartlett, 1994).

Linear methods calculate a model based on linear combinations of input data. In contrast, non-linear techniques are based on a non-linear description of the input data. Therefore, these methods can deal with more complex sample mixtures, i.e. more variation within the input data (Otto, 1999).

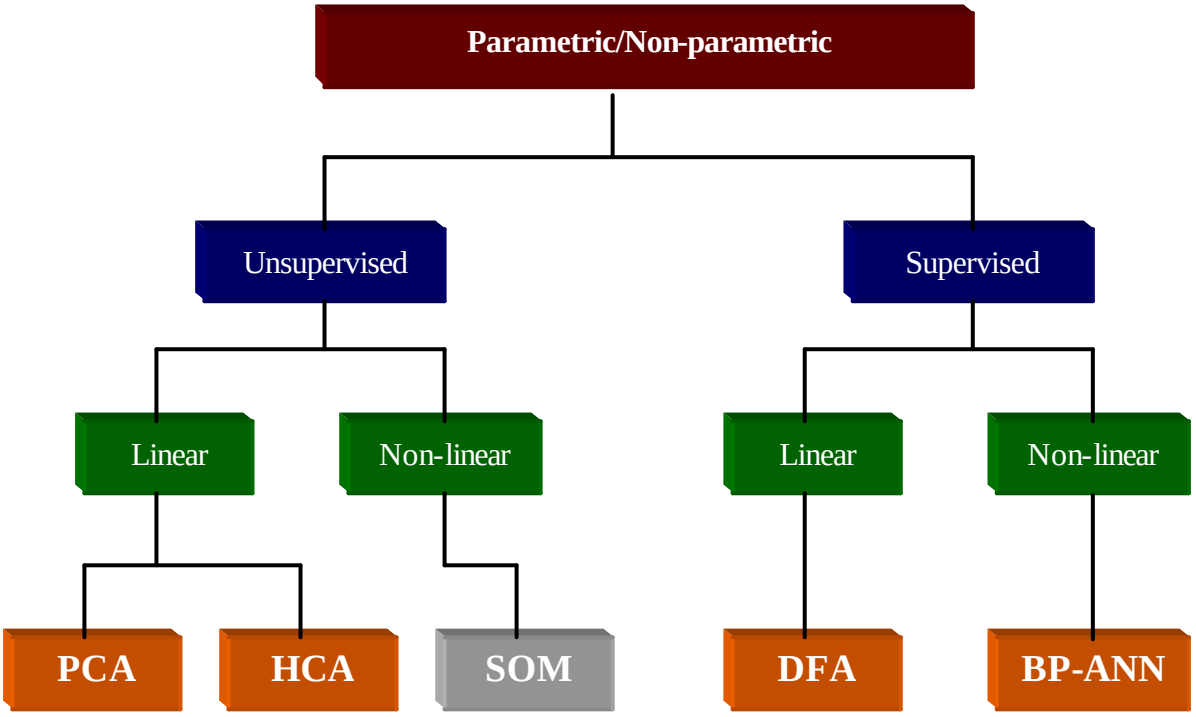

Figure 1.2: Schematic representation of the most frequent used pattern recognition techniques.

Abbreviations: PCA – principal component analysis, HCA – hierarchical cluster analysis, SOM – self organising maps, DFA – discriminant function analysis, BP-ANN – backpropagation-artificial neural network.

Principal Component Analysis (PCA)

PCA is an unsupervised data reduction method. The basic idea of the method is to describe the variation of a multivariate data set in terms of a set of uncorrelated variables, each of which is a particular linear combination of the original variables. In other words, the original data matrix is projected from a high dimensional space into a less dimensional space, preferably a plane or a 3-dimensional space. During the process the original data set is reduced in dimensions, i.e. is compressed, with as little loss of information as possible. This is achieved by filtering out the noise in the original data matrix, without removing essential information described in the variance of the data (Massart *et al*, 1988; Otto, 1999).

Mathematically, the key idea of PCA is to decompose the original $i \; x \; j$ data matrix $\boldsymbol{X}$ into its $i \; x \; k$ score matrix $\boldsymbol{T}$, its $k \; x \; j$ loading matrix $\boldsymbol{P}$ and the residual matrix $\boldsymbol{E}$ according to:

$$X = TP + E \tag{1.5}$$

where i is the number of samples, j is the number of variables and k is the number of principal components (PCs).

PCs are linear combinations of the original variables and can be calculated as follows:

$$t_{11} = x_{11} p_{11} + x_{12} p_{12} + \ldots + x_{1p} p_{p1} \tag{1.6}$$

where t_{11} is the first element of the first PC, x are the original variables and p are the loadings.

The PCs are determined on the basis of the maximum variance criterion. Each subsequent PC describes a maximum of variance, which is not modelled by the previous one. According to this, the first PC contains the most of the variance of the data (Otto, 1999; Everitt and Dunn, 2001). The relationship between samples can be visualised by plotting the scores against each other (score plot).

Hierarchical Cluster Analysis (HCA)

HCA is an unsupervised method that combines individual samples to clusters according to their similarities to each other.

The similarity between two samples is determined by the (Euclidean, that is one measure, but there or others) distance between them, which can be calculated for two samples p_1(x1, y1) and p_2(x2, y2) as follows:

$$d_{(p1,\,p2)} = [(x_1 - x_2)^2 + (y_1 - y_2)^2]^{1/2} \qquad (1.7)$$

where $d_{(p1,\,p2)}$ is the distance between the two samples.

The next step is the reduction of the distance matrix by aggregation of clusters, whereby the clusters with the shortest distances between them are aggregated first. Several different formula exist for the aggregation of two clusters including single linkage, complete linkage, centroid linkage, median linkage and Ward's method (Otto, 1999; Everitt and Dunn, 2001).

Discriminant Function Analysis (DFA)

DFA is a supervised classification procedure aimed at formalising a decision boundary between different classes. The decision boundary is calculated so that the variance between different classes is maximised and within individual classes minimised. Different ways exist to calculate the decision boundary. In a multivariate data set, this is done by solving an eigenvalue problem.

The eigenvector (w) with the greatest eigenvalue (λ) provides the first discriminant function (s1) according to:

$$s_1 = w_{11}x_1 + w_{12}x_2 + \ldots + w_{1p}x_p \qquad (1.8)$$

where w is the eigenvector and x is the original variable.

The second discriminant function (s_2) is calculated from the eigenvector with the second greatest eigenvalue. This procedure is continued until all discriminant functions are found to solve the discrimination problem. The original data set is visualised by plotting the individual discriminant functions against each other (Otto, 1999; Everitt and Dunn, 2001).

Artificial Neural Network (ANN)

The key idea of an ANN is to mimic the human brain by modelling the human nervous system (Kohonen, 1988). An ANN consists of interconnected, and usually adaptive processing elements. The processing elements represent the biological (olfactory) neurons, and their interconnections, the synaptic links. In the biological

neurons the input signals arriving through the axon ends in the synapse. There the information is transformed and sent across the dendrites to the next neuron (Figure 1.3a). In artificial neurons, this signal transfer is simulated by multiplication of the input signal, x, with the synaptic weight, w, to derive the output signal y ((Figure 1.3b) (Otto, 1999).

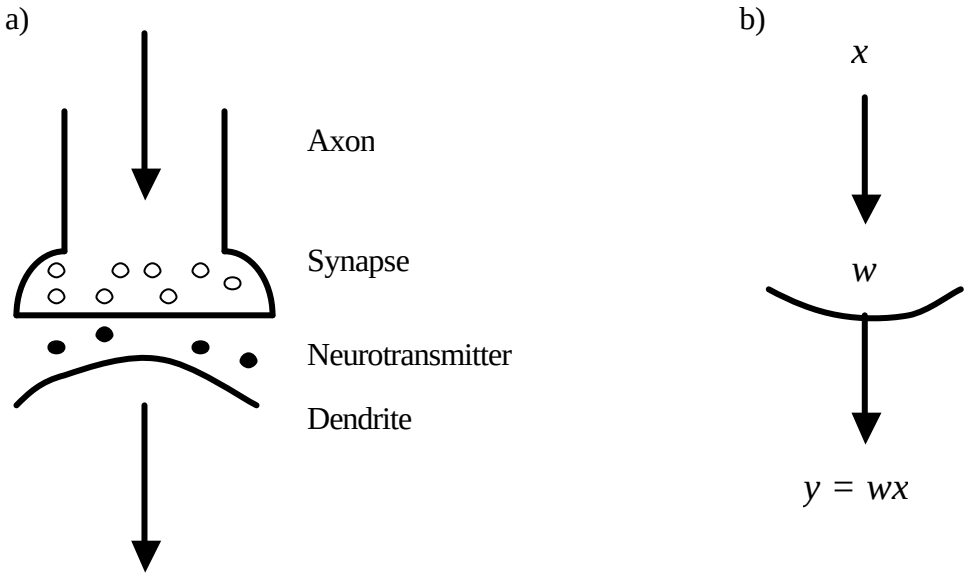

Figure 1.3: Analogy between biological (a) and artificial (b) neurons.

The artificial neuron is the heart of every neural network. In reality, a single neuron receives input signals, x_i, from n neurons, aggregates them by using the synaptic weights, w_i, and passes the result after suitable transformation (transfer function) as the output signal y_i (Figure 1.4). Important transfer functions are given in Table 1.3.

These individual neurons are aggregated to layers. A general neural network consists of an input layer, one or more hidden layer(s), and an output layer. These

layers are usually fully connected (Figure 1.5). As pointed out in Figure 1.5, the output signals (y_i) of the neurons of one layer act as the input signals (x_i) for the neurons of the following layer (Shih, 1994).

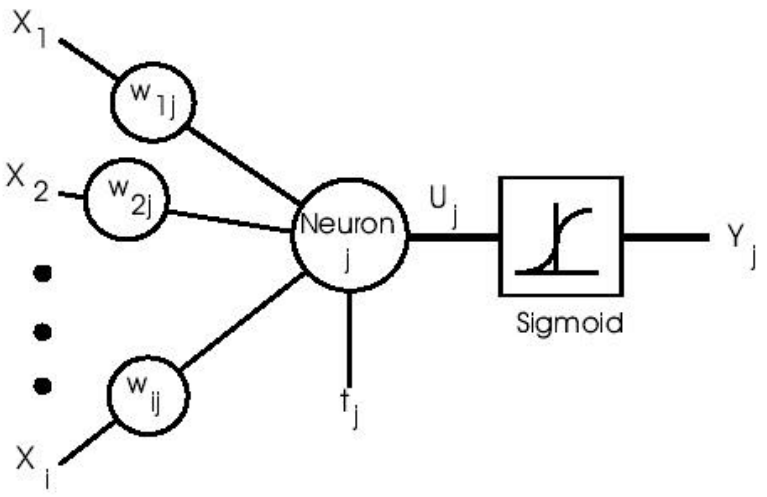

Figure 1.4: Operation of a single neuron.

Table 1.3: Important transfer functions for neural networks (adapted Otto, 1999).

Step function	*Sign function*	*Sigmoid function*	*Linear function*
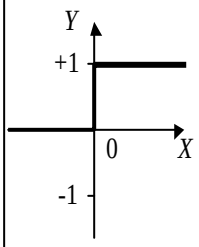	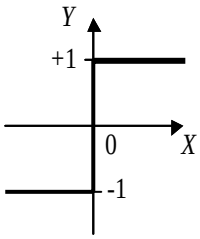	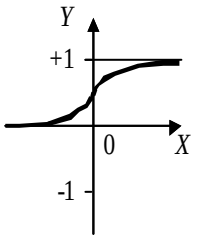	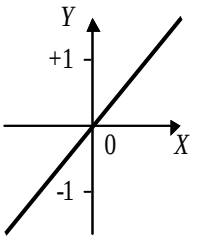
$Y^{step} = \begin{cases} 1, \text{if } X \geq 0 \\ 0, \text{if } X < 0 \end{cases}$	$Y^{sign} = \begin{cases} +1, \text{if } X \geq 0 \\ -1, \text{if } X < 0 \end{cases}$	$Y^{sigmoid} = \frac{1}{1+e^{-X}}$	$Y^{linear} = X$

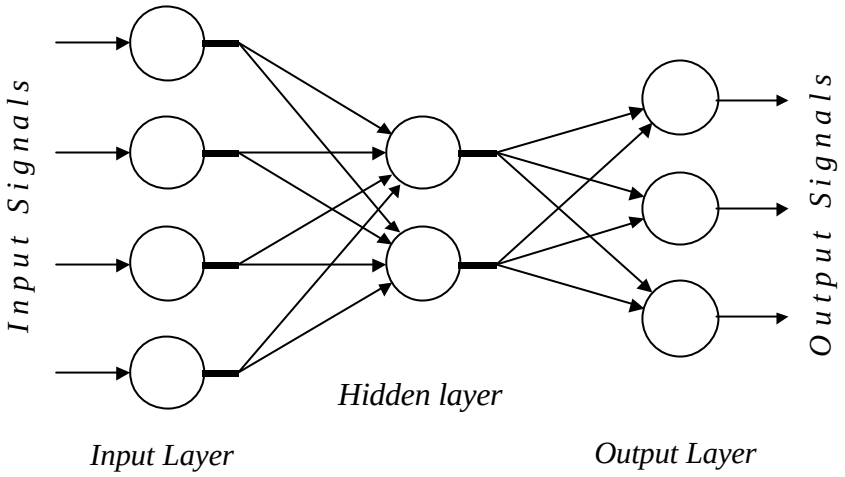

Figure 1.5: Architecture of a neural network.

Generally, the input layer is considered a distributor of the signals from the external world. Hidden layers are considered to be categorisers or feature detectors of such signals. The output layer is considered a collector of the features detected and producer of the response (Shih, 1994).

The main advantages of neural networks are the great adaptability in terms of learning, self-organisation, training, and noise – tolerance. Various algorithms can be used to train an ANN, but the most important one, and the one used in this report, is the back propagation technique (Gardner and Hines, 1997).

The back-propagation algorithm relies on two stages, the first being the learning phase during which the ANN learns how to recognise each of the known odour classes. The second phase is the validation of the model during which the network is

used to classify unknown samples from the same classes as the training data (Gardner and Hines, 1997). As the name back-propagation indicates, the training of the networks starts at the output layer and goes backwards through the layers (Shih, 1994). During the training period, the weights of individual neurons are adjusted so that the error between actual output and target signal is minimised (Otto, 1999).

1.8 RENAL FAILURE AND HAEMODIALYSIS

1.8.1 THE KIDNEYS

The human body contains two kidneys. They form together with two ureters, one urinary bladder, and one urethra the urinary system. The kidneys filter the blood and return most of the water and solutes to the bloodstream. The remaining water and solutes form urine, which is excreted by each kidney through its ureter and stored in the urinary bladder. The urine is expelled from the urinary bladder through the urethra (Tortora and Grabowski, 2000). In Figure 1.6, the organs of the urinary systems are shown.

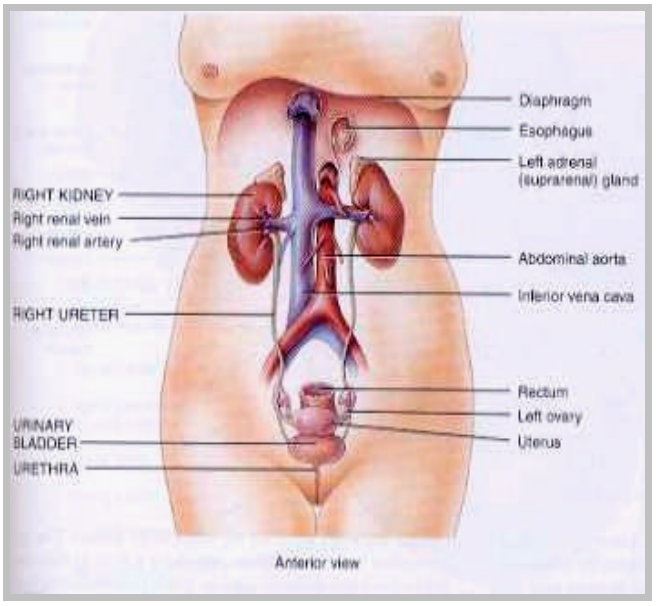

Figure 1.6: The organs of the urinary system (from Tortora and Grabowski, 2000).

Anatomy of the Kidney

The paired kidneys are reddish, kidney-bean shaped organs located just above the waist between the peritoneum and the posterior wall of the abdomen. An average kidney in an adult is 10 – 12 cm long, 5 – 7 cm wide, and 3 cm thick and weighing 135 – 150 g (Tortora and Grabowski, 2000). The concave medial border of each kidney faces the vertebral column and near the centre of this border is a deep vertical fissure, called the renal hilus (Figure 1.7) through which, the ureter, the blood vessels, the lymphatic vessels and nerves leave the kidney. A kidney has two distinct regions, namely the renal cortex and the renal medulla. The renal cortex is a smooth-textured layer underneath the renal capsule (Figure 1.7). The renal medulla consists of 8 – 18 renal pyramids separated by the renal columns, which are an extended part of the renal cortex. Together, the renal cortex and the renal pyramids constitute the

functional portion (parenchyma) of the kidney. Within the parenchyma are the functional units of the kidneys called nephrons. A normal kidney contains about 1 million nephrons (Clancy and Mc Vicar, 1995; Tortora and Grabowski, 2000).

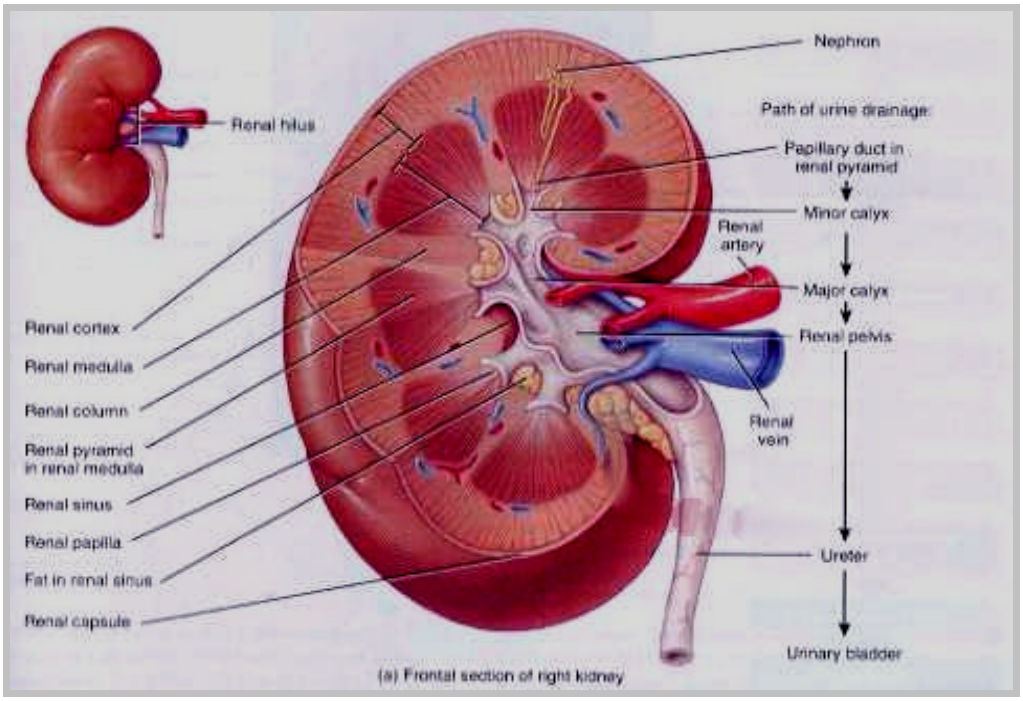

Figure 1.7: Internal anatomy of the kidneys (from Tortora and Grabowski, 2000).

Functions of the Kidney – an overview

The functions of the kidney are:

- *Regulation of the blood ionic composition:* The kidney helps to regulate the blood concentrations of several ions, most importantly being sodium, potassium, calcium, chloride and phosphate ions (Tortora and Grabowski, 2000).

.

- *Regulation of blood osmolarity:* The kidneys maintain a relatively constant blood osmolarity (≈ 290 mOsm/litre) by separately controlling the loss of water and the loss of solutes in the urine (Clancy and Mc Vicar, 1995; Tortora and Grabowski, 2000).

- *Regulation of blood volume:* The blood volume is regulated by either eliminating or conserving water and thus the volume of the interstitial fluid (Clancy and Mc Vicar, 1995; Tortora and Grabowski, 2000).

- *Regulation of blood pressure:* Besides regulating the blood volume, the kidneys are able to contribute to the control of the blood pressure in other ways. Firstly, the kidneys secret the enzyme renin, which converts angiotensiogen to angiotensin I. Angiotensin I is converted into angiotensin II which has a direct action on peripheral vasoconstriction leading to an increased blood pressure. Secondly, the renal glands secret aldosterone which influences the sodium retention and hence, the blood pressure (Clancy and Mc Vicar, 1995; Tortora and Grabowski, 2000).

- *Regulation of blood pH:* The kidneys excrete hydrogen ions (H^+) into the urine and retain bicarbonate ions (HCO_3^-). The bicarbonate ion is an important buffer of H^+ (Clancy and Mc Vicar, 1995; Tortora and Grabowski, 2000).

- *Release of hormones:* The kidneys are responsible for the release of two hormones, namely calcitriol and erythropoietin. Calcitriol is the active form of vitamin D, which regulates the calcium homeostasis. Erythropoietin stimulates the

production of red blood cells by the bone marrow (Clancy and Mc Vicar, 1995; Tortora and Grabowski, 2000).

- *Excretion of wastes and foreign substance:* Waste products or useless substances (for the body) are excreted via urine. Waste products result from metabolic reactions, e.g. ammonia, urea (protein metabolism), creatinine (breakdown of creatine phosphate in muscles), uric acid (catabolism of nucleic acids) or bilirubin (catabolism of haemoglobin). Foreign substances include environmental toxins or drugs (Clancy and Mc Vicar, 1995; Tortora and Grabowski, 2000).

1.8.2 EVALUATION OF KIDNEY FUNCTION

The routine assessment of kidney function involves the evaluation of both the quality and quantity of urine and the concentration of waste products in blood (Tortora and Grabowski, 2000).

Urine analysis (= Urinalysis) is the analysis of the volume, physical, chemical and visible (microscopic) properties of urine. A healthy adult excretes approximately 1 – 2 litre of urine per day. The urine volume depends on fluid intake, blood pressure, blood osmolarity, diet as well as general health. Normal urine consists of about 95 % water and about 5 % electrolytes. Typical solutes present in urine are urea, creatinine, uric acid, sodium, potassium and small quantities of fatty acids, pigments, enzymes and hormones. If a disease alters the body metabolism or the kidney function, the

composition of the urine is changed or the concentration of normal constituents appears in abnormal amounts (Tortora and Grabowski, 2000).

Blood tests are performed to measure either blood urea nitrogen (BUN) or creatinine. A number of factors can raise urea levels, and a decreased glomerular filtration rate as in renal diseases is one of them. However, it is a poor surrogate marker for assessing the renal function as it varies with protein intake (Tortora and Grabowski, 2000). Creatinine results from the catabolic degradation of creatine phosphate in muscle. Normally, the blood creatinine level remains constant since the rate of creatinine excretion (via urine) is equal to the production from muscle. A creatinine level above 135 mmol l^{-1} indicates a poor renal function, but this also varies with age, sex and body weight, and renal function (Tortora and Grabowski, 2000).

Renal Plasma Clearance is the volume of blood that is cleared of a substance per unit of time, usually expressed in units of millilitre per minute. A low plasma clearance indicates an inefficient excretion (Tortora and Grabowski, 2000). Generally the creatinine clearance is measured since creatinine passes easily across the glomular membrane and is not reabsorbed and only secreted in small quantities. Normal range for the creatinine clearance is 120 – 140 ml min^{-1} (Tortora and Grabowski, 2000). Of more accurate determination of the GFR is the clearance of ^{51}Cr-label ethylendiaminetetraacetic acid (EDTA) (Haslett *et al*, 1999).

The clearance of a substance can be calculated according to:

$$\text{Clearance of substance } S = \frac{[S]_{urine} \times \dot{V}_{urine}}{[S]_{plasma}} \qquad (1.9)$$

where [S] is the concentration of substance S in either urine or plasma and V is the urine volume per minute (Clancy and Mc Vicar, 1995).

Imaging Techniques are used to visualise the shape of the kidneys as well as to assess the renal function. The main methods are intravenous pyelogram, ultrasound, computer tomography and the application of radionucleotides (Haslett *et al*, 1999).

Renal biopsy is performed to assess the nature and extend of the renal disease. The procedure is carried out under ultrasound guidance for an exact placement of the needle. The obtain tissue sample is then analysed using conventional light microscopes or electron microscopes (Haslett *et al*, 1999; nephrologychannel, 2004).

1.8.3 RENAL FAILURE AND RENAL REPLACEMENT THERAPY

Renal failure

Glomerular and tubular functions are highly dependent on adequate blood supply (Kidneys receive about 20 % of cardiac output). If the blood supply is disturbed, both functions are impaired (Stevens and Lowe, 2000). If one part of a nephron is affected, it is likely that other parts will develop abnormalities due to the close structural and functional relationship of nephrons (Stevens and Lowe, 2000). Renal failure occurs

when a sufficient number of nephrons are damaged and therefore the kidneys unable to perform their tasks (Tortora and Grabowski, 2000; Stevens and Lowe, 2000). Renal failure can be divided into two main types, namely acute and chronic renal failure.

Acute Renal Failure

Acute Renal Failure (ARF) refers to a sudden and usually reversible failure of the renal function, i.e. the majority of the nephrons stop working simultaneously. ARF normally develops over a period of days or weeks (Haslett *et al*, 1999). The clinical manifestation includes oliguria or even anuria, disturbed fluid and electrolyte balance (Stevens and Lowe, 2000). Several diseases can cause ARF, such as central perfusion failure, tubular and interstitial diseases or glomerular diseases (Stevens and Lowe, 2000). If the cause of renal failure is not rapidly corrected, temporary renal replacement therapy (RRT) may be necessary (Haslett *et al*, 1999).

Chronic Renal Failure

Chronic Renal Failure (CRF) is deterioration in renal function, which develops over a long period of time (years). As more and more nephrons are destroyed, renal function becomes progressively worse (Haslett *et al*, 1999; Stevens and Lowe, 2000). Several diseases can lead to CRF, all of which cause a slow, progressive destruction of the nephrons. The most common causes are diseases of the glomeruli (glomerulonephritis and diabetic glomerular disease) and diseases of tubules and interstitium (infective, toxic and obstructive damage to tubules) and vascular diseases (Stevens and Lowe, 2000). Among the main consequences of CRF are uraemia,

polyuria, abnormalities in biochemical homeostasis (electrolyte imbalances, metabolic acidosis, etc.), secondary hyperparathyroidism, bone disease (renal osteodystrophy) and finally anaemia (Stevens and Lowe, 2000). In contrast to the other forms of renal failure, CRF is not usually reversible and if it progresses may require permanently a kind of RRT.

Renal Replacement Therapy

The ability to replace the kidney function by means of "artificial devices" has been available for 40 years (Stevens and Lowe, 2000). Nowadays, several treatment modalities are available including haemodialysis (HD), haemofiltration (HF), continuous ambulatory peritoneal dialysis (CAPD), and transplantation. However, dialysis using an artificial kidney can only replace a part of the excretory function, whereas the endocrine and metabolic function of the kidney cannot be restored. In contrast, transplantation can replace all kidney functions (Stevens and Lowe, 2000). The distribution of the treatment modalities in the United Kingdom in 2002 is shown in Figure 1.8. As can be seen, transplantation accounts for 37 %, HD for about 46 % and CAPD for 17 %.

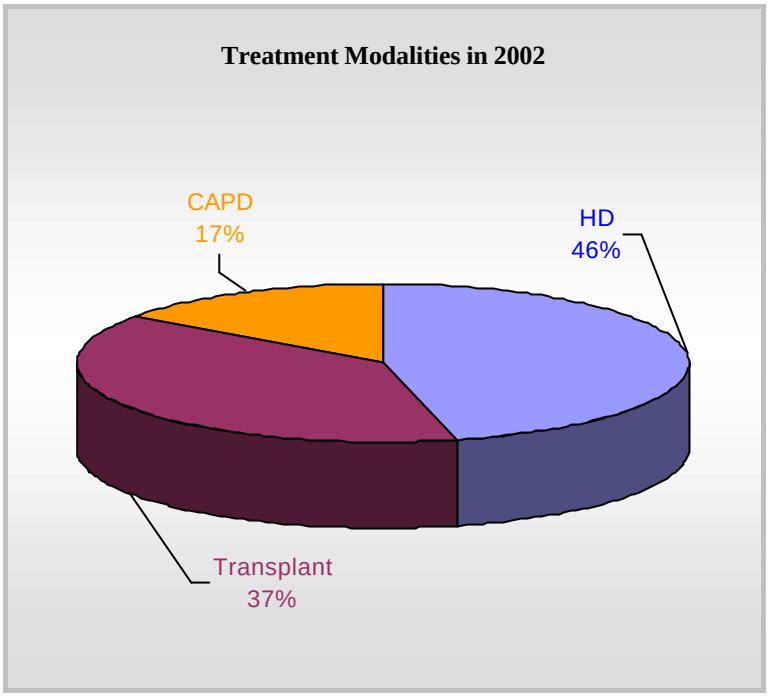

Figure 1.8: Treatment modalities in the United Kingdom in 2002 (modified, UK Renal Registry Report 2003).

Key: CAPD: Continous Ambulatory Peritoneal Dialysis, HD: Haemodialysis

Haemodialysis, Haemofiltration and Continuous Ambulatory Peritoneal Dialysis

These three treatment modalities apply semipermeable membranes to separate the dialysis fluid from the blood stream. Accumulated waste products and excessive body fluid diffuse from the blood stream across the membrane into the dialysis fluid. Haemodialysis and haemofiltration employ artificial membranes, whereas CAPD utilises the body's own peritoneal membrane (Haslett *et al*, 1999). Haemodialysis removes waste product via diffusion across a transmembrane concentration gradient. In contrast, haemofiltration provides solute clearance solely by convection, as solutes are dragged down a pressure gradient with water (Levy *et al*, 2001). A more detailed description of haemodialysis is given in section 1.8.4.

Transplantation

This is the only possibility to restore normal kidney function and correcting all metabolic abnormalities of CRF (Haslett *et al*, 1999). The kidney graft is taken either by a dead donor or from a living relative. It is essential, that blood group compatibility is guaranteed. Donor kidneys are usually matched with the recipient human leukocyte antigens (HLA) to increase the graft survival (Haslett *et al*, 1999). The problem associated with transplantation is the requirement for long-term immunosuppression leading to a higher incidence of infections and malignant neoplasm, especially of the skin. However, transplantation is the best treatment modality and is also the most cost-effective treatment for CRF (Haslett *et al*, 1999).

1.8.4 HAEMODIALYSIS

The invention of dialysis dates back to the 19th century, when Thomas Graham discovered a method for separating gases by diffusion (Drukker, 1983). However, haemodialysis was not widely available till 1960, when the first patient was treated for CRF by intermittent haemodialysis. The milestones in the development of haemodialysis are shown in Figure 1.9.

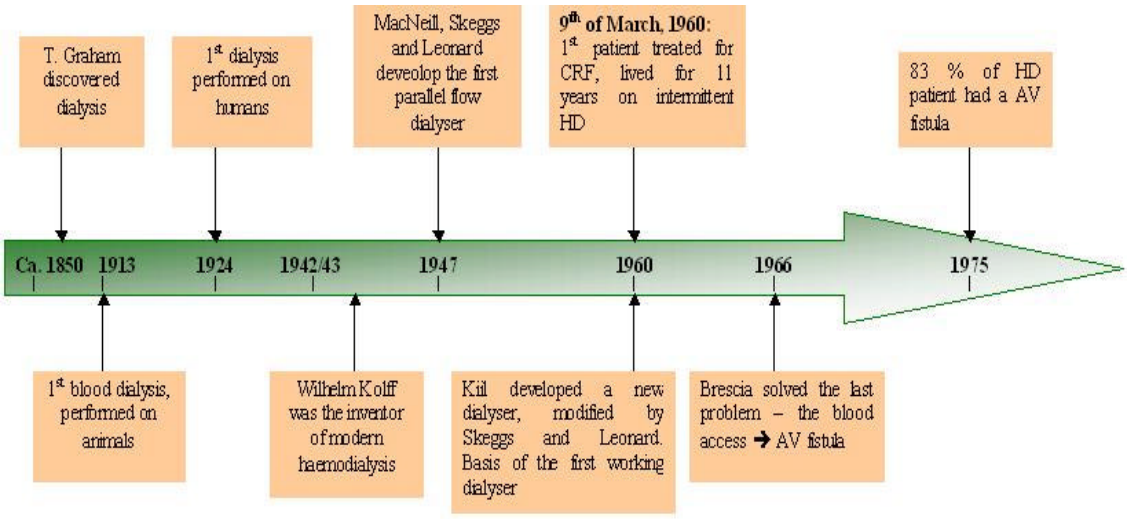

Figure 1.9: Milestones in the development of haemodialysis (Drukker, 1983).

Key: CRF: Chronic Renal Failure, HD: Haemodialysis, AV: Arteriovenous

Fundamentals of Haemodialysis

Insufficient kidney function can lead to the accumulation of excess electrolytes, waste products and fluid. The concentrations of these compounds can reach toxic levels and need to be removed from the blood stream (Patzer, 2001). To perform haemodialysis, vascular access is required, which is normally obtained by an arteriovenous (AV) fistula (Figure 1.10). The fistula, usually in the forearm of the patient, should be formed before the treatment starts, so that it has time to become established (distension and arterialisation). Large-bore needles can then be inserted into the vein for each HD session. HD is normally performed 3 – 5 hours three times a week (Haslett *et al*, 1999).

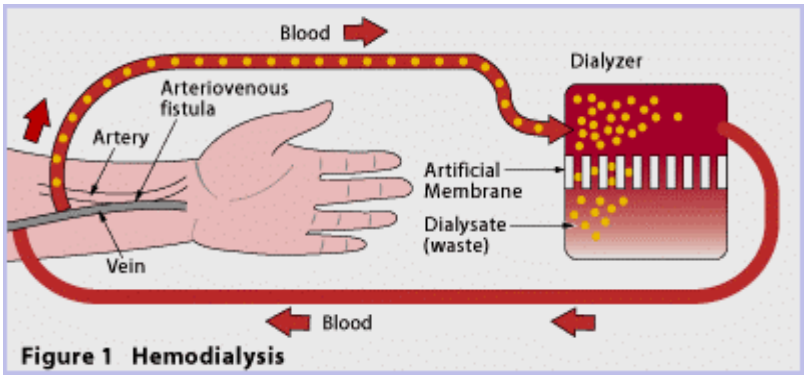

Figure 1.10: Schematic diagram of the fistula and the dialyser (Patzer, 2001).

A typical hollow-fibre dialyser is shown in Figure 1.11. The dialyser consists of a bundle of semi-permeable tubes (hollow-fibre) surrounded by a hard plastic shell. At the top and bottom of the shell, distribution caps are placed. Blood from the AV-fistula enters the dialyser through a distribution cap on one side, flows along the interior of the fibres and exits on the other side through a distribution cap and re-enters the blood circulation via AV-fistula. The dialysate (composition see Appendix C) flows counter-current to the blood on the outside of the fibres (Patzer, 2001).

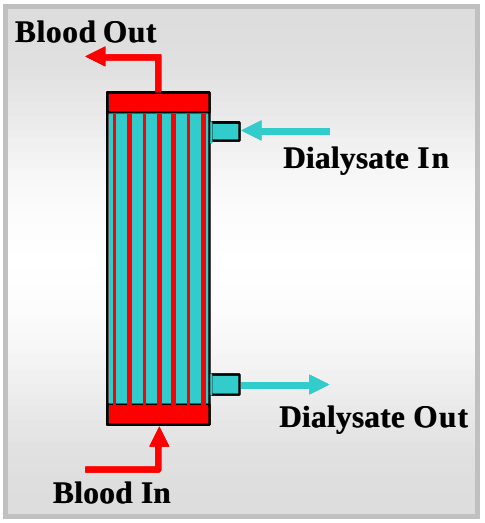

Figure 1.11: Schematic diagram of a hollow-fibre dialyser.

Molecules in the blood, with a molecular size smaller than the pore size of the membrane, can diffuse across the semi-permeable membrane into the dialysate. The driving force for the diffusion is the concentration difference between the blood (high concentration) and the dialysate (low concentration). The diffusion is governed by Fick's law according to:

$$J = -DA\frac{dc}{dx} = -DA\frac{\Delta c}{\Delta x} \qquad (1.10)$$

where J is the flux [mmol l^{-1}], D is the diffusity [cm^2 s^{-1}], A is the area of the membrane [m^2], and dc/dx is the concentration gradient (Sargent and Gotch, 1983).

The diffusity *D* is a unique property of the solute-solvent system at a specific temperature. The sign convention is adopted, which states that diffusion occurs in positive direction, i.e. from the region of higher activity (conc.) to that of lower so that the concentration will be decreasing in the direction of flux. Therefore, the right hand side of equation 1.10 must carry a negative sign (Sargent and Gotch, 1983). The Diffusity *D* is a constant at any particular temperature. Therefore, equation 1.10 can be written as:

$$J = -K_0 A\overline{\Delta C} \tag{1.11}$$

where K_0 is the mass transfer coefficient [cm min^{-1}] and $\overline{\Delta C}$ is the concentration difference [mmol l^{-1}] (Sargent and Gotch, 1983).

Equation 1.11 states that with a specific dialyser (K_0A is constant), the transfer of solutes from blood into dialysate will depend directly on the concentration difference (ΔC). This concentration difference is the driving force of dialysis. The concentration of solutes in blood and dialysate will linearly change, when solutes are transferred from one to the other (Figure 1.12). The solute concentration in blood decreases whilst in the dialyser (c_{Bi} ➔ c_{Bo}). In contrast, the concentration in the dialysate increases (c_{Di} ➔ c_{Do}). The concentration difference at any point in the dialyser is the difference between these two lines (red and blue) and this concentration (violet line) determines the flux.

Figure 1.12: Blood and dialysate concentration as a function of flux between the two fluids in counter current flow (Sargent and Gotch, 1983).

On the other hand, excessive body fluid has also to be removed from the body. However, the driving force for the removal of excessive body fluid is not same as for the solute removal (ΔC). The transfer of water form the patient to the dialysate is determined by a pressure difference (ΔP). The water flux can be calculated as follows:

$$Q_F = K_{UF} \times (\overline{P_B} - \overline{P_D}) \qquad (1.12)$$

where Q_F is the ultrafiltration rate [ml min^{-1}], and $\overline{P_B} - \overline{P_D}$ is the pressure difference (driving force) between the pressure on the blood side and the dialysate side (Sargent and Gotch, 1983).

Adequacy (dialysis dose) of Haemodialysis

Dialysis dose can be defined as the amount of haemodialysis received per dialysis and the dialysis frequency per week (De Palma and Pittard, 2001). It is a measure of how effective a dialysis treatment (HD or CAPD) removes waste products from the body (NIH, 1999)

The concept of dialysis adequacy was developed in the early 1970s to assess the treatment efficiency of end-stage renal disease (ESRD) patients (Canaud *et al*, 2000). From the very beginning the removal of small molecules was considered important as they were directly linked to the symptoms and signs of renal failure (Lindsay and Sternby, 2001; Keshaviah, 2002). Therefore, urea has been suggested as a surrogate marker for small toxic solutes (Keshaviah, 2002). In 1975 urea gained wide acceptance as a marker of solute removal in dialysed patients (Vanholder *et al*, 1994).

Urea Reduction Ratio (URR)

The URR is a formula (equation 1.13), which expresses the reduction in blood urea during a dialysis session (De Palma and Pittard, 2001).

$$URR = \frac{(BUN_{predialysis} - BUN_{postdialysis})}{BUN_{predialysis}} \times 100 \qquad (1.13)$$

where BUN is the blood urea nitrogen.

The URR is the simplest way to measure the delivered dialysis dose. It does not include the time of dialysis, the body size and effects of ultrafiltration (Levy *et al*,

2001). Hence, the URR does not consider the residual renal function. The URR should be continuously higher than 65 % (with a three times per week HD schedule) to ensure an adequate treatment (UK Renal Registry Report, 2003)

Normalised dose of dialysis (Kt/V)

Gotch and Sargent (1985) introduced the Kt/V ratio as a result of their "mechanistic" analysis of the National Cooperative Dialysis Study (NCDS). The study was performed between 1976 and 1981 in the USA with the aim to find a correlation between the dialysis dose and morbidity (Lindsay and Sternby, 2001).

K represents the dialyser urea clearance (known from in-vitro studies), t is the dialysis time and V is the urea distribution volume (Levy *et al*, 2001). The Kt/V – value is the ratio between the volume of blood cleared of urea during a dialysis session (Kt) and the distribution volume of urea (V) which is equivalent to the total body water (Kemp *et al*, 2001). The gold standard for determining Kt/V in HD is by urea kinetic modelling (UKM) (Kemp *et al*, 2001). UKM is based on the principle of mass balance to describe urea nitrogen production and urea removal in the body (Shak, 1999).

The analysis of the NCDS by Gotch and Sargent (1985) revealed that a Kt/V < 0.8 (three times per week HD schedule) was associated with an increased morbidity. They concluded that a Kt/V of 1.0 was adequate (Gotch and Sargent, 1985). Since then, there is a controversial discussion about the appropriate Kt/V value to ensure an adequate treatment (Kemp *et al*, 2001). The UK Renal Registry (2003) recommends a Kt/V value greater than 1.2 as an appropriate dialysis dose.

1.8.5 MONITORING OF HAEMODIALYSIS

Urea Monitoring

As mention above, the Kt/V –value and the URR value are the most commonly used parameter to judge the adequacy of HD treatment. For both values, the determinations of pre- and post-dialysis urea concentrations are necessary (Levy *et al*, 2001; Lindsay and Sternby, 2001). The urea concentrations can be measured either on the blood side (BUN) or on the dialysate side (Dialysate Urea Nitrogen: DUN). BUN values can be inferred from DUN values using well-established relationships (Knocki *et al*, 2000a).

In the past few years, several devices have been developed that can measure urea more of less continuously in blood or in spent dialysate (Lindsay and Sternby, 2001). The majority of urea measurements are based on an enzymatic reaction. The enzyme urease catalyses the following reaction (Sternby, 1999):

$$(NH_2)_2CO + 2H_2O \Leftrightarrow NH_3 + NH_4^+ + HCO_3^- \qquad (1.14)$$

The amount of urea is measured indirectly by measuring the products of reaction in equation 1.14. This can be done by either measuring the breakdown products directly (NH_4^+) or indirectly by measuring a secondary parameter (pH, conductivity) (Sternby, 1999; Lindsay and Sternby, 2001). It is important, that enough urease is present to convert all of the urea (Sternby, 1999).

There are at least four devices commercially available, which can measure urea on-line in spent dialysate or ultrafiltrate (Sternby J., 1999). Three of them, namely the Baxter Biostat 1000 (Baxter Healthcare Corp., McGaw Park, IL), the Bio Care Device (Bio-Care Corp., Hsinchu, Taiwan), and the DQM 200 – Device (Gambro Lund AB,

Lund, Sweden) measure the urea concentration on the dialysate side, whereas the Bellco – Device (Bellco SpA, Miranda, Italy) measures the urea concentration on the blood side.

The following table summarises the four commercial available urea-monitoring devices.

Table 1.5: Summary of the four commercial available urea-monitoring systems.

Device	Place and Method of Measurement	Reference
Baxter Biostat 1000	Dialysate Ammonium-sensitive electrode	Depner *et al*, 1996 Hasper *et al*, 1997
Bio – Care	Dialysate Ammonium-sensitive electrode	Sternby, 1999 Lindsay and Sternby, 2001
DQM 200	Dialysate Conductivity change	Sternby, 1999 Lindsay and Sternby, 2001
Bellco – Device	Blood - ultrafiltrate Conductivity change	Colasanti *et al*, 1995 Santoro *et al*, 1996

The Bellco – Device is designed for a combined Haemofiltration/Haemodialysis treatment. The urea concentration is measured in the ultrafiltrate from the haemofilter (Lindsay and Sternby, 2001).

Knocki *et al* (2000a) could show that a potentiometric urea sensor (urease – coupled ammonium – selective electrode) is useful for fast and accurate DUN determination in a wide concentration range from 50 to 500 mg l^{-1}. This group also observed that cations influence the sensor response, which leads to an overestimation of the urea concentration. However, using an uncoated ammonium – selective electrode as a reference electrode, can eliminate the interferences. The urea

concentration is equal to the difference between the two sensor responses (Knocki *et al*, 2000b). Current research is focused on the development of new urea kinetic models, in particular multi-compartment models to provide a more accurate estimate of the Kt/V value (Shinzato *et al*, 1994; Daugirdas *et al*, 1997; Canaud *et al*, 2000). The single pool model assumes that urea equilibrates instantaneously among all body compartments, but in fact urea behaves as if it is distributed between two distinct compartments, intra- and extracellular. As urea is removed from the blood during dialysis, a concentration gradient is set up between the compartments. Single pool models are overestimating the dialysis efficacy by ignoring the intracorporeal compartment urea disequilibrium phenomenon. In contrast, multi-compartment models account for intracorporeal dialysis disequilibrium and post-dialysis urea rebound effects. However, multi-compartment models require multiple blood tests to solve the complex equations. These difficulties preclude its use in routine clinical practice (Daugirdas *et al*, 1997; Canaud *et al*, 2000).

Another area of research is based on the spectroscopic determination of urea and other small molecules retained in ESRD patients. Recently, two research groups published their results. Fridolin *et al* (2002) applied UV – spectroscopy to measure small waste products in spent dialysate. This group observed a good correlation between the UV – absorbance (285 nm) and the removal of small molecules such as urea, creatinine and uric acid. Similar results were found by Olesberg and co-workers (2002), who used an FTIR (Fourier Transform Infrared) spectrometer. They found, that the absorption spectrum of urea in the range between 5000 – 4000 cm^{-1} (λ = 2.0 – 2.5 μm) is relative strong and distinct from other components. In both cases, the results need to be validated.

Monitoring of Ionic Dialysance

Dialysance (*D*) is a measure of the magnitude of flux (leakiness) of a dialysis membrane as a function of the concentration of solute across the membrane. It is an indicator of how easy molecules will pass across a membrane from blood into the dialysis fluid. The measurement of the ionic dialysance provides an estimation of the urea clearance with good correlation (Mercadel *et al*, 1998; Petitclerc, 1999; Lindsay *et al*, 2001). Other authors suggest that the ionic dialysance may be equivalent to the effective urea clearance (urea clearance corrected for recirculation), however the topic remains controversial (Polaschegg, 1993; Manzoni *et al*, 1996; Di Filippo *et al*, 2001; Teruel *et al*, 2001).

For the measurement of the ionic dialysance, two conductivity probes are placed at the dialyser inlet and outlet (Manzoni *et al*, 1996; Petitclerc, 1999). The conductivity of a solution is a function of the concentration of the ionic substance and their electrical charges (Santoro *et al*, 2000). In other words, the difference between the two conductivity probes varies as a function of the ionic dialysance and thus the dialyser efficiency (Santoro *et al*, 2000). Hence, from the difference in the conductivity an indirect measurement of the effective dialysance can be obtained (Santoro *et al*, 2000).

A commercially available biosensor (Diascan^{TM}, Hospal, Italy) enables the on-line monitoring of HD based on ionic dialysance measurements (Levy *et al*, 2001; Teruel *et al*, 2001). Katopodis *et al* (2002) compared the Kt/V value with the Dt/V value, derived from ionic dialysance measurements for assessing the dialysis dose. The findings of this group are similar to those of Del Vecchio *et al* (1998), who found

that the Dt/V value is a suitable and promising parameter for quantifying the dialysis dose.

Monitoring of the nutritional status of Haemodialysis patients

The prevalence of protein/energy malnutrition is high in patients undergoing RRT (Wolfson and Strong, 1996; Kemp *et al*, 2001). It has been shown in several studies, that nutrition is as important as the quality of dialysis in determining the outcome (Laird, 1983; Mc Cusker *et al*, 1996).

Among many parameters indicating protein malnutrition, the most commonly used are serum albumin, dietary protein intake (indicated by PCR), creatinine and pre-dialysis serum urea nitrogen (Kopple, 1997; Qureshi *et al*, 1998).

The protein catabolic rate (PCR) is derived from the urea generation rate (G_U), which is calculated during UKM (equation 1.15). PCR is the amount of protein that the patient is catabolising per day. In a nutrionally stable dialysis patient (zero nitrogen balance) the PCR equals the dietary protein (Shak, 1999; Levy *et al*, 2001).

$$PCR = 6.25\ x\ [G_U + 1.81 + (0.031\ x\ m)] \qquad (1.15)$$

where G_U is the urea generation rate (g day^{-1}) and m is the lean body weight (kg).

The PCR is often normalised to the body weight (nPCR) (Levy *et al*, 2001). In nutritional stable patients the PCR is equal to the dietary protein intake (Shak, 1999). Patients with nPCR > 1.0 g $kg^{-1}day^{-1}$ can show a positive nitrogen balance and hence, a lower morbidity and mortality (Levy *et al*, 2001).

Creatinine is a routinely measured parameter and its production rate reflects the magnitude of the muscle mass (Bergström, 1997). In haemodialysis patients, high serum creatinine levels correlate with lower morbidity and mortality which may seem paradoxical but the higher creatinine reflects higher protein stores (muscle mass) and hence implies better overall nutritional status (Bergström, 1997; Olesberg *et al*, 2002). Almost all commercial available laboratory analysers are based on spectroscopic detection of the Jaffe reaction (Soldatkin *et al*, 2002). The reaction itself is not very specific and many substances present in blood such as glucose, pyruvate can interfere (Soldatkin *et al*, 2002).

A promising step towards the on-line measurement of creatinine is the progress in the development of creatinine – selective biosensors (Soldatkin *et al*, 2002). Several different types of sensors were developed. They can be divided into two main groups, namely amperometric – based sensors (Schneider *et al*, 1996; Kahn and Wernet, 1991) and potentiometric – based sensors (Campanella *et al*, 1990; Narinesingh *et al*, 1991). Soldatkin *et al* (2002) presented a new type of creatinine – selective biosensor. This sensor is based on ion-sensitive field – effect transistors (ISFET) coated with creatinine deiminase. The results are promising but more work need to be done before the sensor can be implemented into routine monitoring of HD (Soldatkin *et al*, 2002).

1.8.6 URAEMIA AND URAEMIC TOXINS

The uraemic syndrome, one of the main consequences of CRF is attributed to the retention of a number of different molecules, collectively termed uraemic toxins. However, the toxicity of the syndrome has not been attributed to any single

compound; it is most likely to be due to a spectrum of compounds, and indeed the list of potential candidates is complex and growing, and now numbers over 90 (Bergström, 1997; Vanholder *et al*, 2003). Their molecular weight, and degree of protein binding have largely defined the categorisation of these retained compounds in renal failure. They comprise a) small water-soluble compounds, MW < 500Da, b) protein bound solutes, and c) 'middle molecules' MW >500Da. Which compounds exert a toxic effect within the body, and which accumulate innocently, is currently not known with certainty (Vanholder *et al*, 2003).

Uraemic toxicity has been studied for several years. Indirect evidence has been obtained from bioassay studies *in vivo* and *in vitro* (Bergström, 1997). Substances known to be present in an elevated concentration in uraemic serum have been given to humans or experimental animals, or added to tissues, cells, or enzymes *in vitro* to prove whether they exert toxic effects (Bergström, 1997). It has been observed that after infusion of plasma, serum, ultrafiltrate or dialysate of uraemic patients into animals, several biological processes are affected (Bergström, 1997).

Patel and co-workers (1994) found that infusion of uraemic ultrafiltrate to normal rats results in a decreased number of intestinal calcitriol receptors and an increase of receptor mRNA concentration. Whereas uraemic serum inhibits *in vitro* erythropoiesis (Kuroyanagi and Saito, 1966), fibroblast growth (Mc Dermott, 1971), natural killer cell activity (Asaka *et al*, 1988), mononuclear phagocyte function (Wessel-Aas, 1981) as well as platelet function (Bergström, 1997).

The characterisation of the specific toxins that may be responsible for the uraemic symptom has been evolving over the years and so has the application of these ideas into general clinical practice (Vanholder *et al*, 1994). Initially, small molecules (e.g.

urea and creatinine) were held responsible for causing the uraemic syndrome. In the period between 1965 and 1975 a new group of pathobiological active substances were discovered, the so-called middle-molecules (Bergström, 1997). This discovery is based on the observation of Scribner and his group, who found that CAPD is superior to HD in the management of uraemic neuropathy. The peritoneal membrane is more effective at removing middle molecules than a dialysis membrane presumably due to the difference in the pore size of the membrane. (Bergström, 1997).

The composition of the middle molecule fraction is chemically diverse. Different authors reported the presence of peptides, oligosaccharides, organic acids, alcohols, and derivates of glucuronic acid (Le Moel *et al*, 1980, Zimmermann *et al*, 1980; Vanholder *et al*, 1994; Henderson *et al*, 2001). However, the main attention was directed to the peptides, which were thought to be the primary cause of endogenous intoxication signs in the organism (Zimmermann *et al*, 1980; Kovalishin, 1987) Among the many effects caused by peptides are the following: neurotoxicity (Kumegawa *et al*, 1980), cardiotoxicity (Bernard *et al*, 1982), inhibition of platelet aggregation (Bazilinski *et al*, 1985), inhibition of protein synthesis and amino acid transport (Cernacek *et al*, 1982), polymerisation of tubulin (Brauger *et al*, 1983) and the inhibition of various enzymes such as lactate dehydrogenase (Lutz *et al*, 1974), adenylate cyclase (Cloix *et al*, 1976), catalase (Leber *et al*, 1980) and acetylcholinesterase (Smolenski *et al*, 1993).

With improved analytical techniques, it has become evident that several presumed middle molecules are in fact heterogeneous mixtures containing numerous lower molecular weight compounds (Vanholder *et al*, 1994), but these molecules behave like middle molecules during HD, due to steric configuration, electrostatic charge,

lipophilicity and multicompartmental behaviour (Vanholder *et al*, 1994; Bergström, 1997).

A selection of major "small", "middle" and "large" molecules found in uraemic blood are summarised in Table 1.6 (Vanholder *et al*, 2003).

Table 1.6: Established and Suspected (*) Uraemic Toxins.

Small Molecules		**Middle and Large Molecules**
Urea, Uric acid	Oxalate	Advanced glycosylated end products (*)
Creatinine	Myoinositol (*)	Parathormone (PTH)
Guanidine Derivates	Phenols	
Methylguanidine		β_2-microglobulin
Guanidinosuccinic acid	Magnesium	
Pyrimidine Derivates	Sodium	Peptides
Pseudouridine		Beta-endorphin
Orotic acid	Water	Methionine-enkephalin
Orotidine, Uridine		Granulocyte inhibiting protein I and II (*)
	Amines	Degranulation-inhibiting protein (*)
	Methylamine	
Purines	Tyramine	**Protein bound**
Uric acid	Putrescine	Indoles and Indoxyl sulphate
Xanthine, Hypoxanthine	Spermidine	Hippuric acid, P-cresol
Guanosine		
Indoxyl Sulphate	Hydrogen ions	Homocysteine, Polyamines

The uraemic syndrome itself comprises a wide variety of signs and symptoms (Hörl, 1998) including neuropathy, encephalopathy, hypertension and cardiomyopathy (Smogorzewski and Massry, 1997). Several identified (and yet unidentified) uraemic toxins are at least partially removed by HD which may result in an improvement of the many clinical signs and symptoms (Hörl, 1998; Dhonth *et al*, 2000).

1.9 PULMONARY TUBERCULOSIS

Pulmonary tuberculosis (TB) is a notifiable infectious disease affecting the lungs of humans, and certain mammals such as cattle and badgers. In humans, pulmonary TB is caused by *Mycobacterium tuberculosis.* In 1993, the World Health Organisation (WHO) declared TB a global emergency (Dolin *et al*, 1994). There are yearly an estimated 8 – 9 million new case, killing nearly 2 million people each year (Frieden *et al*, 2003). The majority of these new cases occur in sub-Saharan Africa, South and Southeast Asia, Latin America and the former Soviet Union (Raviglione *et al*, 1992; Raviglione *et al*, 1995; Frieden *et al*, 2003). In contrast, case numbers in the past have continuously declined in Western and Central Europe, North and South America (Frieden *et al*, 2003). Nevertheless, a global increase of TB is observable. The reasons, however, depend strongly on the country/region. In Africa, the increase is mainly caused as a result of the burden of HIV infection, and in the former Soviet Union due to socio-economic change and decline of the health care system (Raviglione *et al*, 1995; Shilova and Dye, 2001). Immigration and increased travel are the main reasons for the remaining prevalence in the western world (Rieder *et al*, 1994).

1.9.1 PATHOPYSIOLOGY OF PULMONARY TUBERCULOSIS

TB is spread by airborne droplets, particles of 1 – 5 μm diameter, which contain *M. tuberculosis*. Due to their small size, these particles can remain airborne for hours after expectoration by infected patients through coughing, sneezing or talking (Riley *et al*, 1959; Louden and Roberts, 1966).

The infectious droplets are inhaled and stay in the alveoli of the lung. *M. tuberculosis* is taken up by alveolar macrophages initiating a cascade of events

resulting either in successful containment or progression to active TB (Woolf, 2000). *M. tuberculosis* is able to replicate slowly but continuously inside macrophages. Cell-mediated immunity occurs in most individual within 8 weeks after infection. Alveolar macrophages infected with the organism interact with T-lymphocytes via several cytokines. The released cytokines (especially IL 12 and IL 18) stimulate T lymphocytes (predominantly CD4-positive T lymphocytes) to produce interferon-γ (Schluger and Rom, 1998). Interferon- γ, in turn, stimulates the phagocytosis of *M. tuberculosis* in the macrophage. However, interferon-γ does not directly stimulate the killing of the organism but is important in the control of the infection via the stimulation of the macrophage to release tumour necrosis factor α (TNF-α). TNF, in turn, plays a key factor in the formation of a granuloma. The T-lymphocyte response is specific (Flynn *et al*, 1999).

When the host immune response cannot inhibit the replication of *M. tuberculosis* associated with the initial infection, active disease occurs (Frieden *et al*, 2003). This progression is most common in young children (under 5 years of age) and adults with severe immunosuppression (e.g. AIDS/HIV). Primary tuberculosis can affect almost every organ of the human body, but predominantly the lungs.

1.9.2 CURRENT DIAGNOSTIC TOOLS FOR PULMONARY TUBERCULOSIS

Rapid and accurate diagnosis of symptomatic patients is a cornerstone of the global tuberculosis control strategy. Diagnostic tests for TB can be divided into direct and indirect methods (Figure 1.13). Direct methods are based on the detection of the causative bacilli (*M. tuberculosis*) or their product including chromatographic methods or immunoassays. Indirect methods measure either the specific host immune

response (anti-mycobacterial antibodies) or the cellular response (skin test or lymphocyte stimulation assays).

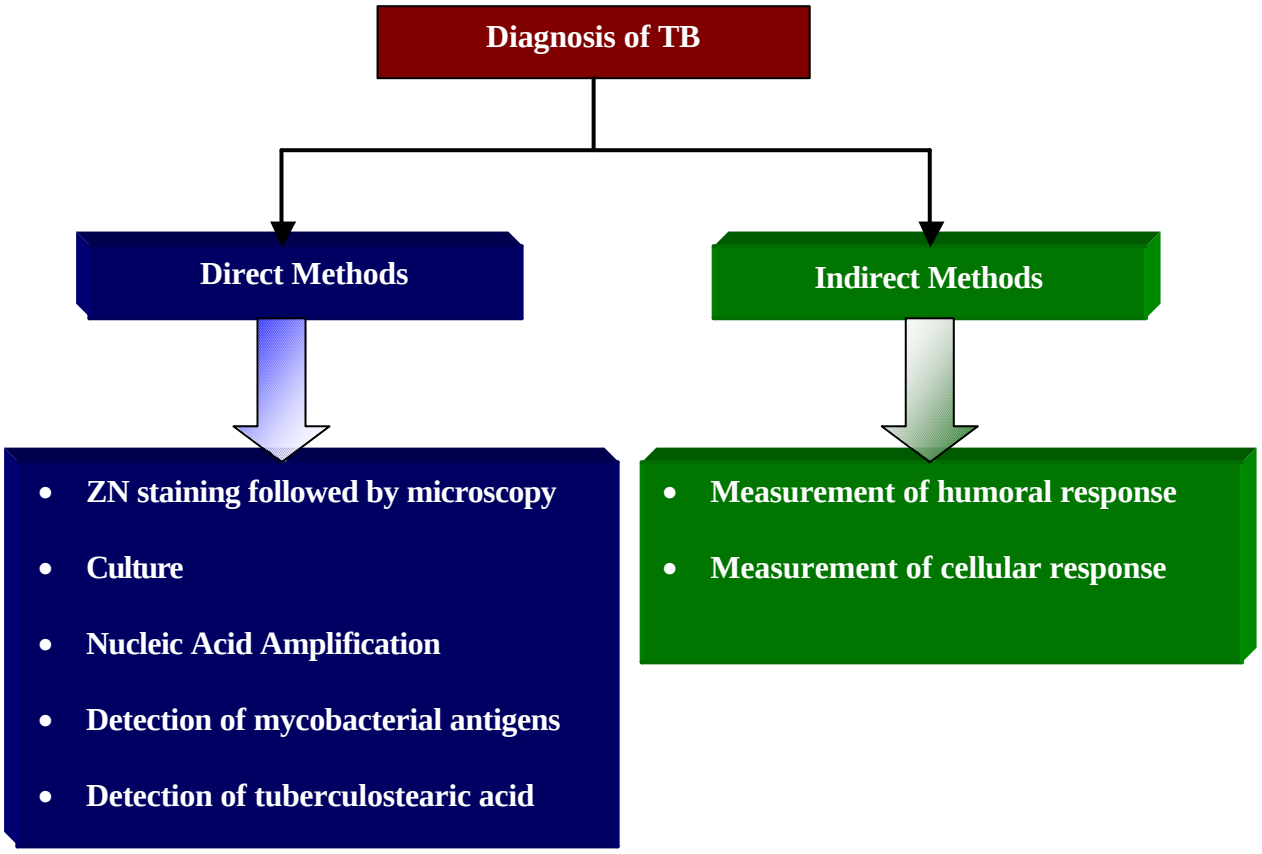

Figure 1.13: Overview of current diagnostic tests for pulmonary tuberculosis.

Direct methods for the diagnosis of pulmonary tuberculosis

Microscopy

Robert Koch was the first who isolated the tubercle bacilli in 1882. In the same year, a simple staining procedure was developed by Ziehl and later modified by Neelsen. The method is based on the staining of *Mycobacteria* in a sputum smear followed by direct microscopic examination. The method is based on the stability of mycobacteria towards acids: the bacteria withstand the acidic decolourisation step during the staining procedure.

A positive ZN (smear-positive), however, is only an indicator for the presence of mycobacteria in sputum, but is no definite diagnosis for pulmonary TB. Sputum microscopy for acid-fast-bacilli (AFB) is recommended by the WHO and IUATLD as the most appropriate technique for case finding especially in high-prevalence countries. Nevertheless, about 40 – 60 % of patients with pulmonary TB and up to 75% of extra-pulmonary cases remain undiagnosed by this method (Garg *et al*, 2003).

Culture

Culture is still widely accepted as the "gold standard" for the diagnosis of TB. In the past, solid media were used for the isolation of *M. tuberculosis*. The main disadvantage of this method is the slow growth rate of mycobacteria resulting in incubation periods ranging from three weeks (AFB positive) to eight weeks (AFB negative). Traditional solid media are either egg-based (e.g. Löwenstein-Jensen) or agar-based media (e.g. Middlebrook 7H10 or 7H11). The most common used liquid media are the Middlebrook 7H9 or 7H12 broth. Over the years, culture systems have

been improved to reduce the incubation period. These improvements were achieved by combing mild specimen decontamination, antibiotics, liquid media and growth indicators (Kolk, personal communications). Nowadays, automated systems are available to detect the bacterial growth. The BACTEC 460 (Becton Dickinson Instrument Systems, Sparks, MD, USA) is a radiometric system based on the production of radioactive carbon dioxide ($^{14}CO_2$) by growing bacteria. Bacteria convert ^{14}C-labelled palmitic acid present in Middlebrook 7H12 broth into radioactive carbon dioxide (Garg *et al*, 2003). The mean detection time of the radiometric system for *mycobacteria* is 13 days, which in turn means a dramatic time reduction compared to traditional culture (Roggenkamp *et al*., 1999). The second commercial available automated culture system is the BacT/Alert instrument (BioMerieux, Marcy-l'Etoile, France). The BacT/Alert utilises a colorimetric sensor to continuously monitor the production of CO_2 concentration in the culture medium. The sensor placed at the bottom of the culture tube changes its colour in the presence of mycobacteria from dark green to yellow. The specificity and sensitivity of the BacT/Alert is comparable to the radiometric system (Brunello *et al*, 1999; Palacios *et al*, 1999).

Traditionally the identification of mycobacteria cultured on conventional solid media was based on growth characteristics or biochemical properties such as growth rate, colony morphology and pigmentation, niacin production, catalase test. New identification methods include specific DNA probes or polymerase chain reaction. DNA probes have been developed to identify *M. tuberculosis*, *M. avium*, *M. kansaii*, *M. intracellulare*, and *M. gordonae* directly in broth or solid culture (Ichiyama *et al*, 1997; Badak *et al*., 1999).

Nucleic acid amplification

Nucleic acid amplification techniques include polymerase chain reaction (PCR), strand displacement amplification (SDA) (Walker *et al*, 1992) and transcription-mediated amplification (TMA) (Jacobs *et al*, 1993). These techniques are based on the detection of mycobacterial DNA or RNA in clinical specimens. PCR technique uses oligonucleotide primers to direct the amplification of target nucleic acid sequences via a three-step process: denaturation, primer annealing, and primer extension (Mullis *et al*, 1987).

The most commonly used target in "home-made" tests is IS*6110*, a specific sequence for bacterial strains belonging to the *M. tuberculosis* complex (Kolk *et al*, 1992, Kox *et al*. 1994). PCR is an important tool for the diagnosis of extrapulmonary TB but also valuable for the diagnosis of pulmonary TB. The sensitivity of PCR in extra-pulmonary TB is lower than for pulmonary TB. Nevertheless, in modern laboratories PCR on cerebrospinal fluid is the method of choice for the detection of tuberculosis meningitis (Nguyen *et al*, 1996).

Several commercial nucleic acid amplification kits are available. The AMPLICOR MTB assay (Roche Diagnostic System, Based, CH) is based on the amplification of the 16s rDNA sequence followed by hybridisation with a *M. tuberculosis* complex specific capture probe. The AMTD assay from Gen-Probe (Gen-Probe Inc San Diego, CA, USA) combines the amplification of rRNA and detection with an acridinium ester-labelled DNA probe specific for *M. tuberculosis* complex. PCR procedures are nowadays widely used in microbiological laboratories. Nevertheless, the high costs and required expertise have limited the implementation of

these methods as routine tests for TB in high burden countries (Ross *et al*, 1998) but also in the Western world (Doern, 1996).

Detection of mycobacterial antigens

Mycobacterial detection assays were largely developed 20 years ago but still need to prove their value in a routine laboratory. Sada *et al* (1983) develop an enzyme-linked immunosorbent assay (ELISA) for the detection of mycobacterial antigens in cerebrospinal fluid for patients with tuberculous meningitis. A few "defined" antigens have been identified for the detection of TB. Among these, are the Antigen 5 and a 45/47 kDa protein complex. Antigen 5, a 38 kDa protein is excreted by growing mycobacteria found in serum (Radhakrishnan *et al*, 1992), cerebrospinal fluid (Radhakrishnan *et al*, 1991) or bronchoalveolar lavage fluid (Raja *et al*, 1988). The 45/47 kDa protein complex is immunodominant and is excreted by growing mycobacteria. Chanteau *et al* (2000) developed an ELISA for the detection of this protein complex in sputum and serum. The sandwich ELISA is based on a polyclonal capture antibody and a mixture of three monoclonal antibodies as secondary antibodies.

Another interesting antigen is lipoarabinomannan (LAM), an immunodominant lipopolysaccharide with a molecular weight between 30 and 40 kDa. LAM is a major cell wall component of mycobacteria. LAM has been detected in serum (Sada *et al*, 1992), sputum (Pereira *et al*, 2000) and cerebrospinal fluid (Chandramuki *et al*, 1985) using different ELISA formats. None of these tests have been properly validated.

Detection of tuberculostearic acid

One easily detectable marker of *M. tuberculosis* is tuberculostearic acid (TBSA), which can be detected by liquid chromatography (Garg *et al*, 2003). TBSA is a lipid component present in the mycobacterial cell wall. It can be detected in clinical samples using liquid chromatography or gas chromatography – mass spectroscopy. The presence of TBSA in cerebrospinal fluid is thought to be a marker for tuberculous meningitis (Brooks *et al*, 1990) and in sputum for pulmonary TB (French *et al*, 1987). Organisms other than *M. tuberculosis* present in pulmonary specimens can generate false-positive results (Garg *et al*, 2003).

Indirect methods for the diagnosis of pulmonary tuberculosis

Measurement of the humoral response

The measurement of the humoral response is based on the detection of specific anti-mycobacterial antibodies. Arloing first described the idea of serodiagnosis of TB in 1898. Since then, many reports describing new methods have been published. In the past, the majority of tests were made with crude mycobacterial preparations and therefore lacking in specificity (Verbon *et al*, 1990). The use of purified antigens has improved the serodiagnostic tests in terms of specificity (Jacket *et al*, 1988). Nevertheless, the sensitivity of antibodies to single antigens is 75% at best, even in patients with smear-positive pulmonary TB (Bothamley, 1995).

Examples of purified antigens are the 38 kDa protein , 30/31 kDa protein, and several heat shock proteins such as 14 kDa, 65 kDa and 70 kDa proteins (Garg *et al*,

2003). Over-expression of recombinant proteins, e.g. the 38 kDa protein in *E. coli* has dramatically simplified the production of antigens (Wilkinson *et al*, 1997).

The diagnostic antigen of choice is currently the 38 kDa protein (Garg *et al*, 2003). This protein was evaluated in an ELISA by Bothamley *et al* (1992). In smear-positive TB patients a sensitivity and specificity of 85% and 97%, respectively was achieved. However, the sensitivity in smear-negative patients was with 15% dramatically lower.

Commercially available serological kits are based on the detection of antibodies against lipoarabinomannan (LAM) (MycoDot^{TM} assay, Genelabs, Geneve, CH) or the 38 kDa protein (ICT Diagnostics, Sydney, Australia). Both tests lack sensitivity when properly evaluated (Perkins, 2000).

Measurement of the cellular response

The Mantoux test is by far the most frequently used test in the history of TB diagnosis. A purified protein derivative (PPD) is used as a skin test reagent for measuring the delayed hypersensitivity reaction of a patient or infected person. PPD contains many mycobacterial antigens, not all of them belong to the *M. tuberculosis* complex. A positive test may be caused by active TB, past infection, BCG vaccination or through environmental mycobacteria (Garg *et al*, 2003). Recently, a recombinant antigen encoded by a gene specific to the *M. tuberculosis* complex replaced the PPD. It showed better results leading to increased diagnostic value of the Mantoux test (Garg *et al*., 2003).

Recently, the gamma interferon (IFN-γ) assay was evaluated as a potential replacement of the Mantoux test. The IFN-γ test is comparable to the Mantoux test in

terms of sensitivity and specificity. However, it requires better-equipped laboratories to culture viable lymphocytes and an ELISA to quantify IFN-γ (Garg *et al*, 2003).

1.9.3 DIAGNOSTIC NEEDS OF LOW AND HIGH PREVALENCE COUNTRIES

The diagnostic pathway for pulmonary TB depends strongly on the setting, i.e. on the available resources. The usefulness of a test depends not only on specificity and sensitivity but also on factors given in by local circumstances such as costs, available laboratory facilities and skills of technicians.

Low-income countries are often characterised by high TB prevalence and poor laboratory facilities. The only means of diagnosis TB is the ZN stain followed by microscopic examination. In these endemic regions, the result has to be obtained quickly before patients disappear and no adequate treatment is possible. Since the prevalence is high, the identification of the causative mycobacterium is often not required. In TB endemic areas, infection with non-tuberculous mycobacteria remains uncommon and therefore the positive predictive value of AFB microscopy is high. Nevertheless, new tests are urgently needed to directly replace microscopy and culture (Perkins, 2000).

The situation in developed countries is different. The low prevalence and the well-equipped laboratories allow a definite diagnosis of TB. Identification of the infecting mycobacterium and drug-susceptibility testing is routine. The diagnostic needs for low prevalence countries are those in support of the elimination of TB and include tests for the identification of latent infections, the detection of TB in immigrants or other high risk groups, the identification of outbreaks and

characterisation of transmission, and the discrimination between *M. tuberculosis* and other non-tuberculous species (Perkins, 2000).

The WHO recommends the following specifications for a new diagnostic test for developing countries:

- Detection limit $\leq 10^4$ AFB ml^{-1} sputum
- Sensitivity of 85 % compared to culture
- Specificity of 95 % compared to culture
- Require less than 15 minutes preparation time
- Long shelf-life (> 6 months)
- Cost-effectiveness
- Simple and robust

1.10 AIMS AND OBJECTIVES

This thesis is divided into two parts. In the first part, the potential of an electronic nose as a monitoring tool for haemodialysis is investigated (non-infectious application). In the second part, the electronic nose is applied as an early detection system for pulmonary tuberculosis (infectious disease).

1.10.1 AIM

To evaluate the potential of electronic nose technology in point-of-care human diseases management: Studies in renal diseases and tuberculosis.

1.10.2 OBJECTIVES FOR THE MANAGEMENT OF RENAL FAILURE

- To find the optimal sample incubation parameters including incubation temperature and time as well as the minimal sample volume for uraemic blood samples.
- To determine the maximal dilution for uraemic blood samples which allow discrimination between pre- and post-dialysis samples.
- To evaluate the sensor reproducibility towards uraemic blood samples.
- To study the influence of urea and creatinine on the sensor response.
- To evaluate the long term stability of the electronic nose towards uraemic blood samples.
- To evaluate the volatile shift occurring during a single haemodialysis session in both blood and dialysate.
- To compare the electronic nose pattern with traditional biochemical markers

1.10.3 OBJECTIVES FOR THE EARLY DIAGNOSIS OF PULMONARY TUBERCULOSIS

- To investigate the potential of an electronic nose to discriminate between different *Mycobacterium spp*. and *Pseudomonas aeruginosa* in both culture and sputum.
- To determine the detection limit of the electronic nose for *M. tuberculosis* in both culture and sputum.
- To investigate the influence of dead *M. tuberculosis* bacteria on the sensor response.

- To determine the specificity and sensitivity of the electronic nose for *M. tuberculosis* in sputum.

1.11 OUTLINE OF THE THESIS

Chapter 2 describes the general materials and methods used throughout the report. However, to keep a certain structure and clearness, the specific methods including sample procurement and sample preparation are described in Chapter 3 and 4.

Chapter 3 describes the development of an electronic nose protocol for the management of haemodialysis. It also includes specific materials and methods.

Chapter 4 describes the application of an electronic nose as a diagnostic tool for pulmonary tuberculosis. It also contains specific materials and methods.

Chapters 5 and *6* set the results presented in this thesis in perspective to current diagnostic practise and also discuss their implications in the future. It also describes which steps need to be addressed to make electronic nose technology a modern diagnostic instrument.

Chapter 2

General

Materials and Methods

2.1 ETHICAL APPROVAL

Ethical approval for this study was obtained either from the Gloucestershire Research Ethics Committee (Study No's: 01/149G; 03/44G) or from the ethics committee of the Academic Medical Centre (Amsterdam, The Netherlands) (Study No: MEC98/034). All patients and volunteers participating in this study gave informed written consent before samples were taken after oral and written information was provided. Each sample was encoded to ensure anonymity (Appendix A.1 and A.2).

2.2 GAS-SENSING SYSTEM

2.2.1 GAS SENSING SYSTEM AND HEADSPACE ANALYSIS

The electronic nose (Bloodhound BH-114, Bloodhound Sensors, Leeds, UK) used in this study employed 14 conducting polymer sensors (Appendix B.1). The BH114 instrument consists of a fully integrated sampling system with the sensor array and hardware controlled by proprietary Windows based software, which also incorporates data collection and processing software.

The sensor unit automatically sets two calibration points. The first one is the baseline, which is obtained when activated carbon filtered (Carbon Cap 150, Whatman, UK) air is passed over the sensor (purple arrow, Figure 3.1) at a flow rate of 4 ml min^{-1}. The second calibration point is a reference point obtained from the headspace of a control sample vial containing 9 ml of reverse osmosis (RO) -water (blue arrow) (Figure 2.1). The interaction of the volatile compounds and the conducting polymer surface produces a change in resistance, which is measured and

subsequently displayed on the computer screen.

For the analysis of the sample headspace, the sample vials were connected to the electronic nose by inserting a needle into the headspace of the sample vials (Figure 3.1). The unknown headspace is passed over the sensor surface (red arrow, Figure 3.1) at a flow rate of 200 ml min^{-1}, which was automatically set by the sensor unit. Between each measurement, a time delay of 2 minutes was set. The individual samples were analysed in a random order.

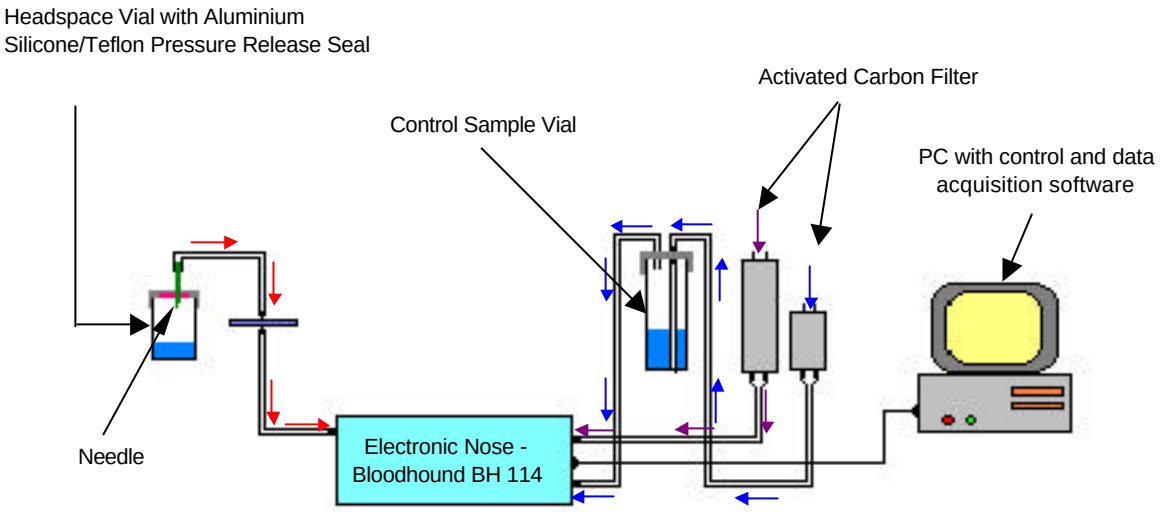

Figure 2.1: Overview of idealised electronic-nose configuration. The set-up consists of the electronic nose sensor array, a sample and a control vial as well as two activated carbon filters and a HEPA-Vent filter. The carbon filters ensure an odourless airflow over the sensor surface and control and sample headspace, whereas the HEPA-VENT filter prevents the fouling of the sensor surface. The electronic nose is connected to a PC running the control software and an appropriate data analysis package.

2.2.2 EXPERIMENTAL PARAMETERS FOR ELECTRONIC NOSE

The adjustable sampling profile consists of five parameters: time delay, adsorption time, baseline length, desorption time, and hold time. The sampling profiles used in this report were set according to Table 2.1.

Table 2.1: Sample profiles used in this report.

	Samples			
	Blood	**Dialysate**	**Culture**	**Sputum**
Time delay (s)	5	5	5	5
Adsorption time (s)	10	10	6	7
Desorption time (s)	15	15	14	21
Baseline length (s)	5	5	5	5
Hold time (s)	0	0	0	0

2.3 DATA ANALYSES AND PATTERN RECOGNITION

To analyse the electronic nose data, two Excel add-in software programs were employed. Principal component analysis, hierarchical cluster analysis, and discriminant function analysis was performed using *XL*stat (*XL*stat©, version 3.4, France) and for the neural network analysis the program Neuralyst™ (version 1.4, Cheshire Engineering Corporation, Pasadena, CA, USA) was used.

2.3.1 SENSOR PARAMETERS

Figure 2.2 displays a typical sensor response to a sample headspace taken over time. The parameters extracted from the sensor response are as follows:

A. Maximum step response (divergence)

B. Maximum adsorption

C. Maximum desorption

D. Ratio between adsorption and desorption

E. Area under the curve (Langmuir adsorption spectrum)

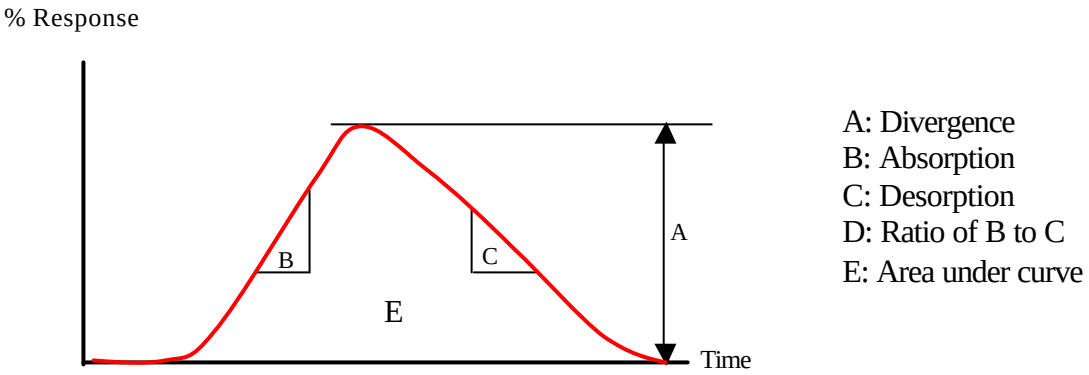

Figure 2.2: A typical sensor response to a sample headspace with the extractable sensor parameters.

However, only two parameters, namely the maximum sensor response and the area under the curve showed good reproducibility and were therefore considered in the data analysis.

2.3.2 PATTERN RECOGNITION

Throughout this report, a common structure for pattern recognition was applied. Figure 2.3 illustrates the two different idealised pathways employed. The normalised/non-normalised raw data were either used as input variables for PCA or ANN. The principal components had a central position and were input variables for DFA and HCA

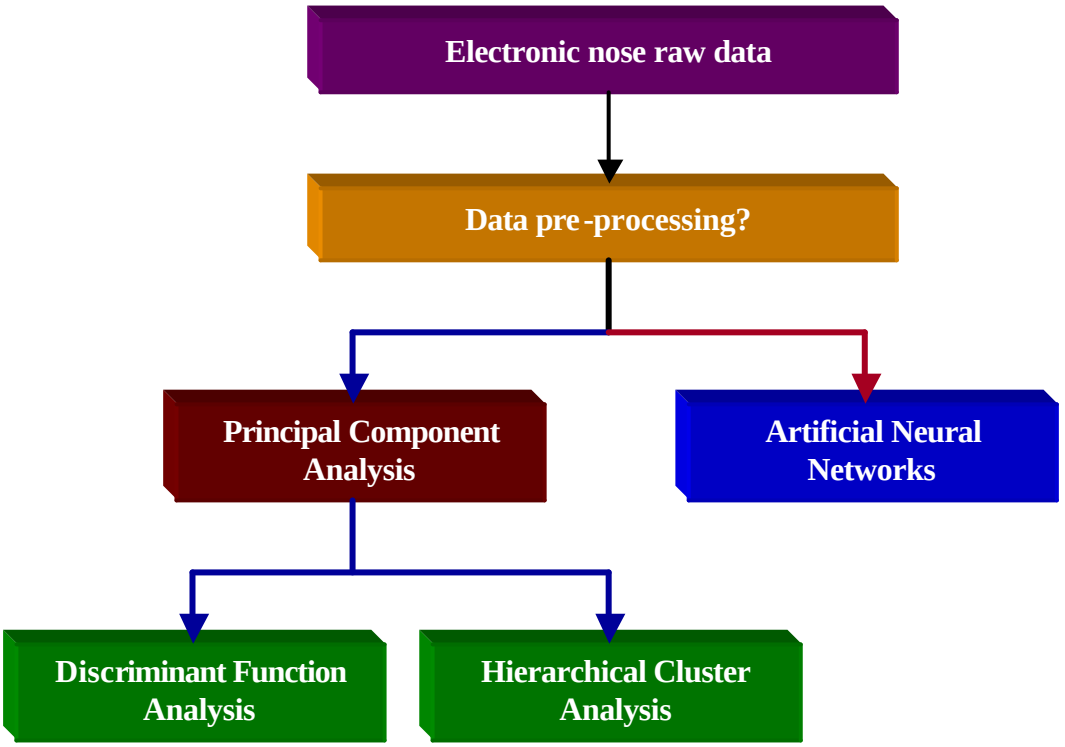

Figure 2.3: Schematic illustration of the data analysis pathways. The blue pathway indicates the central position of PCA (red box). PCs were used as input variables for DFA and HCA (green boxes). In contrast, artificial neural networks were built directly on the pre-processed data matrix (red pathway).

Data pre-processing

The raw data were under circumstances pre-processed to improve the quality of the input data. The method of choice was normalization to vector length one (see equation 1.1). This step was only possible, where no quantitative information was required to solve the discrimination problem.

Principal Component Analysis (PCA)

PCA represents the central point, whereby the principal components were utilized in two separate ways. On one side, they were used to reveal hidden structures (relationships) within the input matrix (score plot), and on the other side, they were used as input variables for DFA and HCA.

However, not all principal components (PC) were used as input variables for the subsequent methods. The number of PCs was determined by the Kaiser criterion, which states, that only principal components with an eigenvector greater or equal than 1 are significant (Jackson, 1991). Applying this rule implicates that approximately 90 – 95 % of the variance (information) of the original data matrix is used for subsequent methods.

Hierarchical Cluster Analysis (HCA)

HCA was used to calculate the distance between individual samples. The result is displayed as clusters of related samples. The initial distance matrix, i.e. the distance between principal components was calculated using the Euclidean distance. The Ward's method was used to aggregate individual sub-clusters. The key idea of this

method is to aggregate clusters in such a way that a minimum increase in the within-group error sum of squares results (Otto, 1999). Two individual clusters were considered significantly different when the distance between them exceeds the 95 % confidence interval (p=0.05) (indicated by the dashed line in dendrograms).

Discriminant Function Analysis (DFA)

DFA, a classification method, was applied to assign unknown samples to one of the pre-defined classes. The model itself was built on a sub-set of the original data and validated with the remaining (unknown) samples. To validate the model, the variables of the withheld samples were inserted into the discriminant functions (obtained during the training period) and subsequently assigned to that class for which its centroid has the smallest Euclidean distance to the unknown sample (Otto, 1999).

Artificial Neural Network (ANN)

The ANN was trained using the backpropagation algorithm with a sigmoid transfer function. The original data set was divided into two groups: the training and the test data set.

Approximately 70 % of the original data were randomly selected and used to train the ANN. The remaining 30 % of the data were used to evaluate the performance of the ANN.

Optimisation of the ANN – Genetic supervisor

To find the optimal network architecture and parameters, a genetic algorithm was applied (genetic supervisor). The key characteristic of a genetic supervisor (GS) is to improve the learning and therefore the discriminatory performance of the neural network. The genetic supervisor optimises the input columns (variables), the configuration, and the network parameters so that the final ANN will perform well as a successful model with a minimum amount of training. Each ANN solution is described by a structure composed of three strings, whereby the strings represent the selection of input variables, ANN configuration, and the ANN parameters (Figure 2.4).

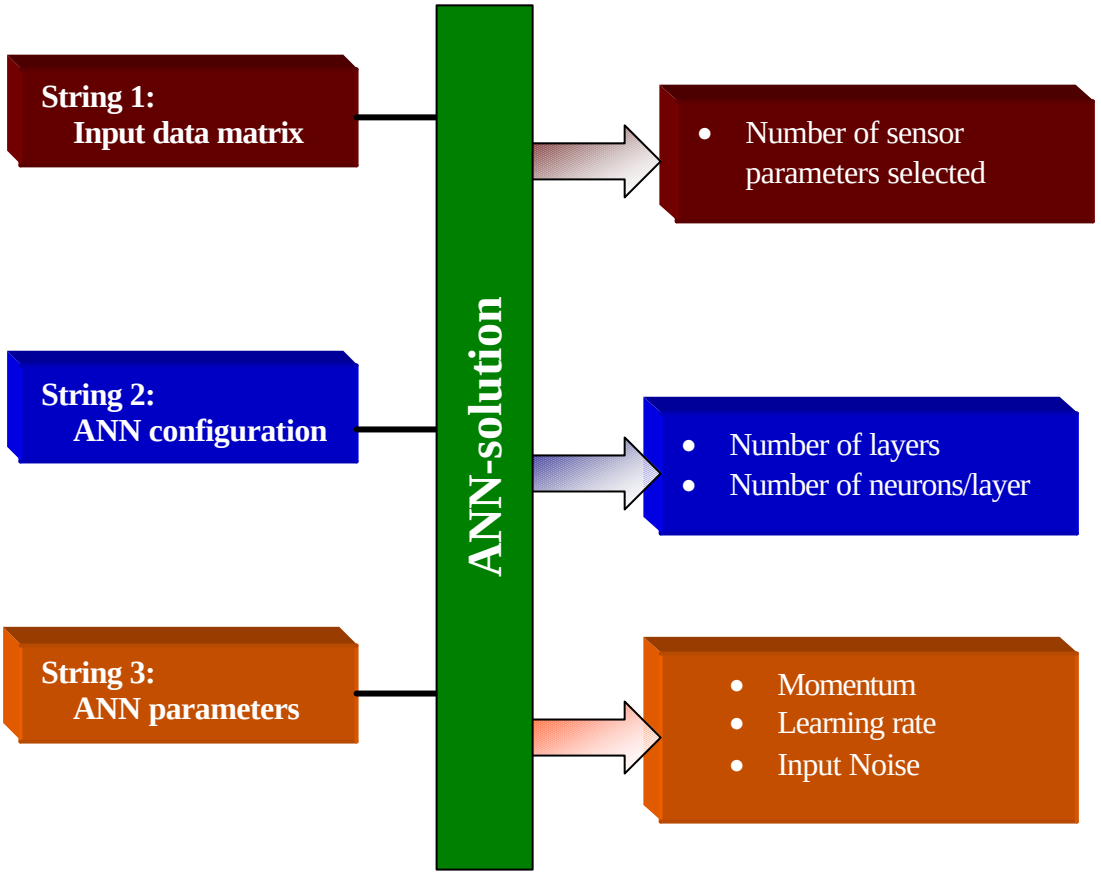

Figure 2.4: Graphic illustration of a single network solution.

String 1 – Input data selection (data matrix): Each sensor parameter is treated separately, i.e. the GS can exclude or include individual parameters to obtain the optimal input data. The inclusion rate determines, how many of the original variables have to be included in the final ANN architecture.

String 2 – ANN configuration: The number of inputs and outputs defined for each ANN solution automatically determines the first and last layer of each neural network. The number of inputs is determined by string 1, and the user defines the number of outputs. The number of outputs is usually equal to the number of different odour classes. It is up to the GS to determine the optimal number of hidden layers and for the optimal number of neurons per layer.

String 3 – ANN parameters: The ANN parameters (momentum, learning rate, and input noise) predominantly control the training behaviour of the neural network. The learning rate applies an amount of correction as a result of the error derived form a given case. The moment averages the current error to a greater or lesser extend with previous errors.

The GS looks for the optimised ANN architecture by selecting input variables, varying the configuration and parameters. Each of the resulting structures is then evaluated in terms of neural network fitness. The network fitness is normally evaluated by calculating the error between ANN output and target output. The optimised neural network is characterised by the smallest error and used ready for training (Shih, 1994).

The following parameters were used for the genetic supervisor.

- Inclusion rate: 75 %
- Momentum: 1
- Learning rate: 0.5
- Input Noise: 0.03

Chapter 3

Electronic Nose in Renal Medicine

3.1 INTRODUCTION

An ever-increasing number of patients have to undergo regular renal dialysis to compensate for acute or chronic renal failure. The estimated annual rate of patients starting renal replacement therapy (RRT) for end stage renal failure in England and Wales is 101 per million population indicating that approximately 5940 patients started RRT in 2002 (UK Renal Registry Report, 2003). Approximately 800,000 patients with end stage renal disease (ESRD) are currently alive throughout the world while being treated with various modes of regular treatment, haemodialysis being the predominant form of RRT (Tetta *et al*, 1999; UK Renal Registry Report, 2003). The annual growth rate of ESRD patients is estimated to be about 9% worldwide (Tetta *et al*, 1999).

Data from renal registries have shown that the average age of patients newly admitted to RRT show a steady increase being now closely to 65 years of age (UK Renal Registry Report, 2003). Such an elderly population shows a variety of co-morbid conditions such as cardiovascular disease or atherosclerosis (Tetta *et al*, 1999; Movilli, 1999). Cardiovascular complications account for 50 – 60 % of all deaths among ESRD patients (Nourooz-Zadeh, 1999). Despite significant improvements achieved in dialysis technology, there is substantially no evidence for a decrease in the prevalence of cardiovascular diseases or amyloidosis during the last decade (Tetta *et al*, 1999; Canaud *et al*, 1999; Levy *et al*, 2001).

The uraemic syndrome is attributed to the retention of a number of different molecules, collectively termed uraemic toxins. However, the toxicity of the syndrome has not been attributed to any single compound; it is most likely to be due to a spectrum of compounds, and indeed the list of potential candidates is complex and

growing, and now numbers over 90 (Bergström, 1997). Which compounds exert a toxic effect within the body, and which accumulate innocently, is currently not known with certainty (Vanholder *et al*, 2003).

Our current approach to the dialytic management of ESRF is to employ urea as a surrogate marker for retained solutes and toxins, and to model the quantity of treatment upon its removal from the body. Urea as such is generally not a particularly toxic compound, and designing treatment strategies using more biologically relevant compounds would be more appropriate, however defining these compounds is problematic (Vanholder *et al*, 1994).

An alternative approach would be to gain information about a wide spectrum of compounds that accumulate in renal failure, and apply the knowledge of changes in the pattern of these compounds to devise and monitor treatment strategies. We have employed the electronic nose (EN) to provide such information.

3.2 SPECIFIC MATERIALS AND METHODS

3.2.1 STUDY DESIGN

The study was divided into four parts to optimise and evaluate the sensor response of the electronic nose to pre and post dialysis blood, and to dialysate samples, from haemodialysis (HD) patients, and to compare responses to blood samples from normal controls (Figure 3.1).

The first part was aimed to find the optimal conditions for the sample pre-treatment to obtain a sufficient sensor response allowing discrimination between pre- and post –dialysis blood. The first part of this study was further divided into four steps

(Figure 3.2). The experimental model obtained from part I was then validated (part II) and finally the performance evaluated in terms of long-term performance and ability to follow the dialysis shift (part III). In the last part (IV) the performance of the electronic nose was compared with biochemical markers traditionally used to assess the efficiency of haemodialysis.

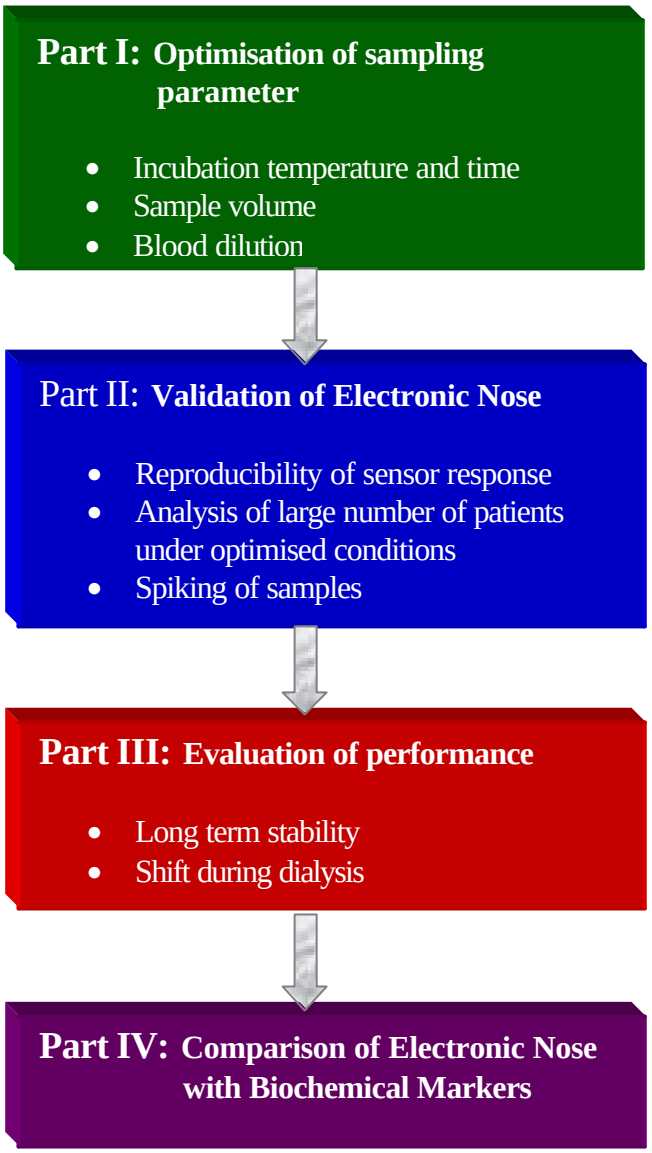

Figure 3.1 Overview of the study design to optimise and evaluate the sensor response of the electronic nose to "uraemic" blood and control blood.

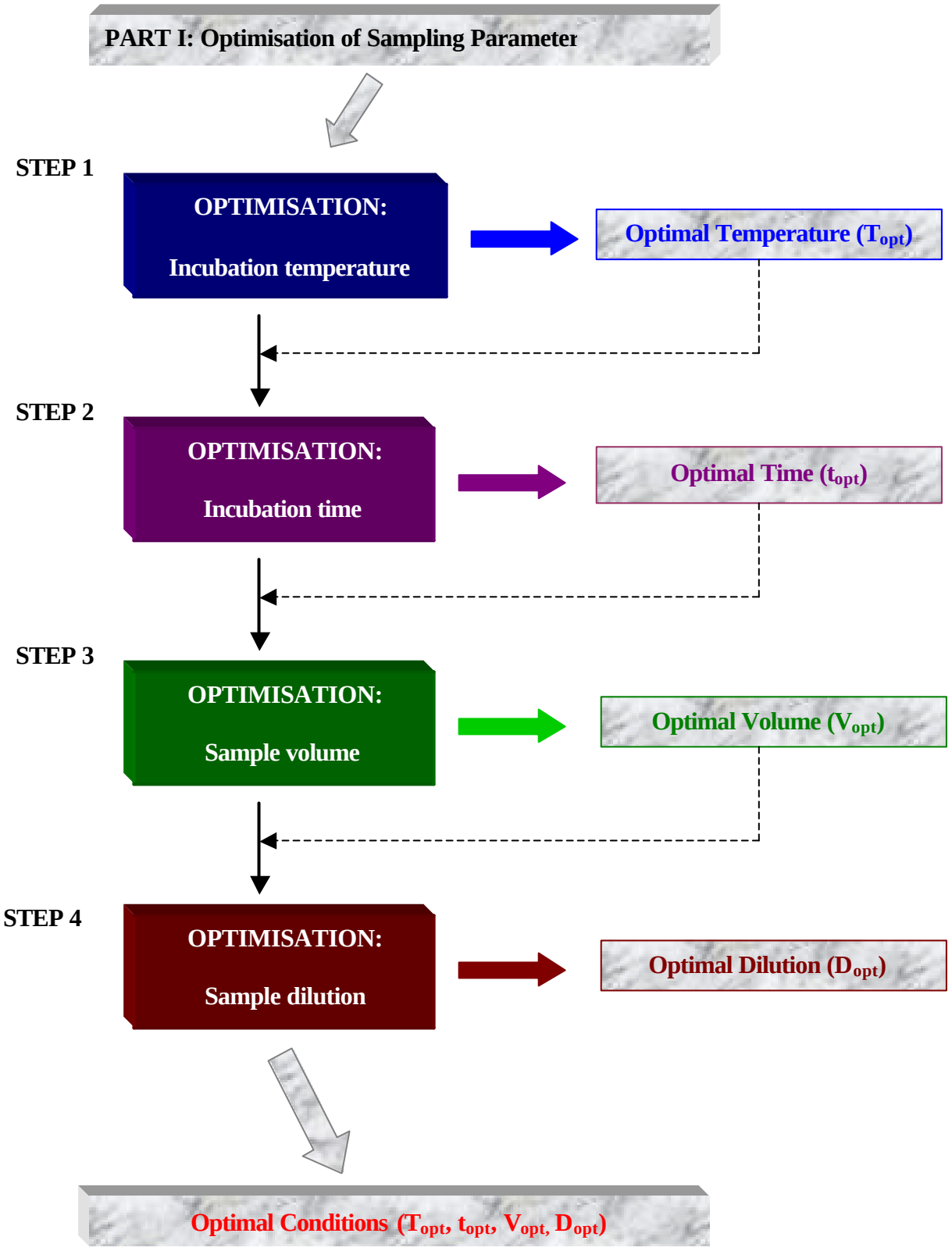

Figure 3.2: The four principal steps for the optimisation of sampling parameters.

3.2.2 SAMPLE PROCUREMENT

All blood samples were collected either from patients undergoing intermittent HD-treatment at Gloucestershire Royal Hospital (Gloucester, UK) or healthy volunteers (Control blood). All patients are treated either with a Fresenius F6 or Fresenius F8 dialyser (Fresenius AG, Bad Homburg v.d.H., Germany) The surface area of the polysulfone membrane is either 1.3 m^2 (F6 dialyser) or 1.8 m^2 (F8 dialyser). The blood flow varied between 200 and 350 ml/min, depending on the patient, whereas the dialysate flow rate was kept constant at 500 ml min^{-1}. All patients included in this study undergo haemodialysis treatment three times a week for four hours per session.

Blood and dialysate collection for analysis of volatiles

Blood samples (4 ml) from patients were collected directly from the HD circuit (pre dialyser) into tubes containing EDTA. (Greiner bio-one, Vacuette®, coagulation tubes). Control samples (10 ml) were obtained by venepuncture. Samples were then immediately frozen and stored at – 20 °C until analysis. Dialysate samples (15 ml) were collected directly from the post dialyser circuit tubing into sterile tubes and stored at –20 °C until analysis.

Blood collection for biochemical analysis

The biochemical analysis was performed on blood serum, therefore sampling tubes with clot-activator (Greiner bio-one, Vacuette®, serum tubes) were used for

blood sampling. From each patient, 10 ml of pre- and post-dialysis blood, respectively and from each volunteer 10 ml of control blood have been taken and analysed by the Clinical Chemistry Laboratory at Gloucestershire Royal Hospital (UK).

3.2.3 SAMPLE PREPARATION (INCUBATION)

All blood samples were stored at - 20 ^{o}C until analysis was performed. The frozen samples were defrosted on ice to minimise the loss of volatiles. Sample aliquots were transferred into a 5 ml headspace vials (Macherey and Nagel, UK) and immediately sealed with a crimp cap with Silicon/Teflon-septum (Jaytee Bioscience Ltd., UK). The sealed headspace vials were subsequently incubated. After the incubation period, the samples were analysed using the electronic nose.

The original sample volume of 2.5 ml of "uraemic" blood was incubated for 30 minutes. As indicated in Figure 3.2, the first step was to find the optimal incubation temperature. The samples were incubated at 20 °C, 37 °C and 70 °C. Thirty seven degree Celsius was chosen because it is the human body temperature. The third incubation temperature of 70 °C was deliberately set very high to investigate if a higher incubation temperature liberates more volatiles compared to 37 °C or 20 °C. After finding the optimal incubation temperature (T_{opt}), the incubation time was varied. Two point five ml of blood was incubated for 30 minutes, 45 minutes and 60 minutes at T_{opt}. In the next step (Step 3, Figure 3.2) all samples (pre- and post-dialysis) were incubated under the best conditions (T_{opt} and t_{opt}). The sample volume was reduced to 2.0 ml, 1.0 ml and 0.5 ml. To reduce the amount of required blood, the smallest possible sample volume was used and further diluted with 0.9 % NaCl

(Sigma, UK). The following dilutions were investigated: 1:2, 1:4 and 1:10. For all subsequent experiments the following parameters were used: optimal incubation temperature, optimal incubation time, optimal sample volume and optimal sample dilution.

3.2.4 SPIKING OF BLOOD SAMPLES

Blood samples were spiked with a) butanol/acetic acid mixture and b) urea/creatinine solution. The samples were prepared and incubated under the optimised conditions (T_{opt}, t_{opt}, V_{opt}, and D_{opt}).

Spiking with butanol/acetic acid mixture

Control blood samples were spiked with a mixture containing butanol (Sigma, UK) and acetic acid (Sigma, UK). The final concentration (in the sample) of each substance was 2 % (v/v).

Spiking with urea/creatinine mixture

Blood samples were spiked with a solution containing urea (Sigma, UK) and creatinine (Sigma, UK). Control blood samples were spiked to a urea and creatinine level found in the average post-dialysis blood, and post-dialysis blood samples were spiked to pre-dialysis concentrations. The average concentrations were calculated from 55 haemodialysis patients and 15 volunteers (Table 3.1).

Table 3.1: Average urea and creatinine concentrations in control and "uraemic" blood.

	Control blood	**Post-dialysis**	**Pre-dialysis**
Urea (mmol l^{-1})	4.5	5.5	21.0
Creatinine (μmol l^{-1})	100	400	850

3.2.5 ANALYSIS OF SENSOR REPRODUCIBILITY

The sensor reproducibility (drift) was studied by analysing one sample for 25 times on three different days. The same experiment was performed with undiluted and diluted (D_{opt}) blood samples (Control blood). An aliquot (V_{opt}) of the same sample was transferred into a headspace vials and immediately sealed. The samples were incubated under the optimal conditions (T_{opt}, t_{opt}).

3.2.6 HEADSPACE ANALYSIS

The incubated sample vials were connected to the electronic nose by inserting a needle into the headspace of the sample (see chapter 2). The sampling profiles used in this study are summarised in Table 3.2.

Table 3.2: Sampling profiles used for the analysis of blood and dialysate samples.

	Samples	
	Blood	**Dialysate**
Time delay (s)	5	5
Adsorption time (s)	10	10
Desorption time (s)	15	15
Baseline length (s)	5	5
Hold time (s)	0	0

3.2.6 DATA ANALYSIS

The original data set was not pre-processed, since the concentration of retained molecules in "uraemic" blood is contains essential information for the discrimination of the different blood types. Only for the analysis of the volatile shift (section 3.3.4), the samples within individual classes (control, pre- and post-dialysis) were normalised to length one prior to the multivariate analysis. This was done by dividing the sensor responses for all samples within a class by the standard deviation of this particular class.

Principal component analysis and hierarchical cluster analysis were applied for the initial experiments, i.e. optimisation of the sampling parameter (part I, Figure 3.1). The purpose was to find a visual difference between the different blood types and not to classify unknown samples.

For all other experiments, principal component analysis and discriminant function analysis were used.

3.3 RESULTS

3.3.1 OPTIMISATIONS OF ELECTRONIC NOSE

Determination of the optimal incubation temperature (T_{opt})

Three different temperatures were studied, namely 20 °C, 37°C, and 70°C. All samples were incubated for 30 minutes. Hence, a sample volume of 2.5 ml was used for the following experiments. The data were analysed using PCA and HCA.

In all three cases, it was possible to discriminate between pre-dialysis blood and post-dialysis blood as indicated by the dotted line in the PCA-charts (Figures 3.3, 3.4, and 3.5). Based on these observations, it seemed that the incubation temperature had little or no influence on the outcome (discrimination). However, when the PCA results were compared with the HCA results, this conclusion appears to be incorrect. No clear discrimination (homogeneous clusters) between pre- and post-dialysis blood was possible to obtain using HCA, independent of the incubation temperature (Figures 36, 3.7, and 3.8). In all three dendrograms (Figures 3.6, 3.7, and 3.8), the two different blood types were clustered into three clusters (C1 – C3). The best differentiation was observed at an incubation temperature of 70 °C as the blood samples of only one patient (patient 1) could not be discriminated (Figure 3.8).

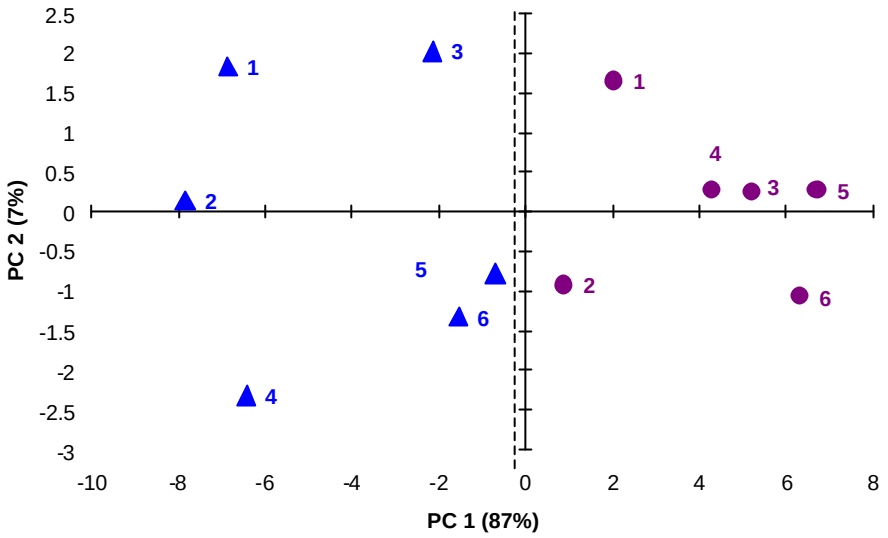

Figure 3.3: Principal component analysis showing separate clusters of post-dialysis blood (6 samples, triangles) and pre-dialysis samples (6 samples, circles). The samples were incubated at 20 °C for 30 min. The blood samples with the same number belong to the same patient.

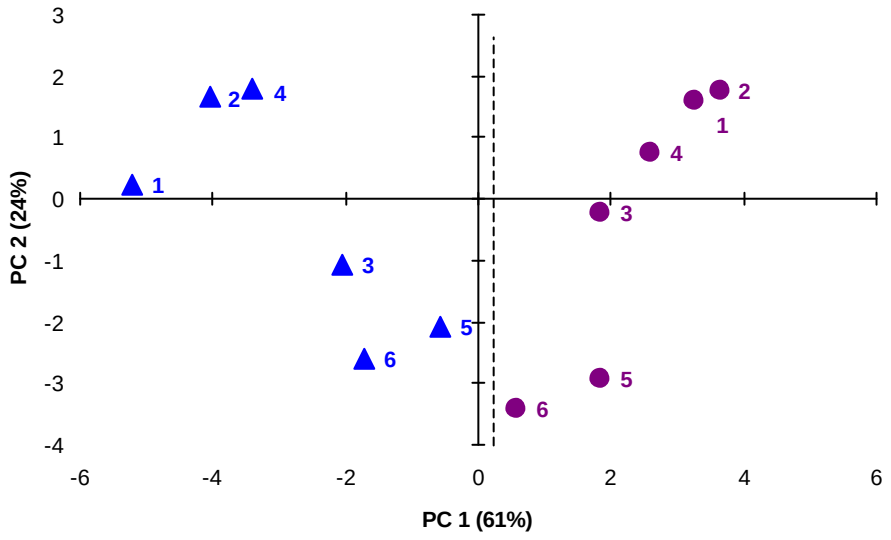

Figure 3.4: Principal component analysis showing separate clusters of post-dialysis blood (6 samples, triangles) and pre-dialysis samples (6 samples, circles). The samples were incubated at 37 °C for 30 min.

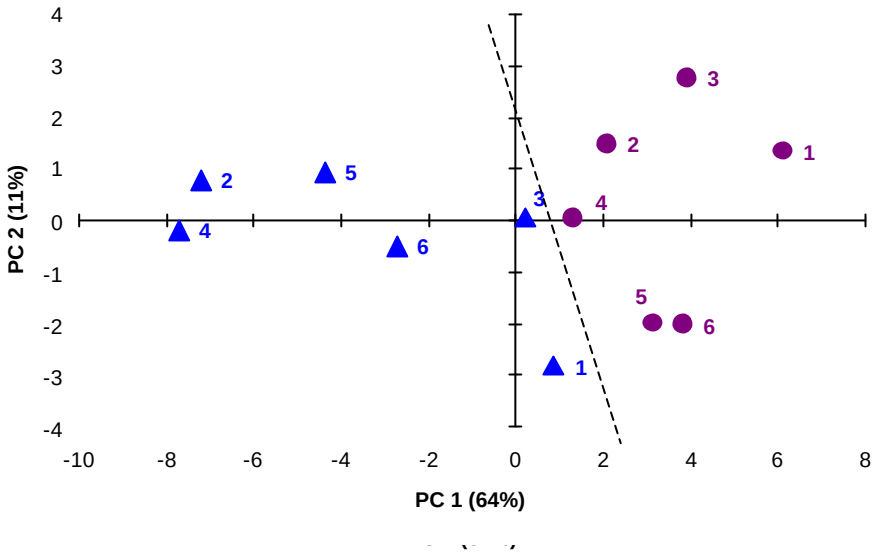

Figure 3.5: Principal component analysis showing separate clusters of post-dialysis blood (6 samples, triangles) and pre-dialysis samples (6 samples, circles). The samples were incubated at 70 °C for 30 min. The blood samples with the same number belong to the same patient.

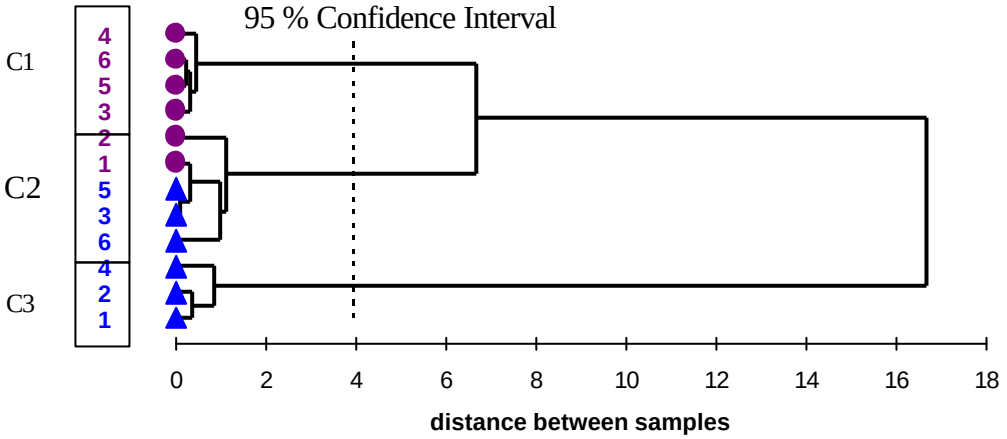

Figure 3.6: Hierarchical cluster analysis of post-dialysis blood (6 samples, triangles) and pre-dialysis samples (6 samples, circles). The samples were incubated at 20 °C for 30 min. The blood samples with the same number belong to the same patient. C1, C2, and C3 represent the three distinguishable clusters (p=0.05).

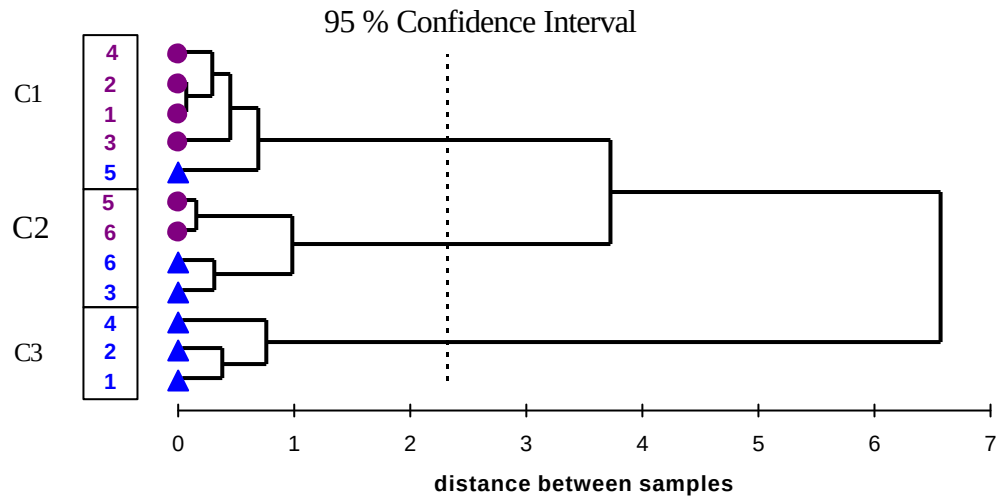

Figure 3.7: Hierarchical cluster analysis of post-dialysis blood (6 samples, triangles) and pre-dialysis samples (6 samples, circles). The samples were incubated at 37 °C for 30 min. The blood samples with the same number belong to the same patient. C1, C2, and C3 represent the three distinguishable clusters (p=0.05).

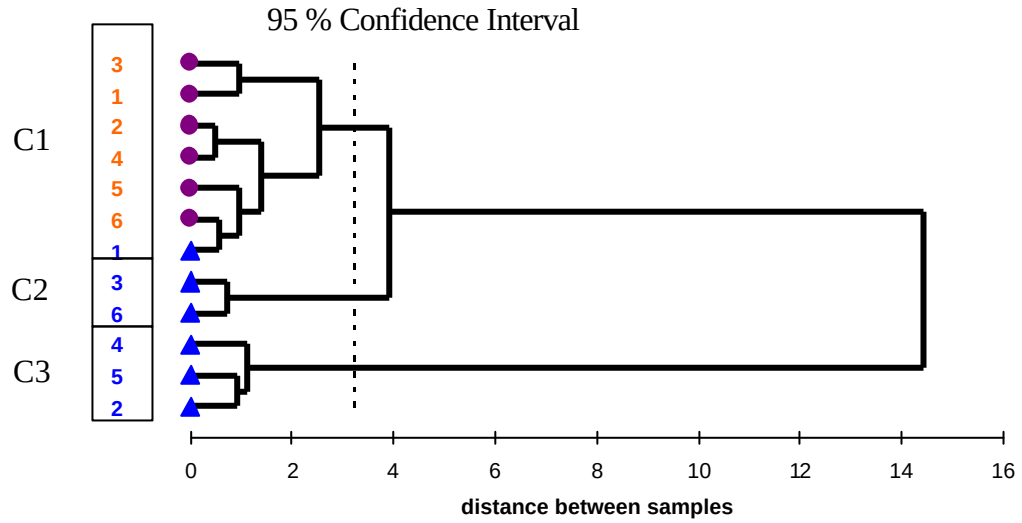

Figure 3.8: Hierarchical cluster analysis post-dialysis blood (6 samples, triangles) and pre-dialysis samples (6 samples, circles). The samples were incubated at 70 °C for 30 min. The blood samples with the same number belong to the same patient. C1, C2, and C3 represent the three distinguishable clusters (p=0.05).

The best discrimination was obtained at 70°C. However, one of the problems encountered at 70 °C was that blood proteins started to denature and therefore made this temperature unsuitable for an on-line monitoring system. Having the end application in mind, 37 °C is the incubation temperature of choice since the dialyser circuit is operated at 37 °C and therefore no additional heating element has to be installed in an on-line monitoring device. For further experiments, the **incubation temperature** was set at **37 °C.** This decision is justified since enough information could be extracted as indicated in Figures 3.4 and 3.7.

Determination of the optimal incubation time (t_{opt})

All samples were incubated at 37 °C for the following times: 45, 60 and 90 minutes. The sample volume was kept constant at 2.5 ml during the experiments

With all three incubation times, a separation of pre-dialysis blood and control blood could be obtained as indicated by the dotted line in the PCA – charts (Figures 3.9, 3.10, and 3.11). The best separation was obtained after an incubation period of 45 min (Figure 3.9). These results were confirmed by HCA as shown in Figure 3.12. As can be seen, post-dialysis samples formed a homogenous cluster (C1), whereas pre-dialysis blood is split into two clusters (C2, C3). However, no clear discrimination (homogenous clusters) was observed after an incubation period 60 and 90 minutes when using HCA. Although the pre- and post-dialysis samples of individual patients were distinguishable from each other (e.g.: patients 3 and 4 in Figure 3.13 or patients 1, 2, and 4 in Figure 3.14). Similar results were obtained when the experiments were repeated. For all further experiments, the chosen incubation time was **45 minutes**.

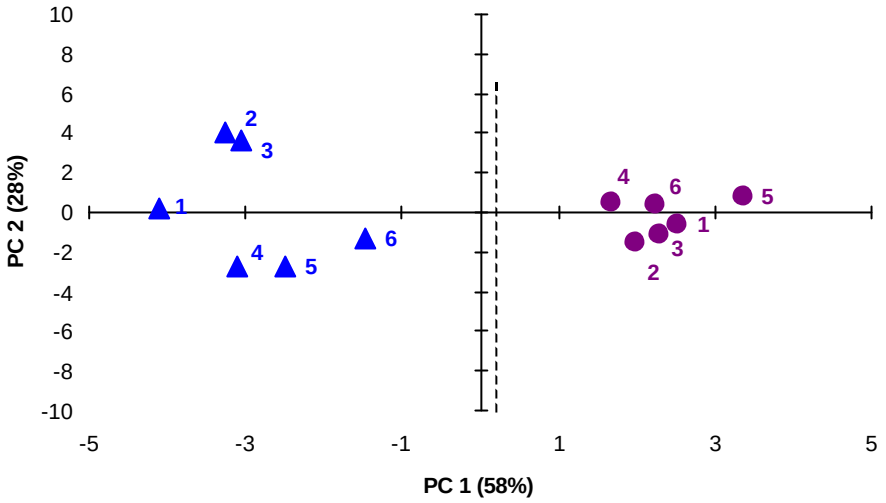

Figure 3.9: Principal component analysis showing separate clusters of post-dialysis blood (6 samples, triangles) and pre-dialysis samples (6 samples, circles). The samples were incubated at 37 °C for 45 min. The blood samples with the same number belong to the same patient.

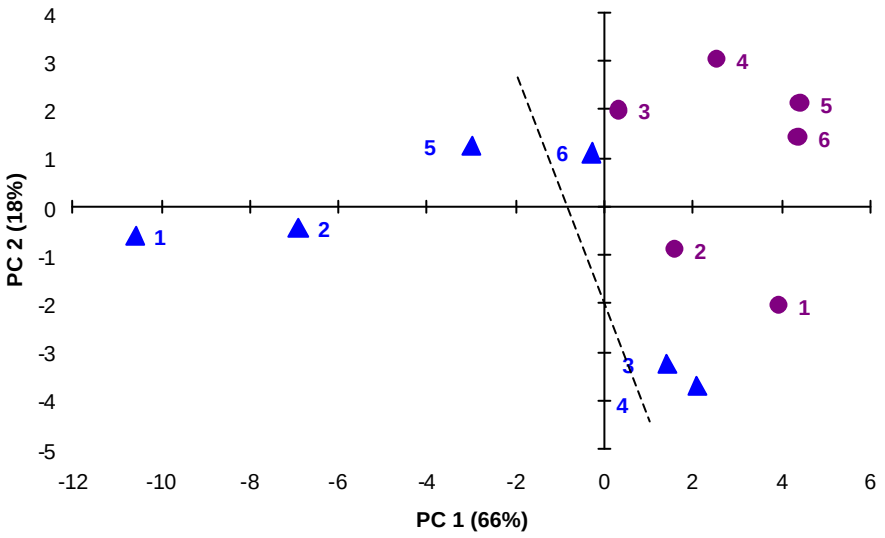

Figure 3.10: Principal component analysis showing separate clusters of post-dialysis blood (6 samples, triangles) and pre-dialysis samples (6 samples, circles). The samples were incubated at 37 °C for 60 min.

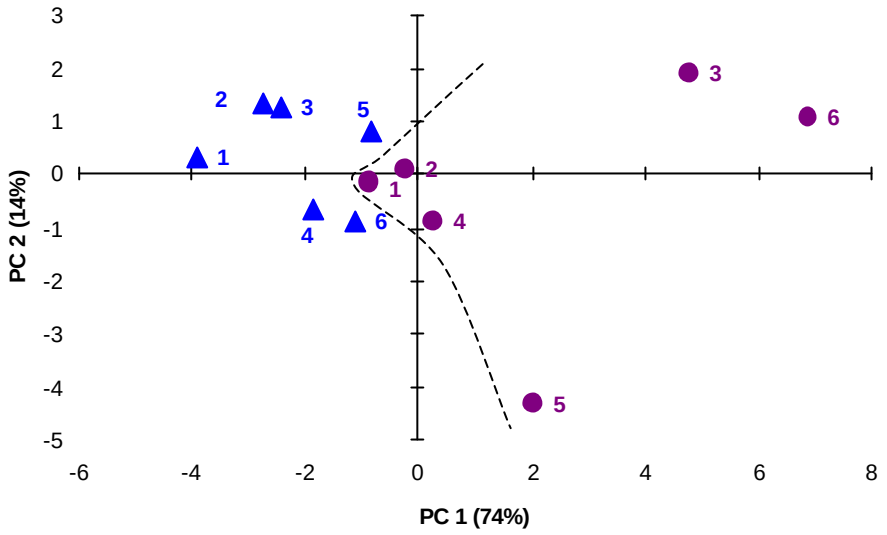

Figure 3.11: Principal component analysis showing separate clusters of post-dialysis blood (6 samples, triangles) and pre-dialysis samples (6 samples, circles). The samples were incubated at 37 °C for 90 min.

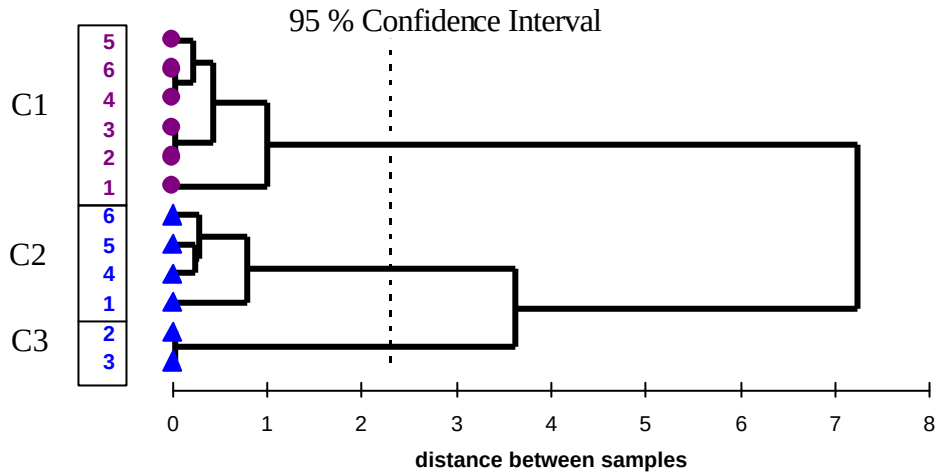

Figure 3.12: Hierarchical cluster analysis of post-dialysis blood (6 samples, triangles) and pre-dialysis samples (6 samples, circles). The samples were incubated at 37 °C for 45 min. The blood samples with the same number belong to the same patient. C1, C2, and C3 represent the three distinguishable clusters (p=0.05).

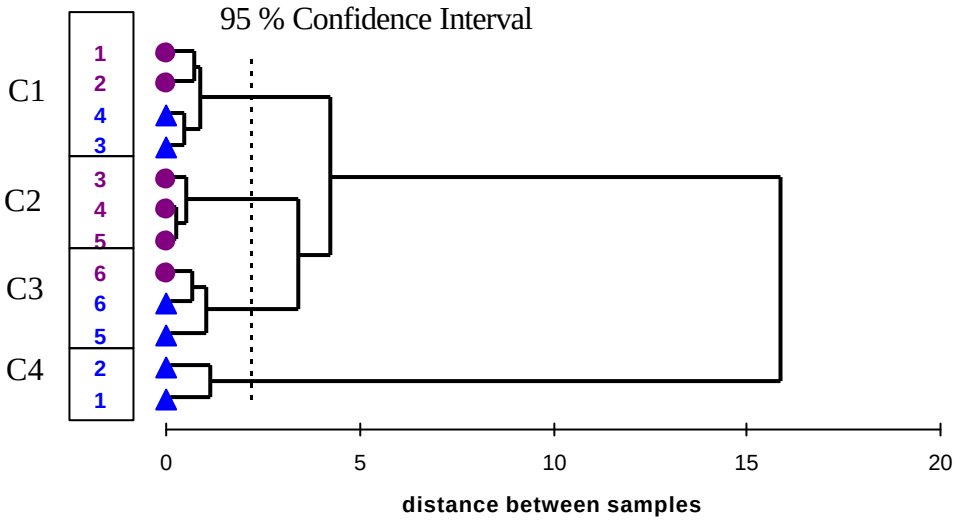

Figure 3.13: Hierarchical cluster analysis of post-dialysis blood (6 samples, triangles) and pre-dialysis samples (6 samples, circles). The samples were incubated at 37 °C for 60 min. The blood samples with the same number belong to the same patient. C1, C2, C3 and C4 represent the four distinguishable clusters (p=0.05).

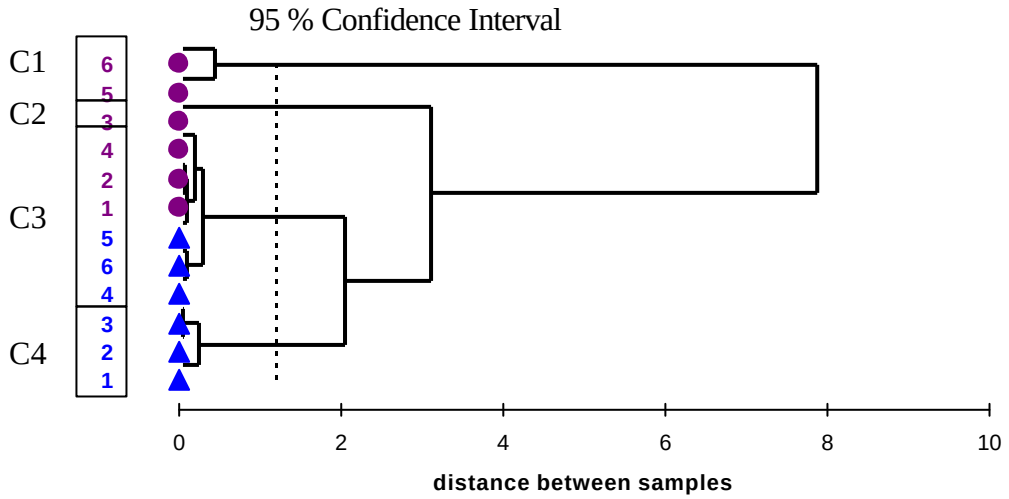

Figure 3.14: Hierarchical cluster analysis of post-dialysis blood (6 samples, triangles) and pre-dialysis samples (6 samples, circles). The samples were incubated at 37 °C for 90 min. The blood samples with the same number belong to the same patient. C1, C2, C3 and C4 represent the four distinguishable clusters (p=0.05).

Determination of the optimal sample volume (V_{opt})

All samples were incubated at 37°C for 45 min. The sample volume was varied as follows: 2.0 ml, 1 ml, and 0.5 ml. The sample volume had no influence on the separation between pre-dialysis blood and control blood as can be seen in the PCA – plots (Figures 3.15, 3.16, and 3.17). For a sample volume of 2.0 ml, the HCA plot was divided into three subclusters (C1-C3) (Figure 3.18). Nevertheless, it was possible to discriminate between all pre- and post-dialysis samples of individual patients (Figure 3.18). However, with a sample volume of 1 ml and 0.5 ml, respectively, no homogenous clusters were obtained using HCA as shown in Figure 3.19 and 3.20. As can be seen in Figure 3.19, only one patient (no. 6) was misclassified, i.e. no discrimination between pre- and post-dialysis sample was possible. In contrast, with a sample volume of 0.5 ml it was impossible to distinguish between all pre- and post-dialysis samples of individual patients (Figure 3.20).

The HCA results are indicating a deterioration of the ability to separate between pre-dialysis blood and post-dialysis blood with a decrease in sample volume. Nevertheless, all further experiments were performed with a sample volume of 0.5 ml because it was still possible to discriminate between pre- and post-dialysis samples of the same patient, even when no homogenous clusters were obtained.

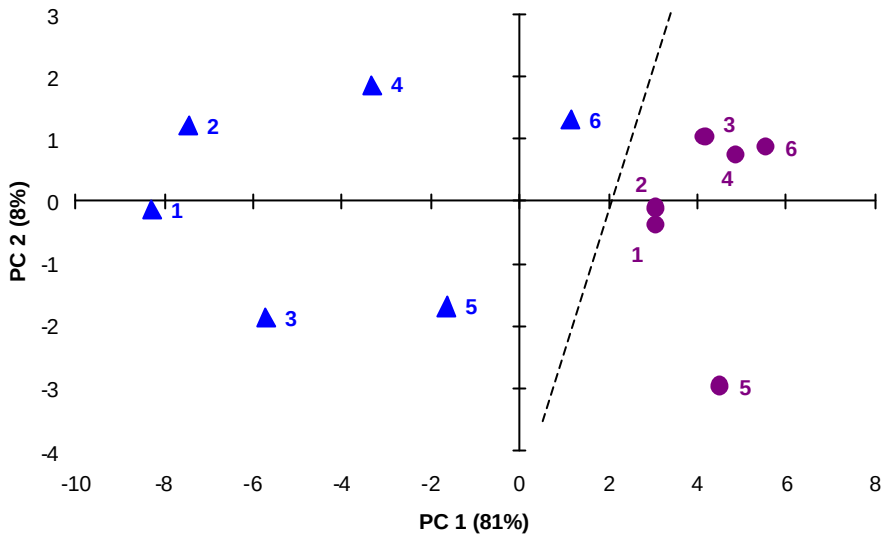

Figure 3.15: Principal component analysis showing separate clusters of post-dialysis samples (6 samples, triangles) and pre-dialysis samples (6 samples, circles). The samples were incubated at 37 °C for 45 min with a sample volume of 2 ml.

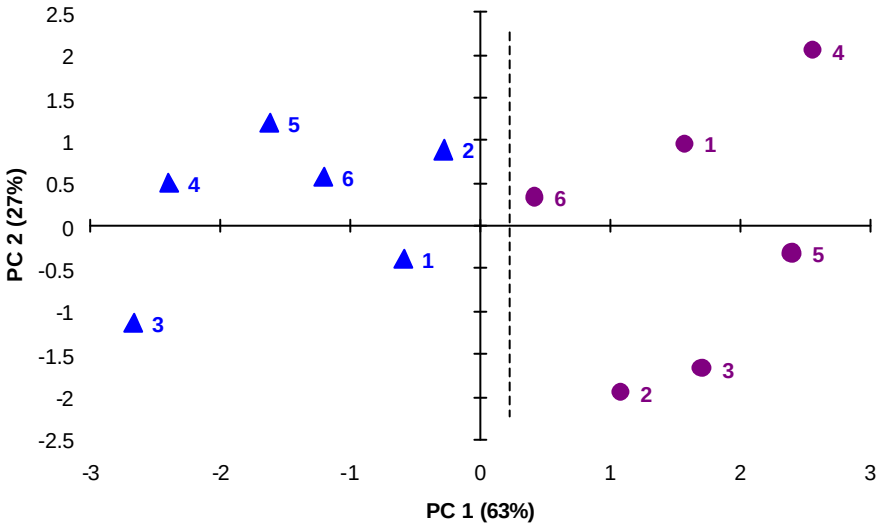

Figure 3.16: Principal component analysis showing separate clusters of post-dialysis samples (6 samples, triangles) and pre-dialysis samples (6 samples, circles). The samples were incubated at 37 °C for 45 min with a sample volume of 1.0 ml.

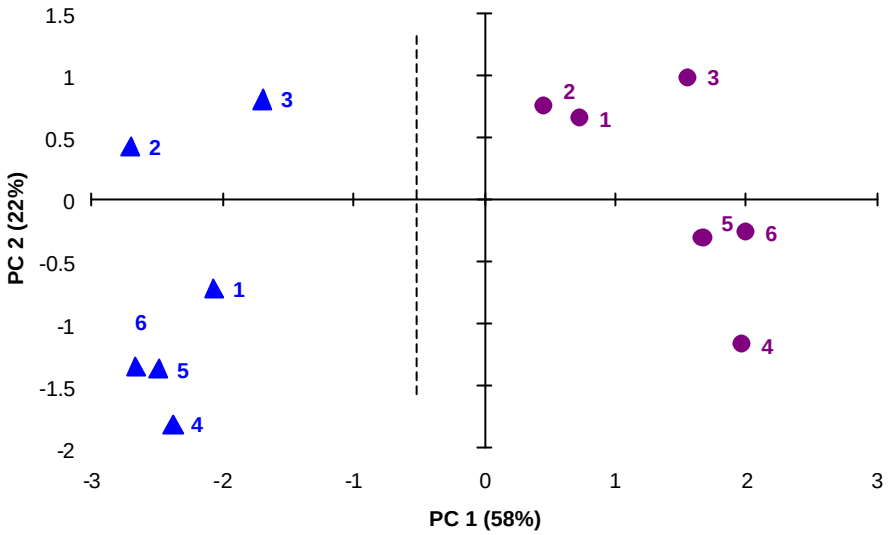

Figure 3.17: Principal component analysis showing separate clusters of post-dialysis samples (6 samples, triangles) and pre-dialysis samples (6 samples, circles). The samples were incubated at 37 °C for 45 min with a sample volume of 0.5 ml.

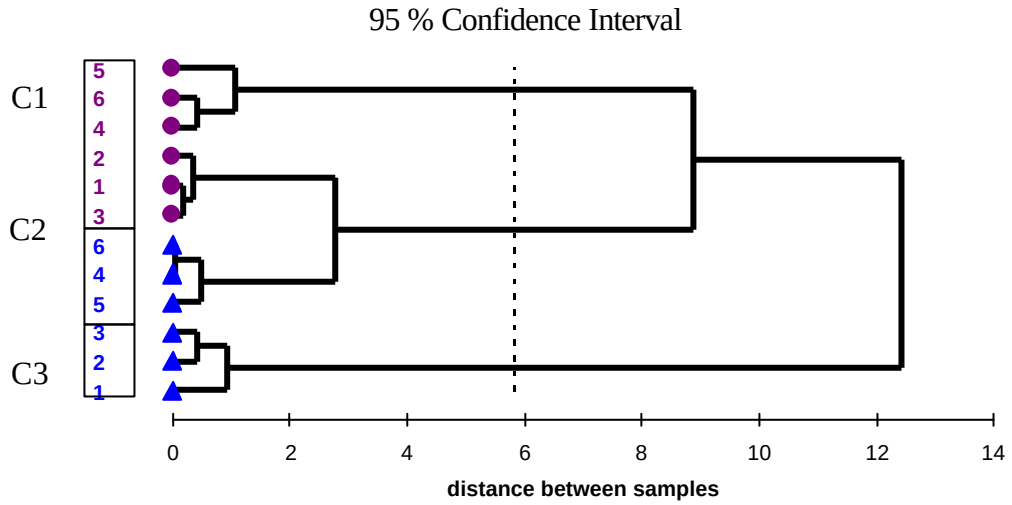

Figure 3.18: Hierarchical cluster analysis post-dialysis blood (6 samples, triangles) and pre-dialysis samples (6 samples, circles). The samples were incubated at 37 °C for 45 min with a sample volume of 2 ml. The blood samples with the same number belong to the same patient. C1, C2, C3 and C4 represent the four distinguishable clusters (p=0.05).

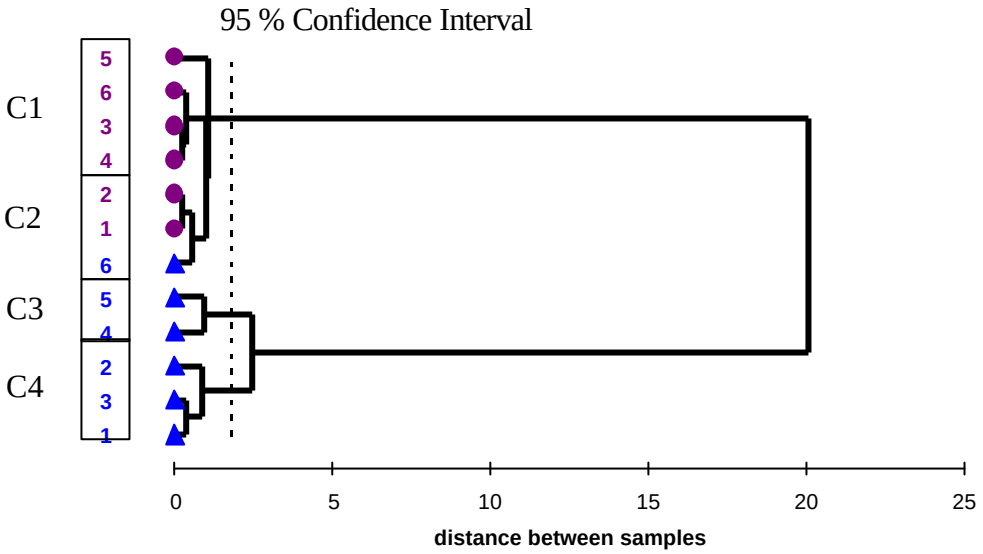

Figure 3.19: Hierarchical cluster analysis post-dialysis blood (6 samples, triangles) and pre-dialysis samples (6 samples, circles). The samples were incubated at 37 °C for 45 min with a sample volume of 1 ml. The blood samples with the same number belong to the same patient. C1, C2, C3 and C4 represent the four distinguishable clusters (p=0.05).

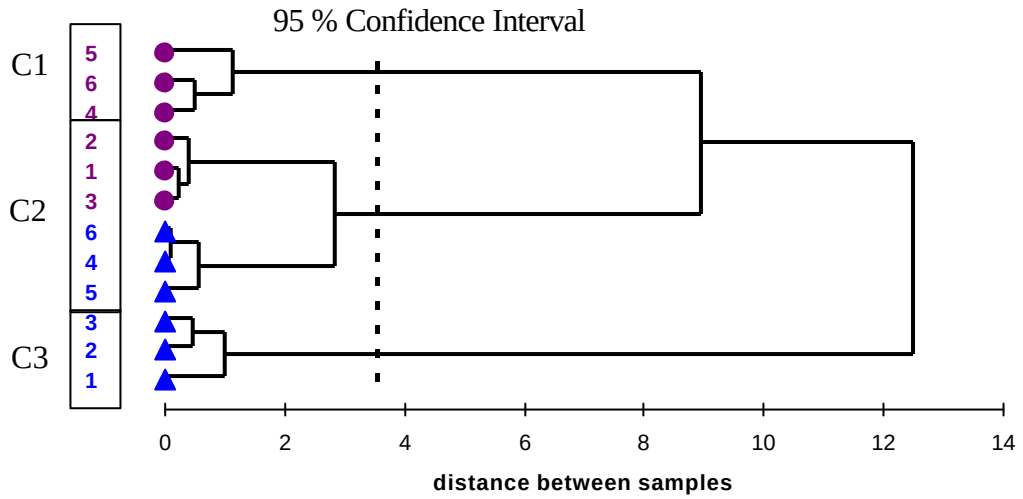

Figure 3.20: Hierarchical cluster analysis of post-dialysis blood (6 samples, triangles) and pre-dialysis samples (6 samples, circles). The samples were incubated at 37 °C for 45 min with a sample volume of 0.5 ml. The blood samples with the same number belong to the same patient. C1, C2, and C3 represent the three distinguishable clusters (p=0.05).

Determination of the optimal blood dilution (D_{opt})

Dialysis patients are anaemic. Hence, one limiting factor is the availability of blood of HD patients. Therefore, the aim was to minimise the required amount of blood needed to obtain a sufficient discrimination between post- and pre-dialysis blood samples. After reducing the sample volume to 0.5 ml, the possibility of diluting blood was investigated. The blood samples were diluted with a sterile 0.9 % NaCl solution to obtained the following dilutions: 1:2, 1:4 and 1:10. The experiments were performed with control blood and after finding the optimal dilution validated with

post- and pre-dialysis blood samples. A visual difference (PCA plot) between diluted control blood samples and blank sodium chloride will be used to determine the optimal dilution, i.e. the highest dilution, which still can be distinguished from the negative controls (0.9 % sodium chloride) will be regarded as optimal dilution.

All samples were incubated under optimal conditions obtained so far (T_{opt}, t_{opt}, and V_{opt}). Undiluted, as well as blood in all dilutions, were analysed together, i.e. in the same experiment. Blank sodium chloride solution served as a negative control. The result of this experiment is shown in Figure 3.21. As can be seen, it is possible to distinguish between undiluted samples and the diluted samples up to a dilution of 1:4. It was impossible to discriminate 1:10 diluted samples from the negative control samples (0.9 % NaCl) indicating that the last concentrations was too low to discriminate between pre- and post-dialysis samples.

Interestingly, on the left hand side of the graph are the concentrated samples (undiluted), whereas the highest diluted samples (1:10) are on the right hand side of the graph together with the negative controls.

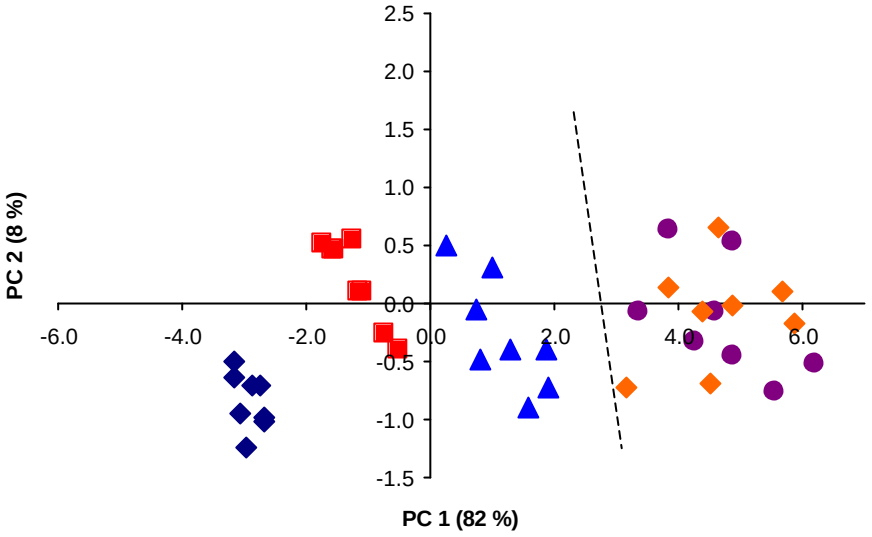

Figure 3.21: Principal component analysis of different diluted control blood samples and blank sodium chloride solution (0.9 % w/v). Different diluted blood samples formed separate clusters, apart from the highest dilution (1:10), which could not be discriminated from blank sodium chloride solution (dashed line).

Key: Undiluted blood (8 samples, dark blue diamonds), 1:2 diluted (8 samples, red squares), 1:4 diluted (8 samples: blue triangles), 1:10 diluted (8 samples, orange diamonds), and blank sodium chloride solution (8 samples, violet circles).

Based on the PCA score plot, a classification model was built using discriminant function analysis. For calculating the model, 2 samples of each sample treatment were withheld and used for cross-validation. As can be seen in Figure 3.22, undiluted blood samples and diluted blood samples (1:2 and 1:4) formed separate clusters. However, 1:10 diluted samples formed a cluster with the negative controls. The analysis of unknown samples (2 of each class) revealed that it is impossible to distinguish 1:10 diluted samples from a sodium chloride solution, whereas the other unknown samples

were correctly identified (Figure 3.22). The result shown in Figure 3.22 indicated that a dilution of 1:4 should not affect the ability to discriminate between pre- and post-dialysis blood samples.

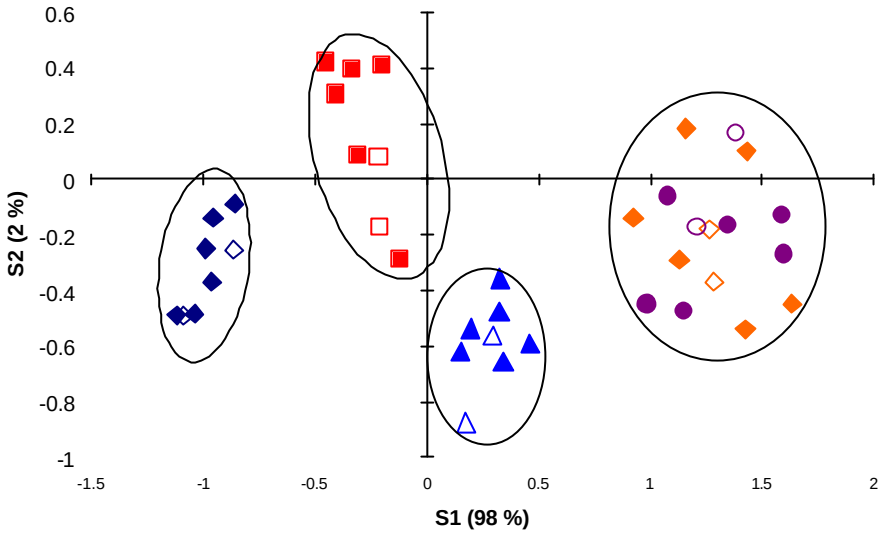

Figure 3.22: Discriminant function analysis of different diluted control blood samples (Undiluted, 1:2, 1:4, and 1:10 diluted) compared to a sodium chloride solution.

Key: Undiluted blood (diamonds), 1:2 diluted (squares), 1:4 diluted (triangles), 1:10 diluted (orange diamonds), and blank sodium chloride solution (circles). Cross-validations: 10 samples (2 of each) were withheld form building the DFA (open symbols).

This observation was evaluated by the analysis of pre- and post-dialysis blood (1:4 diluted). As can be seen in Figure 3.23, it was possible to distinguish between pre- and post-dialysis samples at a dilution of 1:4. Control blood (healthy volunteers) formed a separate cluster compared to “uraemic” blood (Figure 3.23).

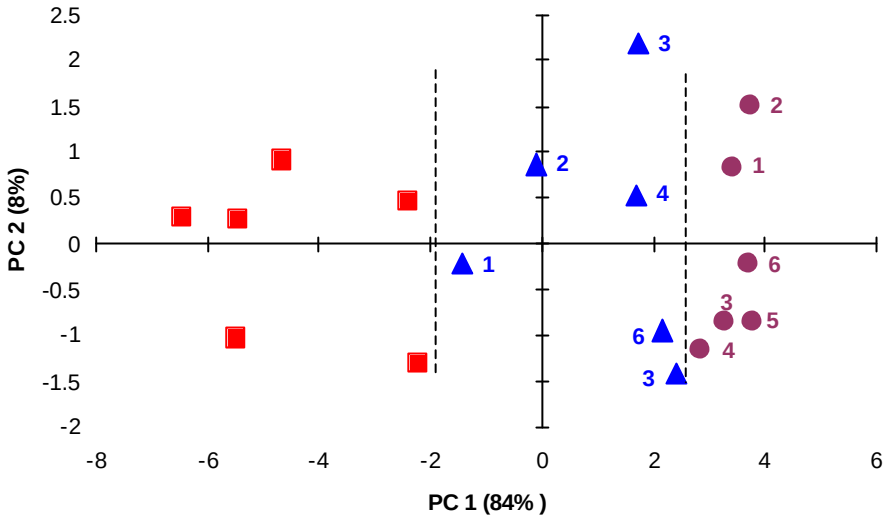

Figure 3.23: Principal component analysis of control blood (6 samples, squares), post-dialysis blood (6 samples, triangles) and pre-dialysis blood (6 samples, circles). The samples were incubated at 37 °C for 45 min with a sample volume of 0.5 ml and a dilution of 1:4. The dialysis blood samples with the same number belong to the same patient.

A perfect discrimination could not be achieved using hierarchical cluster analysis (Figure 3.24). The dendrogram is divided into four sub-clusters (C1 – C4). Cluster C1 contains all post-dialysis blood samples as well as two pre-dialysis samples (patients 3, and 5). Three of the remaining pre-dialysis samples were grouped together in cluster C2. The post-dialysis sample of patient 1 was grouped together with control samples (C3). The control samples itself were divided into two clusters (C3, C4).

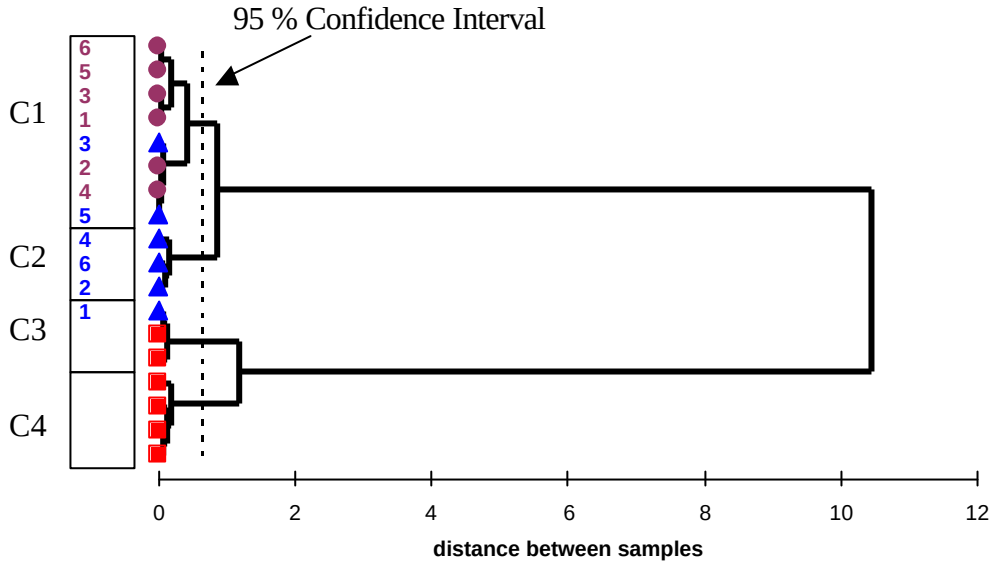

Figure 3.24: Hierarchical cluster analysis of control blood (squares), post- (triangles) and pre-dialysis samples (circles). The samples were incubated at 37 °C for 45 min with a sample volume of 0.5 ml and a dilution of 1:4. The blood samples with the same number belong to the same patient. C1, C2, C3 and C4 represent the four distinguishable clusters (p=0.05).

The overall aim of this study was to discriminate between pre- and post-dialysis blood samples. Therefore, the control samples were removed from the original data set and the remaining data were re-analysed. As can be seen in Figure 3.25, a good separation was obtained between pre- and post-dialysis samples (dashed line). This observation was confirmed by HCA (Figure 3.26). Figure 3.26 shows two separate clusters (C1, C2). Cluster C1 contains all pre-dialysis samples, whereas cluster C2 includes all post-dialysis samples.

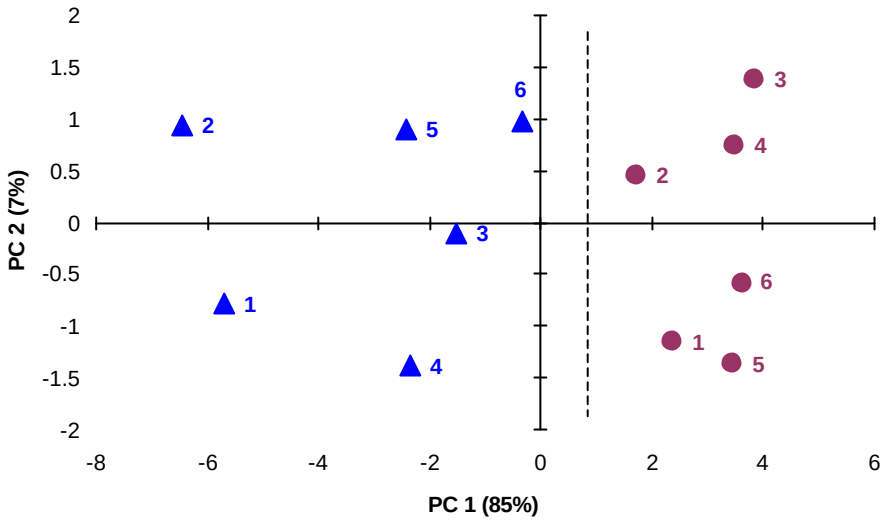

Figure 3.25: Principal component analysis of post-dialysis blood (6 samples, triangles) and pre-dialysis blood (6 samples, circles). The samples were incubated at 37 °C for 45 min with a sample volume of 0.5 ml and a dilution of 1:4. The dialysis blood samples with the same number belong to the same patient.

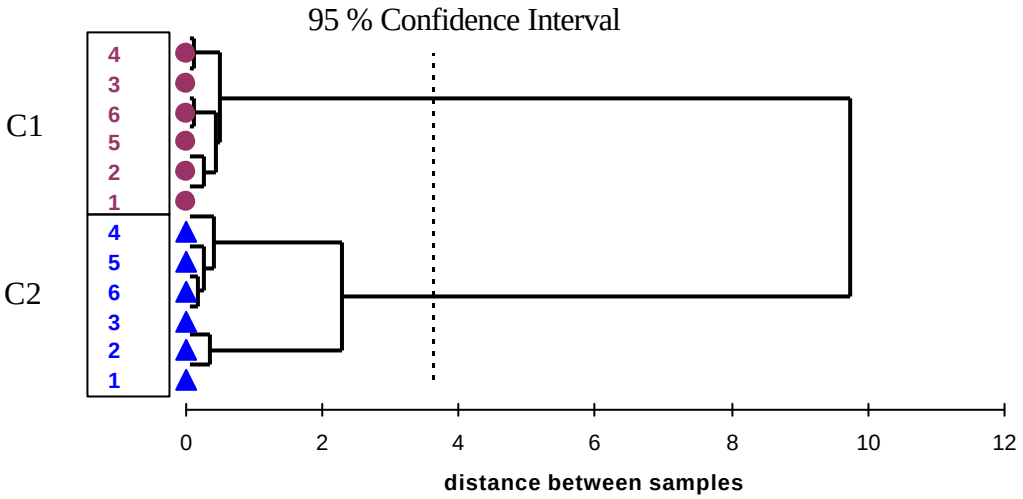

Figure 3.26: Hierarchical cluster analysis of post- (triangles) and pre-dialysis samples (circles). The samples (0.5 ml, 1:4 diluted) were incubated at 37 °C for 45 min. The blood samples with the same number belong to the same patient. C1, and C2 represent the two distinguishable clusters (p=0.05).

The parameters chosen for further experiments are summarised in Table 3.3.

Table 3.3: Summary of the chosen sampling parameters.

Sampling Parameter	
Incubation Temperature (T_{opt})	37 ^{o}C
Incubation Time (t_{opt})	45 min
Sample Volume (V_{opt})	0.5 ml
Sample Dilution (D_{opt})	1:4

3.3.2 VALIDATION OF ELECTRONIC NOSE

After finding the optimal incubation parameters, which allowed a separation of pre- and post-dialysis blood samples it was necessary to validate the electronic nose. The validation included the analysis of more samples (bigger sample size), spiking of blood samples, and investigating the sensor drift.

Reproducibility of sensor response

The sensor drift was determined with 0.5 ml control blood (undiluted and 1:4 diluted). The samples were incubated at 37 ^{o}C for 45 min.

The sensors are generally characterised by a low drift as indicated by the coloured bars in Figures 3.27a/b. Only sensor 11 showed a large variation in the sensor response to undiluted blood on day 1 (Figure 3.27a). However, on following days the drift of sensor 11 was comparable with the others. The day-to-day reproducibility was good as illustrated in both figures. All sensors apart from sensor 11 and 14 showed similar sensor responses, independent on the day and sample dilution (Figures 3.27a/b). The high sensor response of sensor 14 on the second day (Figure 3.27a/b)

might be due to the fact, that the electronic nose was not used for a few days. This break may lead to a full recovery of the sensor and subsequently lead to an increased sensor response.

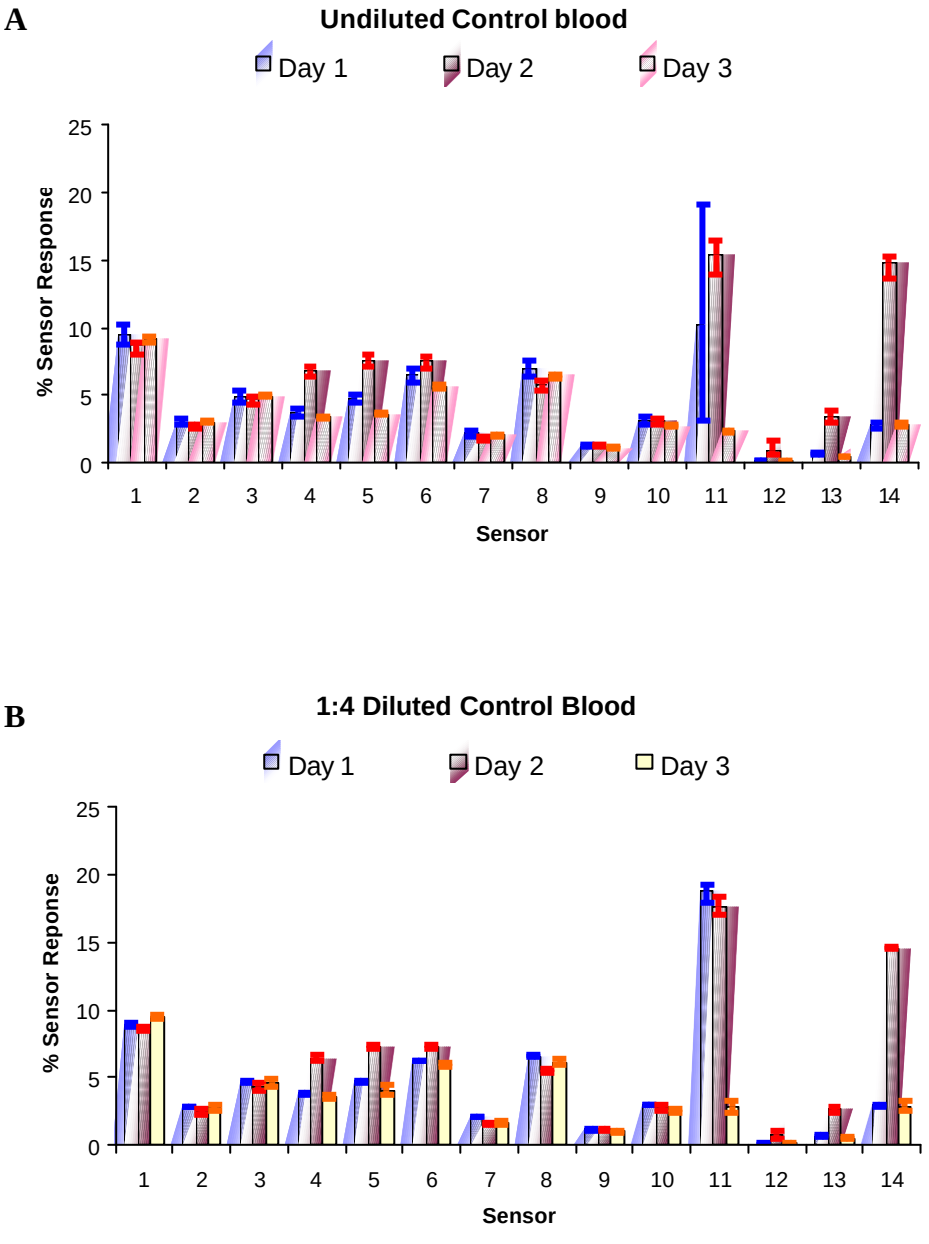

Figure 3.27: The mean sensor response as well as their minimal and maximal response to A) undiluted and B) diluted control blood measured on three different days.

However, it was decided to eliminate sensor 11 and 14 from the data analysis for all further experiments presented in this report due to their lack of reproducibility.

Analysis of larger sample size

The optimisation of the sampling parameter was done on a relatively small sample size due to the blood consumption during the experimental phase. The first part of the validation phase was the analysis of 55 patients and 40 volunteers based on the findings described in section 3.3.1 (Table 3.3).

Blood samples were obtained from 55 patients undergoing intermittent HD. The samples were taken before and after a single dialysis session directly from the HD circuit. Control blood (40 volunteers) samples were obtained by venepuncture.

The result of this experiment is shown in Figure 3.28. The two first principal components account for 88 % of the variance of the original data matrix, and this information was sufficient to easily discriminate between "uraemic" blood and control blood. However, more importantly is the fact that the odour of pre-dialysis blood differs to the odour of post-dialysis samples (Figure 3.28).

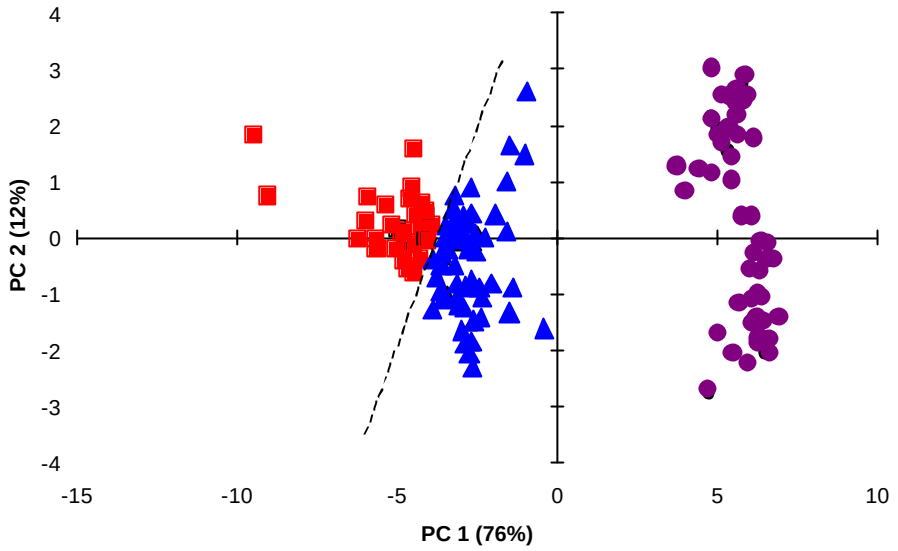

Figure 3.28: Principal component analysis showing the separate clusters of control blood (40 samples, squares), post-dialysis blood (55 samples, triangles) and pre-dialysis blood (55 samples, circles).

Based on the analysis presented in Figure 3.28 (PCA) a classification model was built (DFA) using samples from 47 patients and 32 controls selected at random. The result of the classification model is presented in Figure 3.29. The samples grouped into three clusters (pre-, post- dialysis, and control) with good separation. The model was validated by analysis of the 24 samples (8 of each class) that were not used to construct the classification model, and all 24 samples were correctly classified as either control, post-dialysis or pre-dialysis blood indicating the validity of the model.

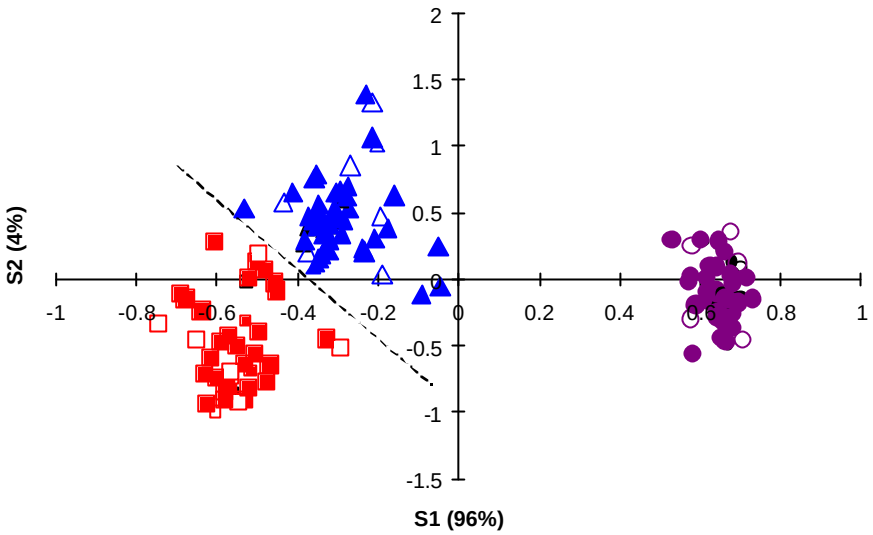

Figure 3.29: Discriminant function analysis showing the separate clusters of control blood (squares), post-dialysis blood (triangles) and pre-dialysis blood (squares). Cross-validation: 24 samples (8 of each), open symbols.

Spiking of blood samples

Spiking of blood samples by adding highly volatile substances was done to investigate if it would give rise to an altered sensor response. In the first set of experiments, control blood was spiked with butanol and acetic acid. In a second experimental series "uraemic" blood (post- and pre- dialysis) was spiked with urea and creatinine.

Spiking of control blood with butanol and acetic acid

Control blood samples were spiked with highly volatile pure chemicals. The aim was to investigate if the electronic nose was able to differentiate between modified samples and unmodified samples. A positive result (discrimination possible) was an indicator that the electronic nose was working properly under the given conditions.

Control blood samples were spiked with butanol and acetic acid so that the concentration of both substances was 2 % (v/v) in the final sample. Two % was chosen because the manufacturer of the electronic nose recommends a 2 % butanol solution as a reference standard (Bloodhound Operating Manual, Version 1.4.2).

The result of the experiment is shown in Figure 3.30. As can be seen, a clear separation between the control blood samples and the spiked samples is observable (dashed line). The two highly volatile compounds caused an additional odour in the spiked samples. Hence, these volatiles gave rise to the altered sensor response allowing the discrimination between the samples (Figure 3.30).

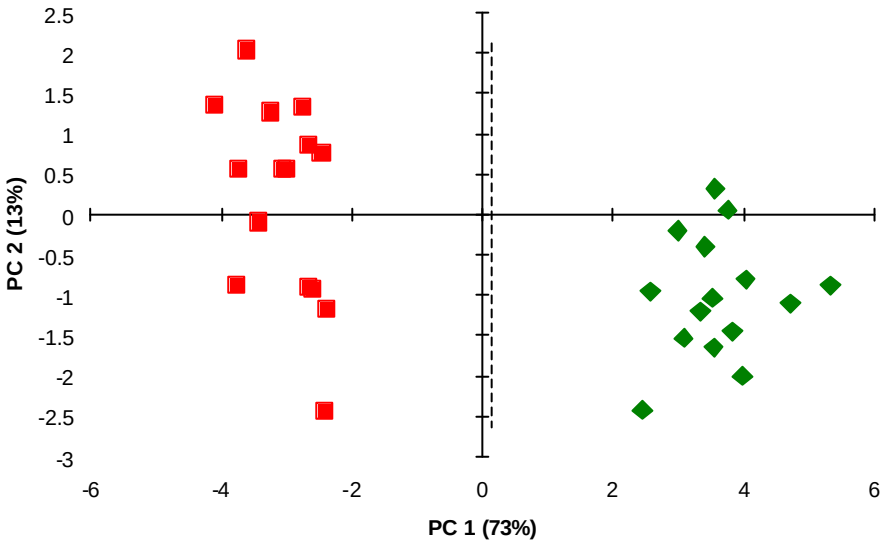

Figure 3.30: Principal component analysis showing the separate clusters of control blood (14 samples, squares) and control blood spiked with butanol (2% v/v) and acetic acid (2% v/v) (14 samples, diamonds).

Spiking with urea and creatinine

The aim of the second experimental series was to investigate if the sensor response is influenced by urea and creatinine. Urea and creatinine are two substances, which are elevated levels in HD patients and currently used to assess the treatment adequacy.

For this reason, blood samples were spiked with urea and creatinine. Control blood (obtained from healthy volunteers) was spiked to an averaged level observed in post-dialysis samples (urea: 5.5 mmol l^{-1}, creatinine: 400 µmol l^{-1}), whereas post-dialysis samples were spiked to an averaged pre-dialysis level (urea: 21.00 mmol l^{-1}, creatinine: 850 µmol l^{-1}).

The result of the spiking experiment is shown in Figure 3.31. As can be seen, it is possible to distinguish between control blood, post- and pre-dialysis blood. The spiking itself did not influence the ability to distinguish between the different sample types. No difference between spiked and unspiked samples was observable, i.e. the formed one cluster.

Based on the PCA, a classification model was built (DFA) using 45 samples (9 of each sample type). The result is shown in Figure 3.32. As can be seen, three different distinctive clusters for control blood, post-dialysis and pre-dialysis blood were formed. It was impossible to distinguish between spiked and unspiked blood samples. The cross-validation revealed that it was only possible to allocate the unknown samples either to control, post-dialysis or pre-dialysis cluster independent of the spiking status. This result indicates that urea and creatinine do not actively influence the sensor response.

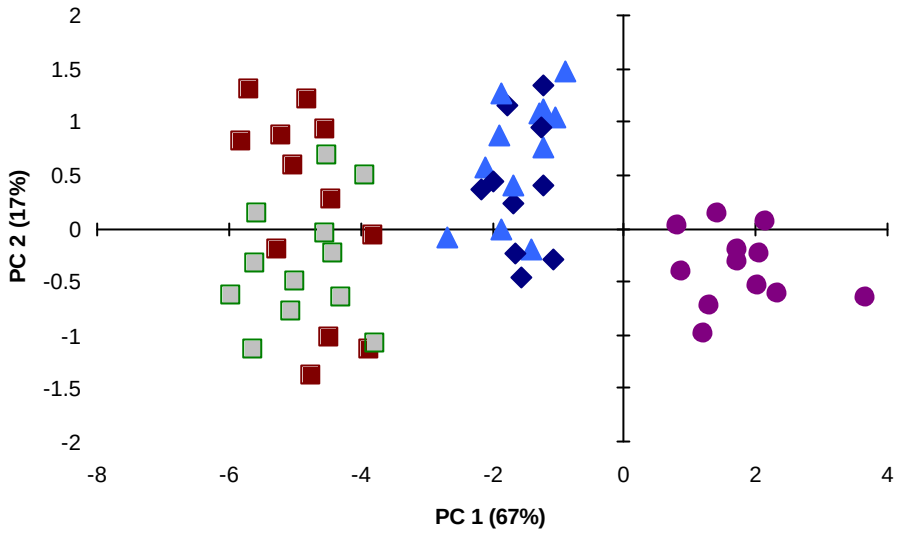

Figure 3.31: Principal component analysis of control blood (12 samples, red squares), spiked control blood (12 samples, green/grey squares), post-dialysis blood (12 samples, triangles), spiked post-dialysis blood (12 samples, diamonds) and pre-dialysis blood (12 samples, circles).

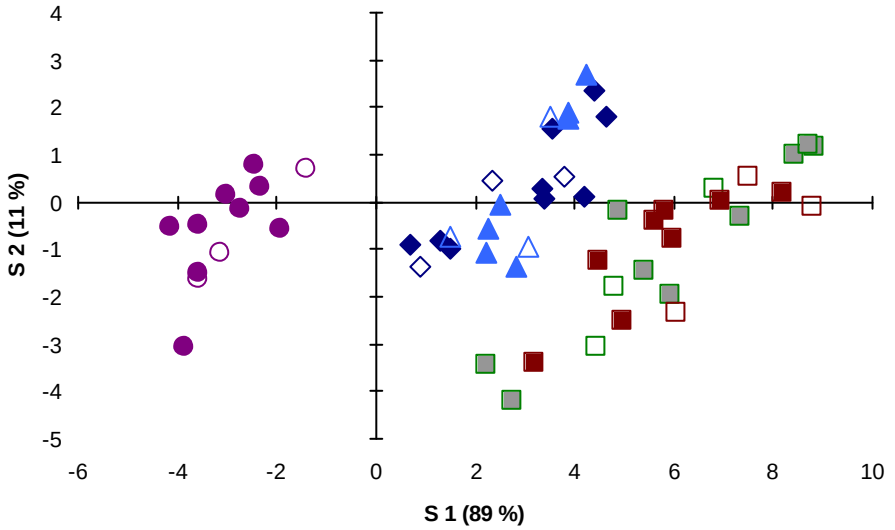

Figure 3.32: Discriminant function analysis of control blood, spiked control blood post-dialysis blood, spiked post-dialysis blood and pre-dialysis blood. Cross validation: 15 samples (three of each type), open symbols.

3.3.4 EVALUATION OF THE ELECTRONIC NOSE PERFORMANCE

The aim of this research project was to investigate the potential of an electronic nose as a new monitoring tool for haemodialysis. In this section, the performance of the gas sensor array is studied in terms of its ability to follow the volatile shift occurring during a single haemodialysis session and also its long-term performance (stability).

Analysis of the dialysis (volatile) shift

This study was designed to explore and characterise alterations in the spectrum of volatile compounds that can be detected by the electronic nose in the blood and dialysate of patients undergoing haemodialysis treatment.

Analysis of the blood-side shift

Blood samples were obtained before, and then hourly until the end of dialysis, from 14 haemodialysis patients. Blood samples were obtained also from 15 healthy controls. The blood samples were diluted and incubated under the parameters described in Table 3.3.

The result of the EN analysis of the blood samples is shown in Figure 3.33. The first two principal components account for 81 % of the variance of the original data matrix, which was sufficient to clearly discriminate the sample groups at different time points.

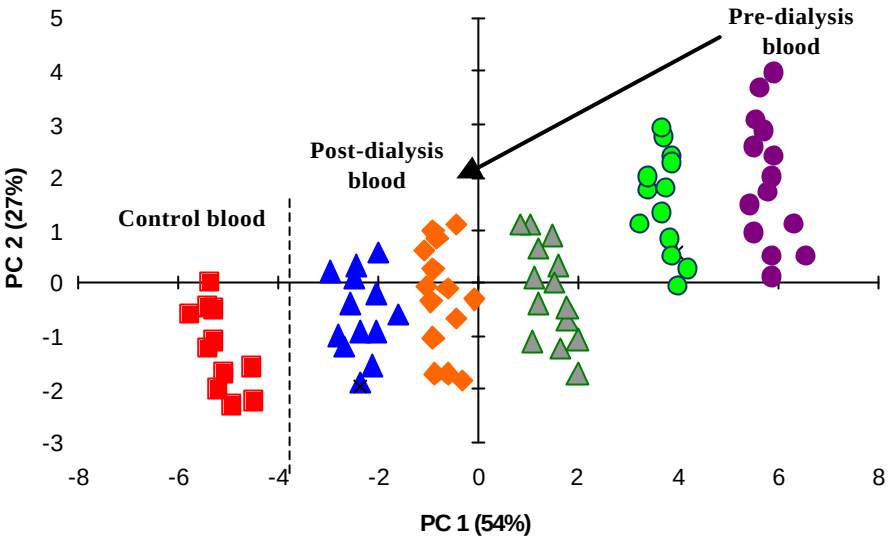

Figure 3.33: Principal component analysis of 15 volunteers (control blood) and 14 haemodialysis patients The uraemic blood samples were taken at the beginning, then every hour and at the end of a single dialysis session.

Key: Pre-dialysis blood (circles), 1 hour after the start of the treatment (circles with green background), 2 hour after the start of the treatment (triangles with grey background), 3 hour after the start of the treatment (diamonds), Post-dialysis blood (triangles), Control blood (squares).

The classification model was built using results of samples from 12 patients and 13 controls and validated by correct classification of the results from 2 patients and 2 controls. As can be seen in Figure 3.34, each group of samples from different time points formed a separate cluster, pre-dialysis samples are clustered on the right, and during the time course of the HD session the sample clusters are plotted progressively

towards the left. Post-dialysis blood samples and control samples are clearly separated at the extreme left of the graph. The discrimination problem was solved by using the first two discriminant functions (s_1, s_2). When the data of 4 unknown samples were inserted into these two discriminant functions, the model reliably predicted the type of sample, i.e. correct classification was possible.

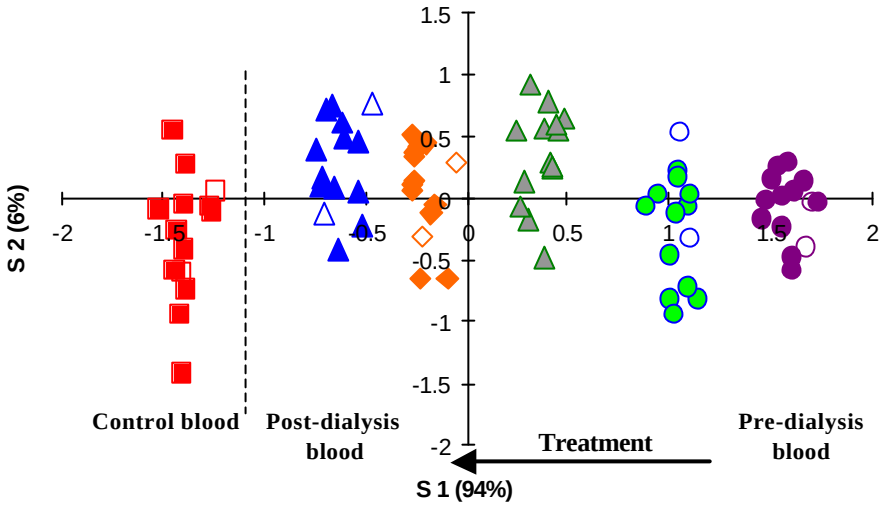

Figure 3.34: Discriminant function analysis of 15 volunteers (control blood) and 14 haemodialysis patients. The uraemic blood samples were taken at the beginning, then every hour and at the end of a single dialysis session.

Key: Pre-dialysis blood (circles), 1 hour after the start of the treatment (circles with green background), 2 hour after the start of the treatment (triangles with grey back ground), 3 hour after the start of the treatment (diamonds), Post-dialysis blood (triangles), Control blood (squares), Cross-validated samples (open symbols).

Analysis of the dialysate--side shift

Dialysate samples (15 ml) were collected directly from the post dialyser circuit of 14 haemodialysis patients (same patients as for blood-side). An aliquot of 2 ml of dialysate was used and incubated at 37 °C for 45 minutes. The larger volume was chosen due to the dilution effect of dialysate and dialysis fluid itself is available in unlimited amounts.

The result of the principal component analysis of dialysate taken at different time points is shown in Figure 3.35. As with blood sample analysis each sample type (corresponding to the time point of sampling) formed a separate cluster, and the first two principal components account for 88 % of the original variance. The inter-cluster variability of the dialysate samples however appears larger than that of the blood samples (Figure 3.33 vs. Figure 3.35).

Again a classification model was built using discriminant function analysis, using 60 samples of dialysate from patients and 13 samples of control dialysate. Different clusters were formed for the different sample types, and the model was validated by cross-validation. Unknown dialysate samples of 2 patients and 2 controls were analysed and correctly identified using the first two discriminant functions (s_1, s_2) (Figure 3.36).

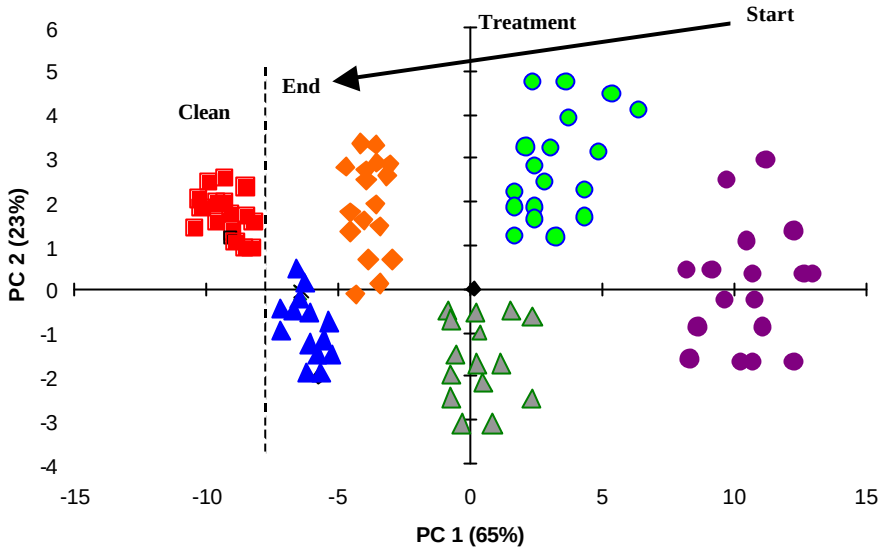

Figure 3.35: Principal component analysis of clean dialysate and dialysate of 14 haemodialysis patients. The dialysate samples were taken at the beginning, then every hour and at the end of a single dialysis session.

Key: Start dialysate (circles), 1 hour after the start of the treatment (circles with green background), 2 hour after the start of the treatment (triangles with grey background), 3 hour after the start of the treatment (diamonds), end-dialysate (triangles), clean dialysate (squares).

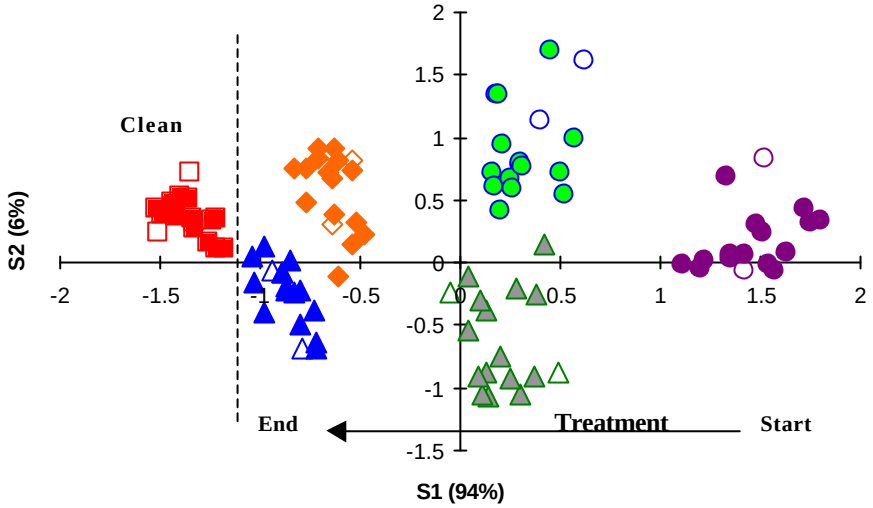

Figure 3.36: Discriminant function analysis of clean dialysate and dialysate of 14 haemodialysis patients. The dialysate samples were taken at the beginning, then every hour and at the end of a single dialysis session.

Key: Start dialysate (circles), 1 hour after the start of the treatment (circles with green background), 2 hour after the start of the treatment (triangles with grey background), 3 hour after the start of the treatment (diamonds), end-dialysate (triangles), clean dialysate (squares).

Long-term Performance (stability)

One of the main drawbacks of electronic nose technology is its lack of long-term reproducibility. This experiment was designed to study the performance of the gas sensor array to blood samples taken over a period of three weeks (9 consecutive dialysis sessions). 11 HD patients were selected and followed for nine consecutive

dialysis sessions. The blood samples were obtained before and after the treatment of each single session.

The result of this long-term experiment is shown in Figure 3.37. As can be seen, control blood is on the left hand side of the graph, post-dialysis is in the middle and pre-dialysis blood is located on the right hand side. No clear discrimination could be obtained as indicated by the overlapping circles (added by author) in Figure 3.37. The first principal components account for 87 % of the variance of the original data matrix. The introduction of a third principal component (see Figure D.1, Appendix D) did not contain any significant information allowing a clear discrimination of the different sample types.

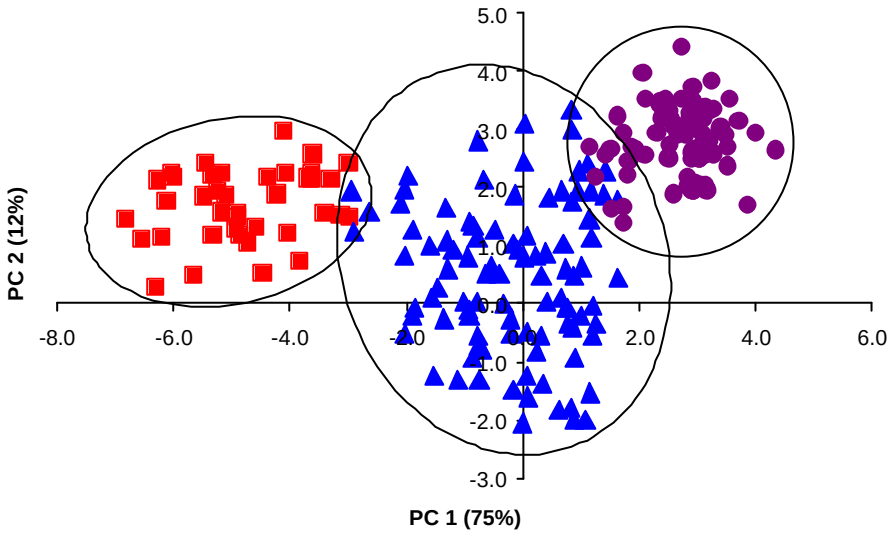

Figure 3.37: Principal component analysis of control blood (45 volunteers, squares), post – dialysis (99 samples, triangles) and pre-dialysis blood (99 samples, circles). The blood samples of 11 HD patients were taken at nine consecutive dialysis sessions.

Based on the principal component analysis a classification model was build using DFA and artificial neural network.

The result of the DFA is shown in Figure 3.38 using 40 control samples and 174 uraemic blood samples (87 samples each). As can be seen, it was impossible to obtain clearly separated clusters (overlapping circles, Figure 3.38). The model was validated by cross-validation. The data features of the withheld samples (5 control samples, 18 uraemic samples) were inserted into the first two discriminant functions (S_1, S_2). The cross-validation revealed that it was impossible to predict the nature of eight unknown samples. One control samples was mistakenly classified as a post-dialysis sample. Among the wrongly classified uraemic samples were four post-dialysis samples and three pre-dialysis samples. Two post-dialysis samples were wrongly identified as control samples and the other two samples were thought to be pre-dialysis samples. All three pre-dialysis samples were mistakenly classified as post-dialysis samples (Figure 3.38).

Based on the cross-validation, the validity of the DFA model was questioned and a more sophisticated classification model was used. The artificial neural network was trained using 60 % of the original data set (27 control samples, 58 post-dialysis samples, and 58 pre-dialysis samples), selected at random. The remaining 40 % (18 control samples, 38 post-dialysis samples, and 38 pre-dialysis samples) of the data set was used to validate the neural network (test data).

The analysis of the test data revealed that the ANN was able to correctly predict all control samples, all pre-dialysis samples and 35 (out of 38) post-dialysis samples. One of the three misclassified post-dialysis samples was identified as a control sample, and two samples were classified as pre-dialysis samples. The result of the ANN validation is summarised in Table 3.4.

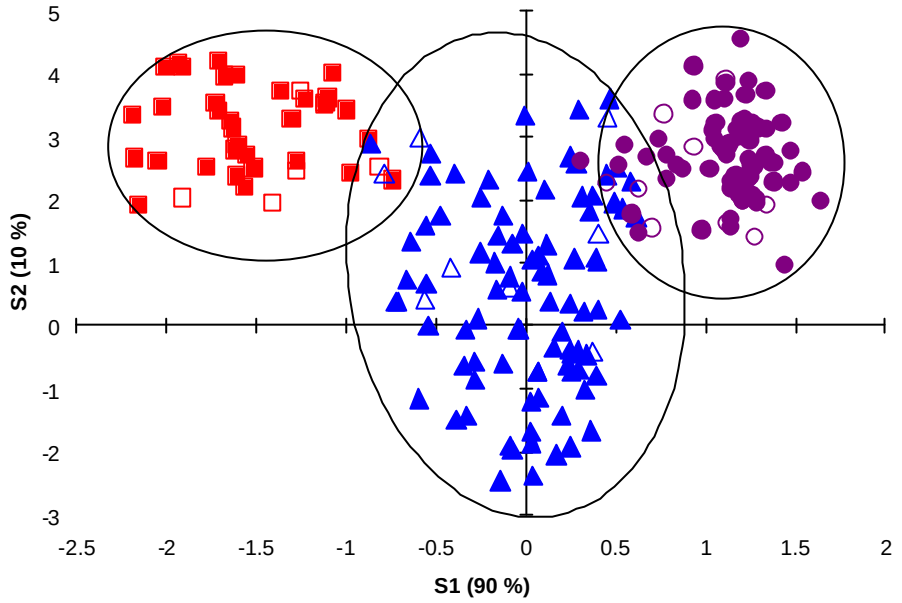

Figure 3.38: Discriminant function analysis of control blood (45 volunteers, squares), post – dialysis (99 samples, triangles) and pre-dialysis blood (99 samples, circles). The uraemic blood samples of 11 HD patients were taken at nine consecutive dialysis sessions. Cross-validation: open symbols (5 control samples, 18 uraemic samples).

Table 3.4: Validation results of the neural network.

	To Control		To Post		To Pre		Total	
From Control	**18**	(19.0%)	**0**		**0**		**18**	(19.0%)
From Post	**1**	(1.0%)	**35**	(37.5%)	**2**	(2.0%)	**38**	(40.5%)
From Pre	**0**		**0**		**38**	(40.5%)	**38**	(40.5%)
Total	**19**	(20.0%)	**35**	(37 5%)	**40**	(42.5%)	**94**	(100 %)

3.3.4 COMPARISON OF TRADITIONAL BIOCHEMICAL MARKERS WITH ELECTRONIC NOSE DATA

This study was designed to compare traditional biochemical markers with electronic nose data. A biochemical blood profile was obtained from 28 HD patients and 15 healthy volunteers. A randomly selected subset (8 controls, 11 HD patients) was used to perform the electronic nose analysis (volatile profile). Finally, any correlation between volatile profile (shift between pre- and post-dialysis samples) and urea reduction ratio (URR). The URR was chosen because it is one most frequently used parameter for assessing the haemodialysis adequacy.

Biochemical Analysis

Five biochemical parameters (urea, creatinine, carbon dioxide, phosphate, and calcium phosphate product) were selected for this analysis and are summarised in Table 3.5.

Table 3.5: Summary of results of biochemical analysis, showing minimal (min) and maximum (max) concentration as well as the mean concentration of control blood, post- and pre-dialysis blood.

		Control blood N=15	**Post – dialysis Blood N=28**	**Pre – dialysis Blood N=28**
Urea [mmol L^{-1}]	Min	3.61	3.0	9.6
	Max	7.37	16.6	36.1
	Mean	4.87	7.45	21.4
Creatinine [µmol L^{-1}]	Min	63.7	183	402
	Max	100.2	659	1194
	Mean	77.2	366.5	788.5
CO_2 [mmol L^{-1}]	Min	23.12	26.0	20.00
	Max	30.38	35.0	31.00
	Mean	25.76	29.8	25.39
Phosphate [mmol L^{-1}]	Min	1.07	0.52	0.79
	Max	1.30	1.65	2.78
	Mean	1.16	0.94	1.64
Ca^{2+} x PO_4^{2-} [mmol L^{-1}]	Min	2.56	1.26	1.90
	Max	3.50	4.31	6.67
	Mean	2.90	2.37	4.17

As expected, small uraemic toxins such as urea and creatinine were effectively removed during haemodialysis. However, the post-dialysis concentrations of these molecules were higher than compared to healthy subjects. These results are well known, but it is almost impossible to present this multivariate data set in a reasonable

way (two- or three-dimensional space) in their raw form. Therefore, the original matrix was reduced in dimensionality using PCA. The results of the PCA are shown in Figure 3.39.

Figure 3.39(a) demonstrates that it was possible to discriminate between post- and pre-dialysis blood (dashed line) by using the first two PCs (axis 1 and 2), which account for 83 % of the variance of the original data matrix. However, it was impossible to separate control blood from post-dialysis blood, but according to Table 3.5, there is a notable difference. After introducing a third PC (vertical axis 3, Figure 3.39b), which accounts for 14 % of variance, it was possible to distinguish between control blood and post-dialysis blood.

The HCA revealed similar results to the PCA, as shown in Figure 3.40. From the original 28-dialysis patients used in this analysis, only in 3 cases (patient: 9, 15, and 24) was it not possible to distinguish between post- and pre-dialysis blood. This is due to small difference between pre – and post-dialysis blood, i.e. there is just a slight decrease of the concentrations of the five biochemical parameters during dialysis treatment (Table D.1, Appendix D).

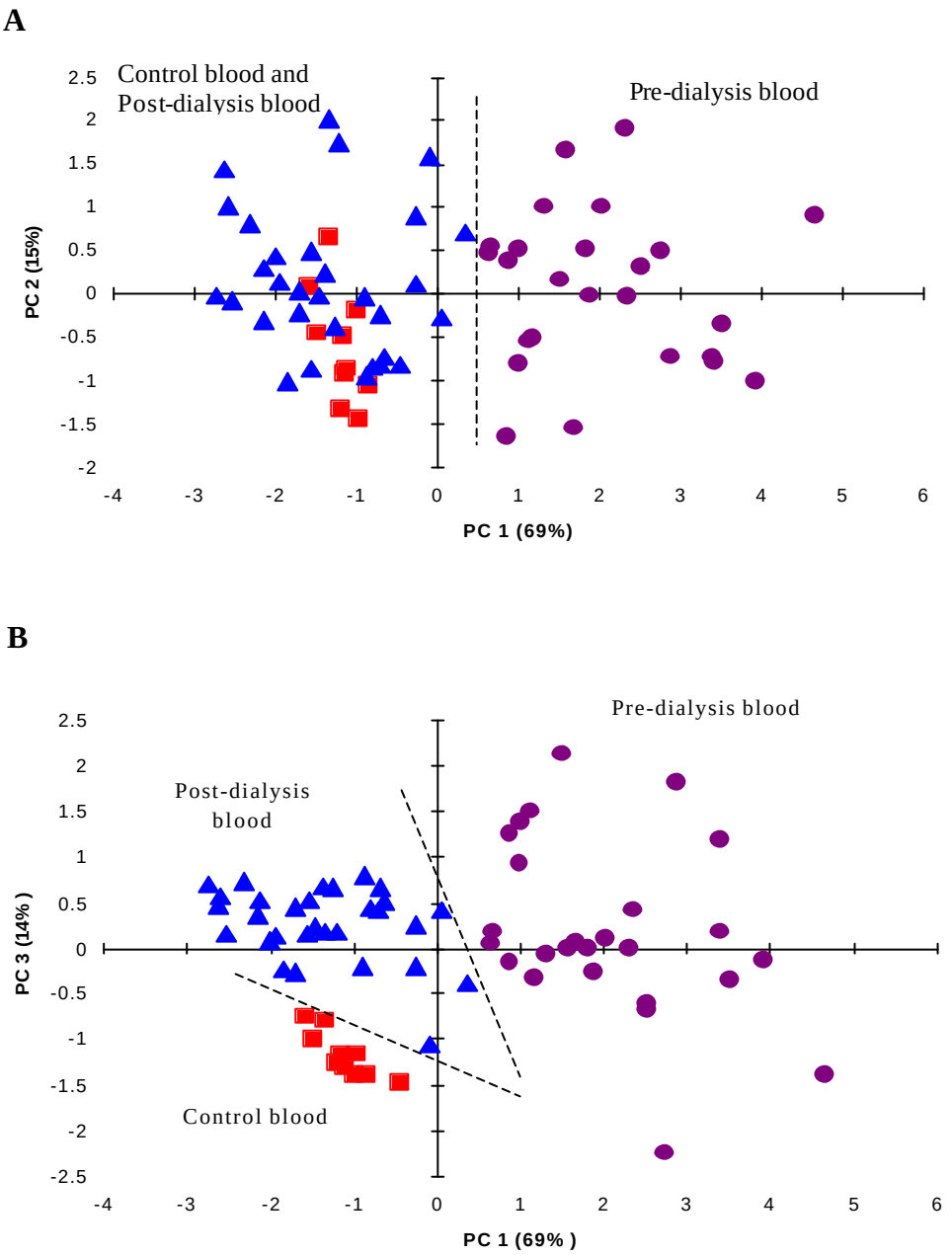

Figure 3.39: Principal component analysis of Control blood (11 samples, squares), Post-dialysis blood (28 samples, triangles) and Pre-dialysis blood (28 samples, circles) based on five biochemical parameters. (A) The first two principal components allow the discrimination between pre-dialysis blood and a mixed cluster containing post-dialysis blood samples and control blood samples. (B) The introduction of a third principal component allows the discrimination between post-dialysis blood and control blood.

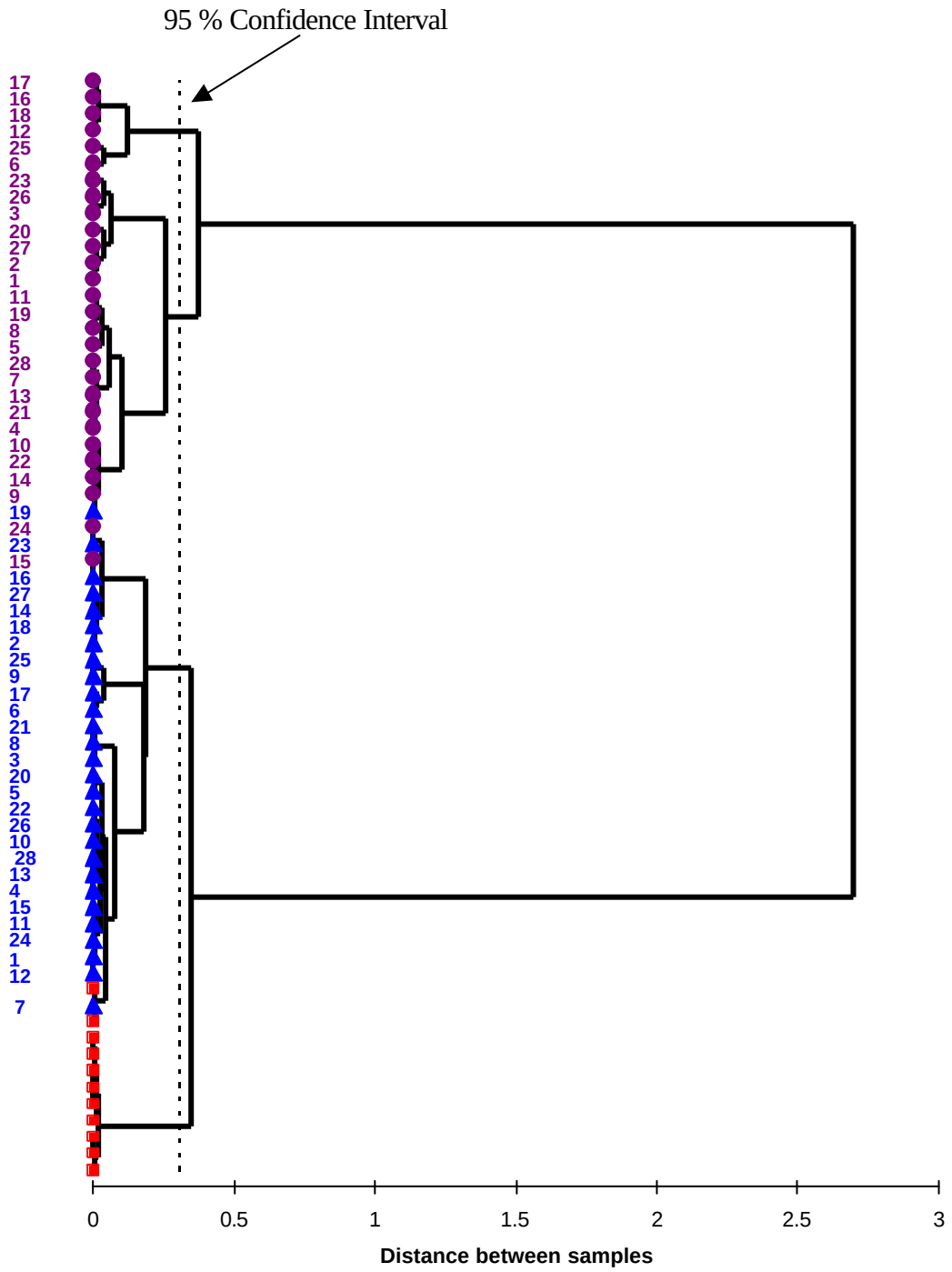

Figure 3.40: Cluster analysis of control blood (squares), post-dialysis blood (triangles) and pre-dialysis blood (circles) based on five biochemical parameters (p=0.05)

Analysis of volatile compounds in blood using an electronic nose

As can be seen in Figure 3.41, a good separation between control blood, pre- and post-dialysis blood was obtained (dashed lines). The first two principal components (PC) account for 94 % of the variance in the original data matrix. The third PC accounts for just 2 % of the variance, and therefore made no significant contribution to the discrimination of the samples.

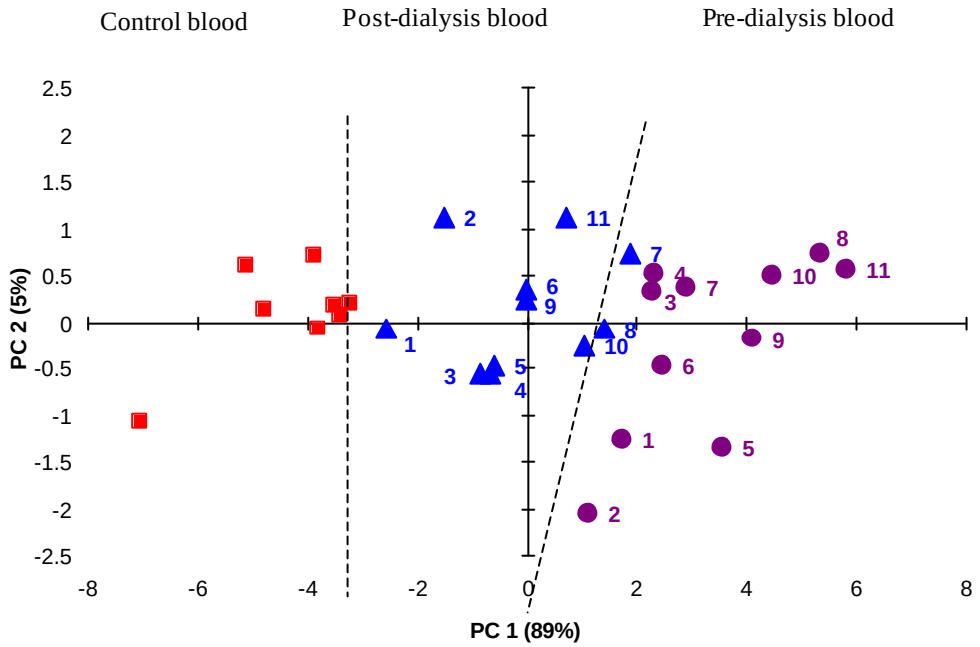

Figure 3.41: Principal component analysis of Control blood (8 samples, squares), post-dialysis blood (11 samples, triangles) and pre-dialysis blood (11 samples, circles) after 45 min incubation at 37 ºC. Post- and pre-dialysis blood samples with the same number belong to the same patient.

Similar results were obtained when using HCA, as shown in Figure 3.42. In one case (patient 9), no difference between pre- and post-dialysis blood was observable. It can be seen that the odour of the post-dialysis sample of patient 1 (PoD1) resembled the odour of control blood, and the odour of the pre-dialysis sample (PD1) was similar to post-dialysis blood.

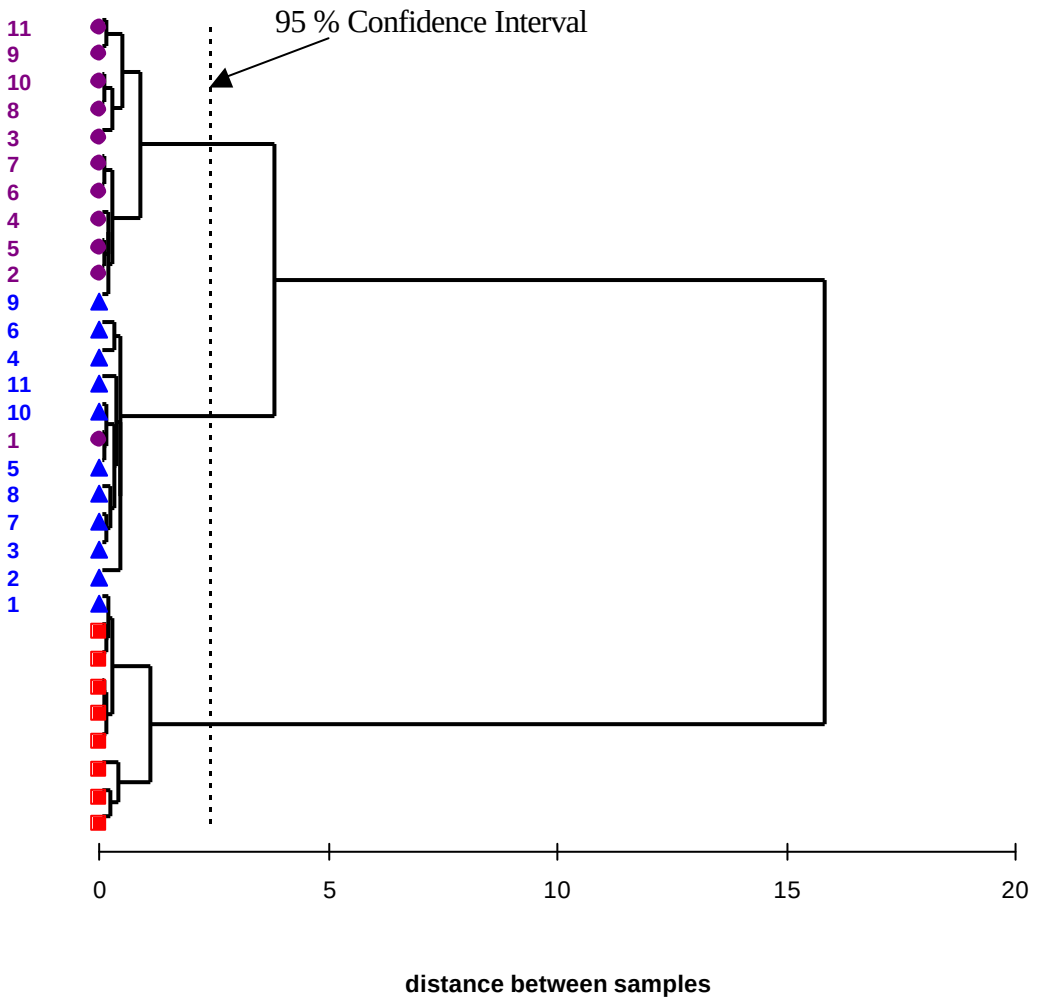

Figure 3.42: Cluster Analysis of Control blood (11 samples, squares), Post- (28 samples, triangles) and Pre-dialysis (28 samples, circles) blood after 45 min incubation at 37 ºC. The post- and pre-dialysis samples with the same number belong to the same patient (p=0.05).

Correlation between volatile profile and urea removal

This experiment was aimed to examine the relationship between the urea removal (expressed as the difference between pre- and post-dialysis concentration) and the volatile shift occurring during a haemodialysis session. In mathematical terms, the volatile shift was expressed as the Euclidean distance between the first two principal components of the pre- and post-dialysis sample of the same patient (see equation 1.7). Blood samples were obtained from 48 HD patients at two different treatment sessions. From all samples, the pre- and post-dialysis urea concentration was determined by the Department of Chemical Pathology at Gloucestershire Royal Hospital (Gloucester, UK). The result of this experiment is shown in Figure 3.43. As can be seen, the urea removal is independent of the distance between the samples. In other words, no correlation between urea removal and volatile shift is observable (R^2 = 0.73).

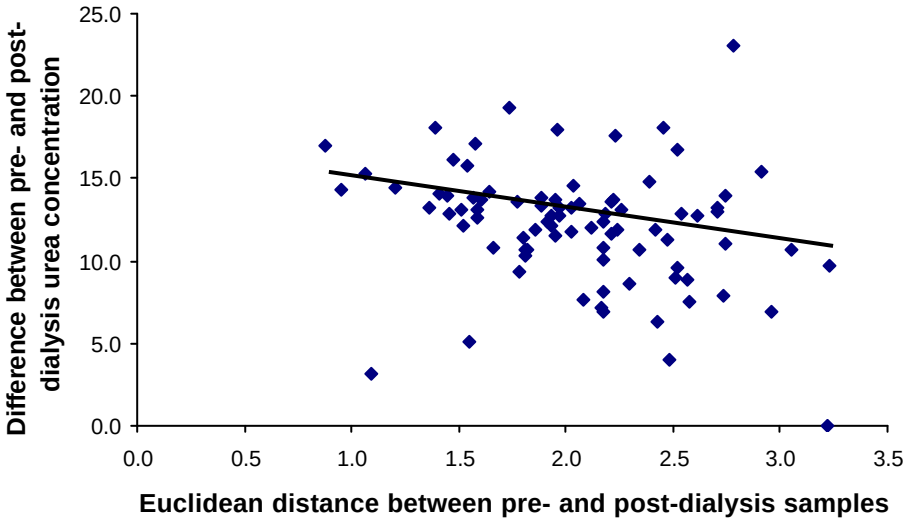

Figure 3.43: Correlation between Euclidean distance and urea removal. The Euclidean distance was calculated from the first two principal components of the pre- and post-dialysis samples.

3.8 SPECIFIC DISCUSSION

The uraemic syndrome is attributed to the retention of a number of different molecules, collectively termed uraemic toxins. However, the toxicity of the syndrome has not been attributed to any single compound; it is most likely to be due to a spectrum of compounds, and indeed the list of potential candidates is complex and growing, and now numbers over 90 (Bergström, 1997). The categorisation of these retained compounds in renal failure has been largely defined by their molecular weight, and degree of protein binding. They comprise a) small water-soluble compounds, MW < 500Da, b) protein bound solutes, and c) 'middle molecules' MW >500Da. Which compounds exert a toxic effect within the body, and which accumulate innocently, is currently not known with certainty (Vanholder *et al*, 2003).

Renal replacement therapy is inevitable for end-stage renal failure (ESRF) patients. The concept of dialysis dose (or adequacy) was introduced around 20 years ago (Canaud *et al*, 2000). Since the early days, urea was and still is employed as a surrogate marker for retained solutes and toxins, and to model the quantity of treatment upon its removal from the body. However, there is still a controversy among nephrologists, whether urea is a suitable surrogate marker molecule or not. Urea is, on one hand, a small molecule with a molecular weight of 60 Da and thus its removal from the blood stream might not reflect the behaviour of other solutes especially larger molecules or protein bound molecules. On the other hand, urea, as such is generally not a particularly toxic compound, and designing treatment strategies using more biologically relevant compounds would be more appropriate, however defining these compounds is problematic and cumbersome (Vanholder *et al*, 1994).

An alternative approach would be to gain information about a wide spectrum of compounds that accumulate in renal failure, and apply the knowledge of changes in the pattern of these compounds to devise and monitor treatment strategies. In this study we employed an electronic nose to provide such information.

3.8.1 OPTIMISATION OF SAMPLING PARAMETER

The aim was to find the optimal conditions under which a separation between pre- and post-dialysis samples is possible with a reasonable amount of blood. As illustrated in Figure 3.2, the initial phase of this research project involved the optimisation of volatile generation (sampling parameters). In other words, it was attempted to release enough volatiles naturally present in uraemic blood only by altering the incubation parameters (temperature, time and volume). This direct release of volatiles from samples was utilised in the past for a broad range of applications. For instance, Guadarrama *et al* (2001) applied it to identify and classify virgin olive oil from different regions. In contrast, for many gas chromatographic (GC) applications pre-column derivatisation is necessary to convert non-volatile substances into volatile derivates. Among the many non-volatile substances analysed by GC are amino acids, steroids or sugars, which are either methylated, acetylated or trimethylsilyliated to become volatile (Pauschmann, 1990). Chandiok *et al* (1997) treated the human vaginal tissue with 10% KOH to release amine compounds which were subsequently detected by an AromaScan electronic nose (today known as Osmetech).

Incubation Temperature

Only a slight improvement in separation of clusters was observed by increasing the static incubation temperature (20 °C ➔ 70 °C). An incubation temperature of 37 °C was chosen due to two main factors. Firstly, the natural body temperature is 37 °C and therefore the HD circuit is operated at this temperature, and secondly a temperature of 70 °C caused a denaturation of the plasma proteins. Both facts mean a simplification of the design of an eventual on-line device. On one hand, an incubation temperature equal to the operating temperature means that no additional heating or cooling element is required. On the other hand, a denaturation of plasma proteins leads to a "fouling" of the flow cell containing the sensor array, which might lead to serious consequences such as cross-infection due to imperfect cleaning and sterilisation process of the on-line device.

Roussel *et al* (1999) reported that the headspace temperature highly influences the repeatability of the measurements, whereby lower temperature (35 °C) yield better results compared to high temperature (> 65 °C). They also found that higher incubation temperatures result in a higher concentrated headspace without significantly improving the outcome (discrimination). Gilbert *et al* (1997) were able to distinguish 12 pure volatile solvents such as butanol and pentanone using a Bloodhound electronic nose after incubation of the samples at 25 °C. Gonzalez-Martin *et al* (2001) used an incubation temperature of 35 °C to characterise vegetable oils. This group found that this temperature is sufficient to release enough information from the samples allowing discrimination between the different types of oil using six metal oxide sensors. In contrast, Guadarrama *et al* (2002) applied a self-made gas sensor array to analyse different plastic films used in the car industry. They were able

to discriminate between different "plastic odours" after a relatively short incubation period of 9 minutes at a high temperature of 80 °C.

For the detection of microorganisms, the incubation temperature is vital since each microorganism has an optimal temperature for growth during which volatile compounds are generated and accumulated in the headspace (Schleger, 1992). Magan *et al* (2001) used an incubation temperature of 30 °C to discriminate between the bacterium *Staphylococcus aureus* and the yeast *Kluyveromyces lactis* in skimmed milk samples. Pavlou *et al* (2000) were able to distinguish between different *Proteus mirabilis, Enterococcus faecalis, Escherichia coli* and *Heliobacter pylori* after an incubation period of approximately 5 hours at 37 °C.

Incubation time

In this specific application, the equilibrium between liquid and gaseous phase was reached after 30 minutes and therefore, an increase of the incubation time from 30 to 90 minutes did not result in a better separation of the individual clusters. The general rule states that the time to reach equilibrium between liquid and gas phase in a given sample vial depends on the ratio between liquid and gas volumes. The higher the liquid volume is the longer the time to reach the equilibrium (Pauschmann, 1990). Gardner and Bartlett (1999) suggest that a longer incubation period should lead to a more homogenous headspace and thus positively influences the sensor response and hence the reproducibility. The incubation times reported in the literature are ranging from a few minutes to several hours depending on the samples. Guadarrama *et al* (2002) for instance, were able to discriminate different plastic films after an incubation time of only nine minutes. Gonzalez-Martin *et al* (2001) choose a volatile

generation time of 7 minutes, which was sufficient to discriminate between different vegetable oils. In contrast, the incubation times are much longer for microbial samples to allow the microorganisms to develop a unique volatile "signature". Canhoto and Magan (2003) found that it was impossible to distinguish between control samples and *Pseudomonas aeruginosa* at a concentration of 10^2 CFU ml^{-1} after an incubation period of 24 hours, however, they were able to distinguish between the same samples after 48 hours of incubation. In a different report Magan *et al* (2001) showed that it was possible to discriminate *Staphylococcus aureus* and *Kluyveromyces lactis* suspensions incubated for two and five hours, respectively from each other independent of the incubation time. However, both microbial suspensions (*S. aureus* and *K. lactis*) "smelled" differently when the incubation time was increased from two to five hours indicating that increasing the incubation period leads to a different headspace.

Nevertheless, an incubation period of 45 min was chosen for the analysis of blood/dialysate samples to ensure equilibrium between liquid phase and headspace as well as a well-mixed headspace.

Sample Volume

The results of these experiments showed that the sample volume did not influence the outcome. This is not a surprise since the only difference between the samples is the concentration of volatiles in the headspace. The applied conducting polymers are able to detect molecules in the ppm range (Gardner and Bartlett, 1999; Frank *et al*, 2000). Stetter *et al* (2000) were investigating the detection thresholds of electronic noses for a range of pure volatile organic compounds (VOCs). For instance, they

found the threshold of ethyl acetate to be between 5 – 25 ppm, for diacetyl between 50 – 100 x 10^{-3} ppm and for butyric acid less than 1 ppm using 13 metal oxide sensors (Fox 3000, Alpha MOS). Therefore, the chosen sample volume of 0.5 ml should generate enough volatiles to cause a notable sensor response and hence, allow discrimination between the samples. Doleman and Lewis (2001) performed similar experiments to Stetter but using conducting polymers. They found that the detection thresholds for VOCs such as pentanol, butanol, heptane and hexane are less than 10 ppm.

Blood Dilution

Blood is the limiting factor in this study, therefore reducing the required amount of blood is a major aim. It was possible to discriminate between the different concentrated blood samples up to a dilution of 1:4. It was impossible to distinguish between a 0.9 % saline solution and 1:10 diluted blood samples. The applied conducting polymers are sensitive enough to be able to distinguish between pre- and post-dialysis blood at a dilution of 1:4. In other words, the headspace concentration at this particular dilution (1:4) was high enough to generate a notable sensor response.

Frank *et al* (2000) reported, that the higher the headspace concentration is the smaller is the deviation of data points within a cluster. This statement is based on the analysis of organic solvents such as toluene, octane, and propanol in concentrations between 1 and 100 ppm. The minimum concentration at which a clear discrimination was still possible was 10 ppm. Our findings presented in this report are in agreement with the findings of Frank *et al* (2000). As shown in Figure 3.21, undiluted blood samples were narrower clustered than the diluted blood samples with the highest

dilution showing the highest intra-sample variability. Therefore, a 1:4 dilution was considered as a good compromise to reduce the blood consumption, as it was possible to discriminate between control blood and a blank sodium chloride solution. The analysis of 1:4 diluted pre- and post-dialysis blood samples revealed that sufficient information could be extracted from the samples to distinguished between them (Figures 3.23 and 3.25).

3.8.2 VALIDATION AND EVALUATION OF ELECTRONIC NOSE

The validation and evaluation of the electronic nose involved the analysis of "uraemic" blood samples under optimised conditions as well as the study of the reproducibility of the sensor array.

Reproducibility of sensor response

As shown in Figure 3.27, the individual sensors showed a small variation between different days except sensors 11 and 14, which showed a significant difference. In general, electronic nose sensors are characterised by a high sensor drift (Gardner and Bartlett, 1999). Sensor 11 had with about 60 % the biggest variation. Sensor drift is generally caused by environmental factors such as humidity or temperature or through contaminations (Gardner and Bartlett, 1999; Persaud and Travers, 1997). Environmental factors can probably be excluded as a reason for the observed sensor drift due to the air-conditioning of the laboratory. Contamination drift in conducting polymers is primarily caused by strong acids (Gardner and Bartlett, 1999). Our findings are in agreement with Gibson *et al* (1997), who also used a Bloodhound

BH114 instrument. This group analysed different bacterial specimens and discovered the existence of consistent patterns, characteristic for each microbial species without the presence of a significant sensor drift. Vanneste (1997) observed that conducting polymers were sensitive to water vapour. In addition, they reported a slow, but significant increase of the sensors' resistance with time (drift) generated by a slow dedoping of the sensor material. Although no significant drift was observed in this work, all sensors showed small differences from day to day (5 – 15 %), even though extreme care was taken to reproduce all experimental conditions completely. Nevertheless, sensor 11 and 14 were not considered in further experiments due to their high variability (Figure 3.27).

Analysis of control blood and "uraemic blood" under optimised conditions

The results of our studies show that by EN analysis, blood samples of haemodialysis patients can be reliably distinguished from those of normal control subjects (Figures 3.28). A slight overlap between pre- and post-dialysis samples was observed when different dialysis sessions were considered, as illustrated in Figure 3.38. The reasons for this overlap are not entirely clear. It could be caused by day-to-day variation of the sensors (drift), which is, however, not very likely (compare Figure 3.27). There is a huge variability within individual patients (Table 3.5), which might influence the data analysis. In contrast, the day-today variation within a patient is minimal (stable HD patients). Nevertheless, it was still possible to distinguish between the majority of pre- and post-dialysis samples (Table 3.4) when a more sophisticated data analysis method was applied. Artificial neural networks are able to cope with non-linear relationships between samples. During the dialysis procedure

there is a shift in the profile towards that of the control sample profile, and the similar phenomenon is detectable in dialysate samples (Figures 3.33, 3.34, 3.35, and 3.36). The conducting polymers used in the EN are very sensitive (0.1 - 5 ppm) and there is a linear relationship between sensor response and concentration (Schiffman *et al*, 1997). Through our data pre-processing (normalisation), the concentration impact on the sensor response was only removed within a particular sample group but not between different groups (time points). This was necessary due to the variability between individual patients. Consequently, each sample is described by numerous volatiles present at the time rather than a single highly concentrated compound. The alteration in the blood profiles in the direction of the control suggests that the changes measured are due to substances being removed from the blood during dialysis. The dialysate profile differs most from control dialysate at the start of dialysis, and the profile changes towards the control sample with time, which corresponds to a higher dialysate concentration of reacting compounds at the start of dialysis compared to the end. This would correspond to the higher removal of substances from the blood at the start of dialysis, and lower concentrations towards the end. This approach would accommodate the current thoughts about the dialysis procedure.

Like the human olfactory system, the EN responds to volatile compounds. The volatility of molecules is influenced by many parameters including concentration, equilibration temperature, equilibration time, and viscosity of the sample (Seto, 1994). Volatile substances are generally characterised by a small molecular weight (MW < 500 Da) and their polarity (Gardner and Bartlett, 1999). At this level of the research project, it is unknown which molecules in the blood/dialysate samples are responsible

for the sensor response. Chronic renal failure is characterised by the accumulation of waste products and excessive body fluids. These metabolic waste products as well as body fluids are normally excreted in urine. Therefore, "uraemic" blood contains numerous compounds, some of them are volatile others are not. In the past, many groups tried to identify "uraemic" molecules, which are generally divided into three groups: small, middle and large molecules (Levy *et al*, 2001). Volatile compounds are generally small and polar (Gardner and Bartlett, 1999). In the past, several research groups identified these molecules using mainly gas chromatography and gas chromatography – mass spectroscopy. The range of molecules retained in uraemia is broad including free organic acids, phenolic compounds, aliphatic amines, alcohols, aldehydes, ketones and guanidines (Liebich and Woell, 1977; Niwa *et al*, 1981; Baba *et al*, 1984; Liebich *et al*, 1984). All of them are present in elevated concentrations in CRF patients. Bowen *et al* (1975) investigated benzyl alcohol present in blood of CRF patients. They found elevated values of benzyl alcohol in dialysis patients before the session and lower levels after the treatment. Benzyl alcohol was not found in normal controls. Baba *et al* (1984) analysed serum aliphatic amines using HPLC. They found a six-fold increase of methylamine and dimethylamine in uraemic serum compared to normal control subjects. The degree of removal of these compounds is smaller than for urea and creatinine and is approximately 55% (Baba *et al*, 1984; Lichtenberger *et al*, 1993). The same group found similar concentration of the volatile ethanolamine in pre-dialysis serum and control serum, but a two-fold increased level in post-dialysis samples (Baba *et al*, 1984). Other investigators found volatiles such as methylmercaptan (Dowty *et al*, 1975), acetone, 2-butanone, chloroform, benzene, toluene, pyridine, dipropylketone, cycloheaxanone, and 4-heptanone in uraemic blood

(Liebich and Woell, 1977). All these substances are characterised by a relatively small molecular weight (MW < 500) and are retained in CRF patients. However, due to their low molecular weight they are most likely to be effectively removed during a haemodialysis session, leading to a decreased concentration in post-dialysis samples.

In addition to substances being removed from the blood by dialysis, which will appear in the dialysate, compounds are also generated during dialysis procedure due to increased oxidative stress (Tetta *et al*, 1999; Erdogan *et al*, 2002). The increased oxidative stress in HD patients is caused by the bioincompatibility of the haemodialysis membrane and the imbalance between oxidant production and anti-oxidant activity. It is reported, that haemodialysis membranes can induce the production of free radical, in particular oxygen radicals, as a result of neutrophil or monocytes activation (Ceballos-Piot *et al*, 1996; Nourooz-Zadeh, 1999; Hegebrant and Hultkvist-Bengtsson, 1999; Srinivasa *et al*, 2001). Reactive free radicals can induce lipid peroxidation, a chain reaction in which one radical can cause the oxidation of a comparatively large number of substrate molecules (polyunsaturated fatty acids) (Abuja and Albertini, 2001). The end products of lipid peroxidation are aldehydes (malonaldehyde, propanal), ketones (acetone) and small carbohydrates (ethane, pentane) (Hageman *et al*, 1992; Capodicasa *et al*, 1999). One example of this is the volatile compound isoprene, which has been detected in the breath of dialysis patients following dialysis (Lirk *et al*, 2003). Isoprene is a highly lipophilic compound that is dialysed minimally, and it is unlikely that it is responsible for any of the changes that we have seen in the profile of the dialysate. But, as we are observing changes in the pattern of sensor response, we cannot exclude the possibility that compounds may appear and disappear during dialysis, and contribute to the pattern of

response that we see in the blood samples. In addition, the currently used marker substances urea and creatinine are not contributing to the sensor response as illustrated in Figures 3.30 and 3.31. There was no observable difference between unspiked and spiked samples leading to the conclusion that urea and creatinine are not volatile under the conditions used in this work.

3.8.3 ELECTRONIC NOSE VS TRADITIONAL BIOCHEMICAL MARKERS

This experiment has shown that by application of multivariate methods combined with traditional biochemistry (Figures 3.39 and Figure 3.40) and modern electronic nose technology (Figure 3.41 and 3.42), respectively, it was possible to discriminate "uraemic" blood from control blood. However, more important is the possibility to distinguish between pre- and post-dialysis blood. It has to be mentioned, that PCA as well as HCA are exploratory data analysis techniques, whose main goal is to visualise the original data matrix, i.e. they are not classification methods. The application of these methods to traditional biochemical data (Figures 3.39 and 3.40), demonstrated the efficacy of these tools, even when the outcome was not "blinded".

As mentioned previously, urea is currently the most frequently applied surrogate marker for assessing the haemodialysis adequacy, whereas creatinine can also be used to assess the nutritional status of HD patients. It is well known that the prescribed dialysis dose differs from the actually delivered dialysis dose (Manzoni *et al*, 1996; Keshaviah, 2002). Therefore, it is necessary to quantify the delivered dialysis dose because the adequacy of the dose has a profound effect on patient morbidity and mortality (Manzoni *et al*, 1996; Shak, 1999). For the quantification of the dialysis

dose two parameters are most commonly used, namely the urea reduction ratio (URR) and the normalised dose of dialysis (Kt/V) (Lowrie, 2000; Lindsay and Sternby, 2001). Both parameters are based on urea. The URR is calculated from the pre-dialysis and post-dialysis blood urea nitrogen value, whereas the Kt/V value is derived from urea kinetic modelling (Kemp *et al*, 2001; Levy *et al*, 2001). In the past several studies showed that an increased Kt/V index leads to a reduced morbidity and mortality risk in HD patients. Held *et al* (1996) analysed 7,096 patients and saw an average 7 % decrease in mortality for every increase in Kt/V of 0.1 up to a value of 1.3. Similar results were reported by Parker *et al* (1994) who found a lower mortality when the Kt/V index was increased from 1.2 to 1.4. However, there is a controversial discussion about whether these parameters are appropriate or not (Lowrie, 2000; Vanholder *et al*, 2002). It has been shown that oversimplification of the "dialysis dose" to the Kt/V index might lead to dramatic underdialysis (Canaud *et al*, 2000). Le Febvre *et al* (1991) showed that the Kt/V value delivered was less than the prescribed value by around 5 % in approximately 60 % of dialysis treatment. In addition, the Kt/V value assesses only the removal of small water-soluble compounds from the body (Vanholder *et al*, 2002). Hence, the molecular size of urea means that convective and/or diffusive transport of larger molecules is unlikely to be described by urea kinetics (Vanholder *et al*, 2002; Lowrie, 2000). Both values (Kt/V and URR) assume a dialysis frequency of three times per week. However, recently published data suggest that 5 % of all American patients skip a dialysis session in any month (De Palma and Pittard, 2001). Other pitfalls in using the URR or Kt/V value come from the incorrect post-dialysis blood sampling such as urea-rebound effect, sample dilution with dialysis fluid or blood recirculation. (De Palma and Pittard, 2001).

However, careful post-dialysis blood sampling minimises the influence of these problems (Levy *et al*, 2001).

In contrast, the electronic nose detects numerous compounds simultaneously. Among the possible candidates (see previous section) are the volatiles p-cresol, phenols, reactive carbonyl compounds and benzylalcohol that have also been found and implicated as uraemic toxins, and potentially these compounds are being detected by the EN. As illustrated in Figure 3.43 the electronic nose pattern (or signature) does not reflect the traditional way of assessing the treatment adequacy. In other words, no correlation between volatile shift (as shown for instance in Figures 3.28 or 3.33) and urea reduction ratio could be established. On one hand, urea itself does not contribute to the sensor response (Figures 3.30 and 3.31). On the other, it was possible to follow the volatile shift occurring during a single HD session as illustrated in Figures 3.33 and 3.35. Although not analysed by GC-MS, the EN pattern of response is likely to be to many compounds rather than one, and importantly the toxicity of uraemia similarly will be to many compounds rather than just one. Currently definition of the response in terms of identifying the compounds has not been performed, and this of course could produce a much more detailed picture. However, an equally valid approach is to define the profile of blood or dialysate, which is associated with better clinical outcomes. This approach has the advantage that it produces a pattern of information about the concentrations of compounds, but also information regarding concentrations relative to other detected compounds. The measurement of one potential toxin without regards for other compounds, or their potential interactions in the uraemic milieu, may

produce a false impression and the overall pattern or balance between substances may be more important.

In the past only a few applications have been described in the literature where electronic noses have been used for renal diseases. Among these is the work of Lin *et al* (2001), who applied an electronic nose for the diagnosis of uraemia. This group found marker substances in the breath of chronic renal failure patients such as di- and trimethylamine, which allowed the differentiation between healthy controls and uraemic patients. They concluded that the electronic nose is a potential tool for diagnosis of uraemia, however, they did not utilise these finding to develop an on-line monitoring system based on breath analysis. Di Natale *et al* (1999) were able to detect traces of blood in urine. However, they could not give an explanation which volatiles are responsible for the sensor response. Interestingly, they found a qualitative correlation between the first principal component and the amount of blood present in urine.

The presented method is not fully optimised yet. The electronic nose, however, was reliably able to distinguish blood samples of HD patients from those of normal control subjects. During the dialysis procedure a profile shift towards the control profile was observed. A similar phenomenon is detectable in dialysate samples. The sensors showed good reproducibility apart from sensor 11 and 14. It offers the possibility to monitor potential uraemic toxins as an automated, on-line system and hence improve the quality/efficacy of haemodialysis.

Chapter 4

Electronic nose for the early detection of pulmonary tuberculosis

4.1 INTRODUCTION

In 1993, the World Health Organisation (WHO) declared tuberculosis (TB) a global emergency. It is estimated that over 1/3rd of the world's population is infected with *Mycobacterium tuberculosis*. An estimated 8 – 9 million new cases occur each year with over 2 million deaths (Dolin *et al*, 1994; Frieden *et al*, 2003). The majority of cases occur in sub-Saharan Africa, South and Southeast Asia, Latin America and the Caribbean (Raviglione *et al*, 1992; Raviglione *et al*, 1995; Shafer and Edlin, 1996). The recent increase in the global TB burden is related to the continuous increase in HIV infections (Frieden *et al*, 2003). The early diagnosis of TB followed by appropriate treatment can dramatically reduce the mortality. Currently, TB is diagnosed by chest X-ray, staining of mycobacteria in sputum (Ziehl-Neelsen), and culture. These methods are not satisfactory. Chest X-ray is not specific enough. A suspected chest X-ray can be caused by other lung diseases and previous TB. Microscopy can detect mycobacteria in sputum but species identification is impossible and it lacks sensitivity (Perkins, 2000). Culture and identification of the isolated mycobacteria is the gold standard. However, this can take up to 4 – 8 weeks to get a final result (Perkins, 2000). Nevertheless, the WHO and the International Union against Tuberculosis and Lung Disease (IUTALD) recommend the Ziehl-Neelsen staining for new case findings (Perkins, 2000; Frieden *et al*, 2003). The staining of a sputum smear sample (followed by microscopic examination is an inexpensive method and is very specific in high prevalence environments. The shortcomings of ZN microscopy such as its low sensitivity, especially in HIV positive patients, the operator dependency and preparation time limit the quality of this diagnostic tool in high burden countries (Perkins, 2000; Cleeff *et al*, 2003). In the

past, new research was undertaken to develop new diagnostic tests fulfilling the requirements set by the WHO. These include: high sensitivity and selectivity, inexpensiveness, robustness and simplicity (WHO report, 1997). The main focus was direct towards antibody/antigen detection assays or nucleic acid amplification reactions (Frieden *et al*, 2003). Against this background, we investigated the possibility of an electronic nose as an early detection system for *M. tuberculosis* in both culture and sputum samples.

4.2 SPECIFIC MATERIAL AND METHODS

4.2.1 BACTERIA ISOLATES, SPUTUM AND CLINICAL SPECIMENS

Bacteria isolates

All *Mycobacterium spp* (*Mycobacterium tuberculosis*, RIVM myc 4514; *Mycobacterium avium*, RIVM myc 3875; *Mycobacterium scrofulaceum*, RIVM myc 3442) were obtained from the National Institute of Public Health and the Environment (RIVM) (Bilthoven, NL). *Pseudomonas aeruginosa* (AMC 23123) was isolated at the Academic Medical Centre (AMC, Amsterdam, NL).

Sputum samples

Sputum samples (1 ml) were collected from non-TB patients attending the chest unit of the AMC. A sputum pool (N=25) was prepared by thoroughly mixing individual sputum samples for 12 hours at 4 °C. The sputum pool was stored at - 70°C until the analysis was performed.

Clinical Specimens

337 sputum samples were obtained from patients attending The Yeta District Hospital in Sesheke, Zambia (87), South Africa (200) (through the WHO Specimen Bank) and the AMC. All patients were examined by ZN staining, liquid culture and chest X-ray examination. Culture was used as the "gold standard" in this study for tuberculosis. Furthermore, from all patients the HIV status and their smoking habits were investigated (Table 4.1). Seven TB negative patients had confirmed pneumonia. The collected sputum samples were stored at -70°C until the analysis was performed.

Table 4.1: Details of clinical samples showing the median age with interquartile range, TB status (culture), HIV status and smoking habits. The total number is given in parenthesis.

	Median age (1^{st}, 3^{rd} quartile)	TB+ (N)	HIV and TB+ (Total HIV+)	Smokers and TB + (Total smokers)
Male	36 (29 – 47.5)	126 (210)	63 (83)	55 (68)
Female	36 (31 – 46)	62 (120)	38 (60)	4 (4)
Total	***36 (29 – 47)***	***188 (330)***	***101 (143)***	***59 (72)***

4.2.2 SAMPLE PREPARATION

Preparation of culture samples

All bacteria isolates were cultured in Middlebrook 7H9 medium with OADC enrichment. The bacteria were incubated at 37 °C until an optical density (420 nm) of 0.15 (≈ 1 x 10^8 bacteria ml^{-1}) was reached. Subsequently, the liquid culture was cooled

to 4 °C and allowed to equilibrate for at least 20 minutes to minimise the loss of volatiles during the transfer into smaller headspace vials. 2 ml of the "cold" culture was transferred into a 5 ml headspace vial (Macherey and Nagel, UK) and immediately sealed with a silicon/teflon crimp cap (Jaytee Bioscience Ltd., UK). The headspace was allowed to equilibrate for 45 minutes at 37 °C.

Dead bacteria were obtained by heating the *M. tuberculosis* suspension for 30 minutes at 60 °C. No growth was obtained after inoculation of 10^8 bacteria ml^{-1} in Middlebrook 7H9 or Loewenstein-Jensen medium.

Preparation of spiked sputum samples

The sputum pool (N=25) was spiked with various numbers of different bacteria isolates including *M. tuberculosis, M. avium and P. aeruginosa* as well as a mixture of *M. tuberculosis* and *P. aeruginosa*, which served as a mixed infection sample (50:50). All bacteria were cultivated in Middlebrook 7H9 (+OADC). The sputum samples were spiked as follows: 1 x 10^8 mycobacteria ml^{-1}, 1 x 10^7 mycobacteria ml^{-1}, 1 x 10^5 mycobacteria ml^{-1} and 1 x 10^4 mycobacteria ml^{-1}. 1 ml of sputum and 1 ml of the "cold and equilibrated" culture were transferred into a 5 ml headspace vial (Macherey and Nagel, UK) and subsequently sealed with a silicon/teflon crimp cap (Jaytee Bioscience Ltd, UK). The headspace was allowed to equilibrate for 120 minutes at 37 °C. As control samples served unspiked sputum and control medium (Middlebrook 7H9 + OADC).

Clinical sputum samples

The frozen sputum samples were defrosted on ice to minimise the loss of volatiles. An aliquot of 0.5 ml of "well-mixed" sputum was transferred into a sterile 5 ml headspace vial (Macherey and Nagel, UK) and mixed with 0.5 ml of a 1 M NaCl solution (4 °C) and subsequently sealed with a crimp cap with Silicon/Teflon septum (Jaytee Bioscience Ltd, UK).

Positive control samples (spiked sputum) were prepared by mixing 0.5 ml of the sputum pool with 0.5 ml of a *Mycobacterium tuberculosis* suspension (2×10^8 bacteria ml^{-1}). Negative control samples were prepared by mixing 0.5 ml of the sputum pool with 0.5 ml of a 1 M NaCl solution (4 °C). All samples were incubated at 37 °C for 330 minutes prior to the headspace analysis.

The protocol for clinical sputum samples was slightly modified compared to protocol for spiked sputum samples. This was necessary due to the small sample volume (< 1ml) obtained from the WHO specimen bank.

4.2.3 HEADSPACE ANALYSIS

The incubated sample vials were connected to the electronic nose by inserting a needle into the headspace of the sample (see chapter 2). The sampling profiles used in this study are summarised in Table 4.2. The adsorption and desorption time was increased for the analysis of sputum samples compared to the profile used for liquid culture samples. This was necessary due to the higher complexity, variability and heterogeneity of sputum.

Table 4.2: Sampling profiles used for the analysis of liquid culture and sputum samples (Pavlou *et al*, 2004).

	Samples	
	Liquid	**Sputum**
Time delay (s)	5	5
Adsorption time (s)	6	7
Desorption time (s)	14	21
Baseline length (s)	5	5
Hold time (s)	0	0

4.2.4 DATA ANALYSIS

The original data sets were pre-processed by normalising the sensor response to vector length one. Principal component analysis and discriminant function analysis were used for liquid culture samples and spiked sputum samples. For the determination of the detection limit, the sensor response was not normalised.

For clinical specimens, principal component analysis and an artificial neural network (ANN) were applied. The ANN was trained using 70 % of the original samples (Table 4.3). In this study, a backpropagation network with a sigmoid transfer function was applied. The performance of the ANN was evaluated using the test set (Table 4.4). The training and evaluation of the artificial neural network was based on the clinical samples, i.e. no "artificial" samples were involved (pos. and neg. controls). Due to the small sample size pneumonia cases in the original sample set, they were excluded from the ANN analysis.

Table 4.3: Details of patients used to train the neural network (training set).

	Median age (1^{st}, 3^{rd} quartile)	TB+ (N)	HIV and TB+ (Total HIV+)	Smokers and TB + (Total smokers)
Male	37 (29 – 48)	86 (126)	49 (64)	41 (51)
Female	36 (29 – 47)	47 (70)	29 (43)	2 (2)
Total	***36.5 (29 – 47.5)***	***133 (196)***	***78 (107)***	***43 (53)***

Table 4.4: Details of patients used to validate the neural network (test set).

	Median age (1^{st}, 3^{rd} quartile)	TB+ (N)	HIV and TB+ (Total HIV+)	Smokers and TB + (Total smokers)
Male	34.5 (32 – 50)	40 (84)	14 (19)	14 (17)
Female	36 (33 – 42)	15 (50)	9 (17)	2 (2)
Total	***36 (32 – 45)***	***55 (134)***	***23 (36)***	***16 (19)***

4.3 RESULTS

4.3.1 ANALYSIS OF LIQUID CULTURE SAMPLES

Analysis of Mycobacterium spp. and Pseudomonas aeruginosa

The "smell" of three *Mycobacterium spp.* cultures (*M tuberculosis, M. avium, M. scrofulaceum*) and one *Pseudomonas aeruginosa* culture were analysed and compared to the "odour" of blank medium. The EN raw data were analysed by PCA followed by DFA. The PCA plot (Figure 4.1) illustrates that it is possible to distinguish between the different bacteria isolates *in vitro*.

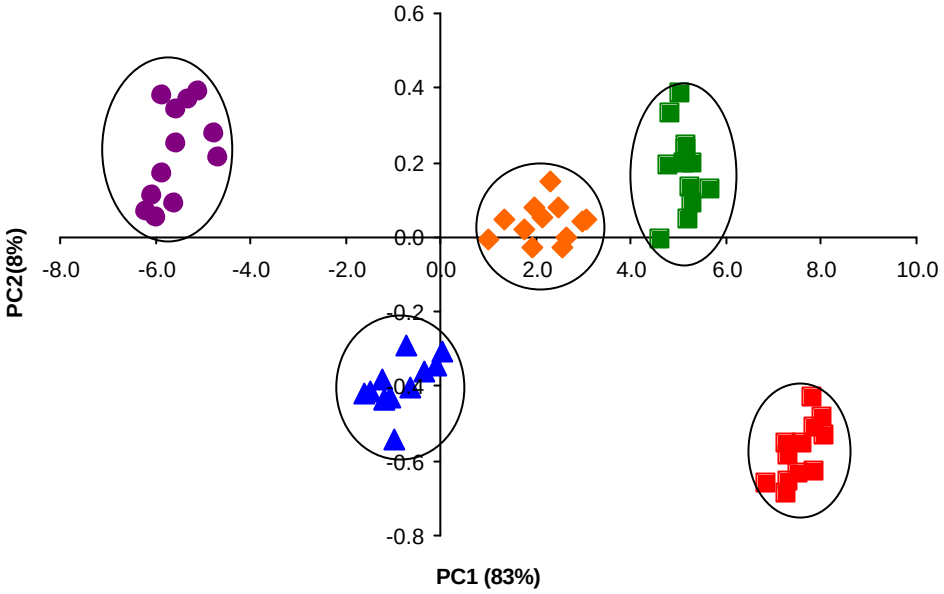

Figure 4.1: Principal component analysis showing the distinguished clusters of liquid cultures of *M. tuberculosis* (triangles, 12 samples), *M. avium* (crosses, 12 samples), *M. scrofulaceum* (diamonds, 12 samples) and *P. aeruginosa* (circles, 12 samples) and blank medium (squares, 12 samples).

The DFA model was built on the first four principal components. Figure 4.2 shows the result of the DFA analysis. It was possible to distinguish between the different bacteria classes using the first two discriminant functions (S_1, S_2). The three different *Mycobacterium spp.* were grouped closely together, but still allowing discrimination (Figure 4.2). The DFA model was validated by the analysis of 15 "unknown" samples. All unknown samples were correctly classified as either one of the three *Mycobacterium spp.*, *P. aeruginosa* or blank medium.

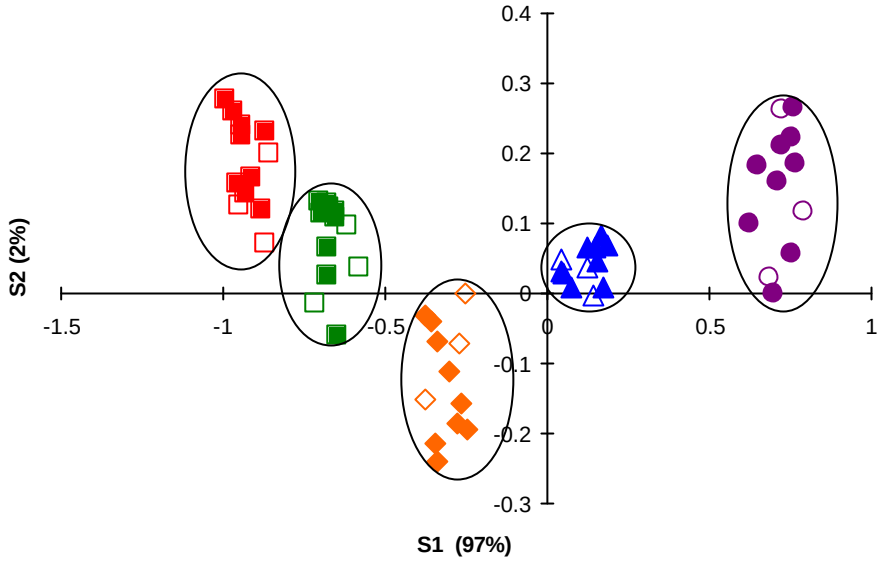

Figure 4.2: Discriminant function analysis of liquid cultures of *M. tuberculosis* (triangles, 12 samples), *M. avium* (green squares, 12 samples), *M. scrofulaceum* (diamonds, 12 samples) and *P. aeruginosa* (circles, 12 samples) and blank medium (red squares, 12 samples). Cross-validation: 15 samples (three from each group) were withheld from building the DFA model but subsequently assigned correctly once the model was built (open symbols).

Determination of the detection limit for M. tuberculosis

The detection limit of the electronic nose for *M. tuberculosis* was determined in culture. Six different concentrated *M. tuberculosis* suspensions (1 x 10^3 mycobacteria ml^{-1} – 1 x 10^8 mycobacteria ml^{-1}) were analysed and compared to blank medium. The EN raw data were analysed by PCA followed by DFA.

The result of the PCA analysis is shown in Figure 4.3. As can be seen, samples with a concentration equal or higher than $1x10^4$ mycobacteria ml^{-1} can be distinguished from blank medium. Samples with a concentration of $1x10^3$ mycobacteria ml^{-1} formed one cluster with blank medium. This indicates that the detection limit is 1×10^4 mycobacteria ml^{-1} as indicated by the dashed line in Figure 4.3. It is also observable that samples with the same concentration form a separate cluster and that different clusters can be discriminated from each other.

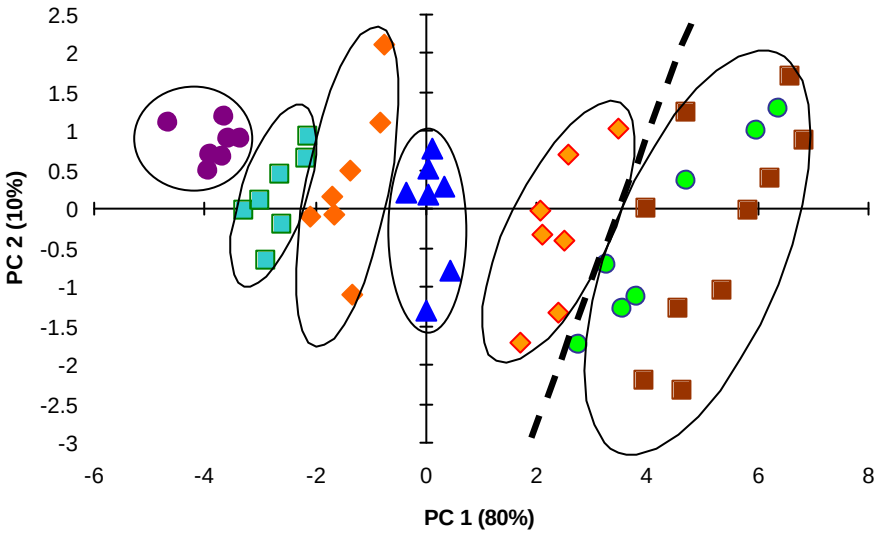

***Figure 4.3*:** PCA plot showing the distinguished clusters of liquid cultures of different concentrated *M. tuberculosis* suspensions. The dashed line indicates the detection limit.

Key: Blank medium (brown squares), $1x10^3$ mycobacteria ml^{-1} (blue circle, green background), $1x10^4$ mycobacteria ml^{-1} (red diamonds, orange background), $1x10^5$ mycobacteria ml^{-1} (blue triangles), $1x10^6$ mycobacteria ml^{-1} (orange diamonds), $1x10^7$ mycobacteria ml^{-1} (light blue squares), $1x10^8$ mycobacteria ml^{-1} (purple circles)

Based on PCA analysis, a classification model was built. The result of the DFA analysis is shown in Figure 4.4. The DFA model was validated by the analysis of 12 "unknown" samples. Two out of 12 unknown samples were incorrectly classified as blank medium (Figure 4.4). Both incorrectly classified samples belonged to the group containing 1 x 10^3 mycobacteria ml $^{-1}$. All other unknown samples were correctly identified. Therefore the detection limit was determined to be as low as 1 x 10^4 mycobacteria ml^{-1} (Figure 4.4).

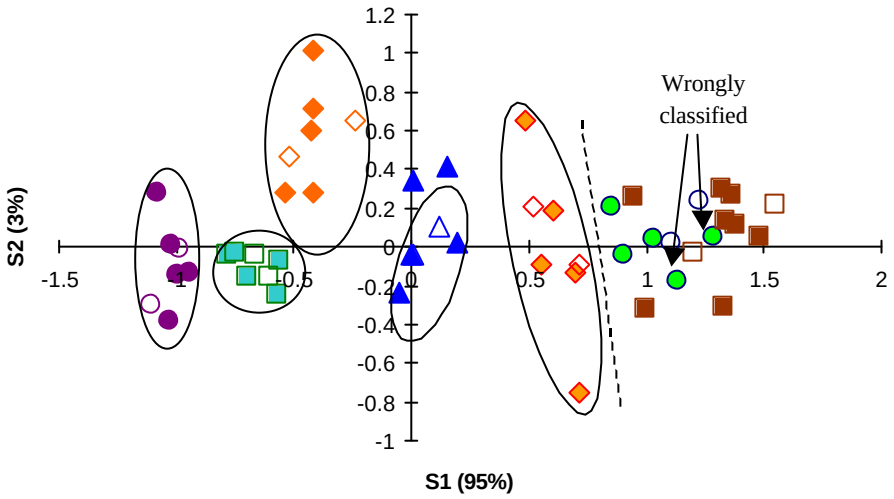

Figure 4.4: Discriminant function analysis showing the different concentration of *M. tuberculosis* in culture. Six different concentrations ranging from 1 x 10^3 to 1 x 10^8 mycobacteria ml^{-1} were analysed (seven samples for each concentration and seven blanks). Cross-validation: 14 samples (two samples from each group) were withheld from building the DFA model. Samples containing more than 1 x 10^4 mycobacteria ml^{-1} were correctly assigned (open symbols). In contrast, blank medium and samples containing 1 x 10^3 mycobacteria ml^{-1} could not be distinguish from each other.

Determination of the influence of "dead" bacteria on the sensor response

The main problem in real samples is the unknown proportion of dead *M. tuberculosis* bacteria. Therefore, we investigated the influence of dead bacteria on the sensor response to find out, if dead bacteria cause a sufficient sensor response allowing discrimination from blank medium. The result of this analysis is shown in Figure 4.5. As can be seen, there is an observable difference in smell of blank medium, dead bacteria, living bacteria and a mixture of dead and living bacteria. There is a slight overlap between the cluster containing the mixture samples and the cluster containing the "living" bacteria (Figure 4.5). The difference between living and mixed samples is not as distinct as between dead and living samples.

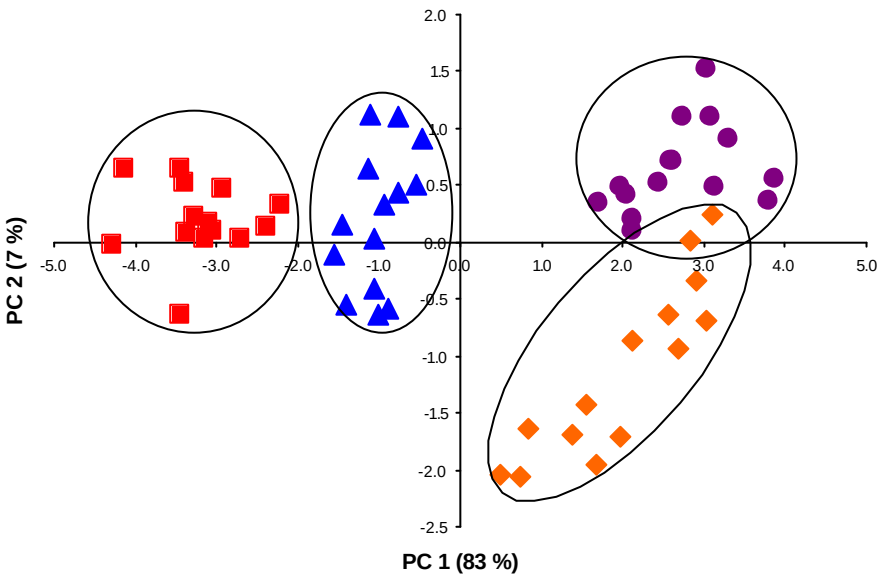

Figure 4.5 Principal component analysis showing the distinguished clusters of a living *M. tuberculosis* suspension (14 samples, circles), a dead *M. tuberculosis* suspensions (14 samples, triangles), and a mixture of it (14 samples, diamonds) compared to blank medium (14 samples, squares).

A classification model was built on 48 samples (12 of each). The result of the DFA analysis is shown in Figure 4.6. This shows that it was possible to discriminate between the four different types of samples. The DFA model was validated by analysis of 12 "unknown" samples. 11 unknown samples were correctly classified as blank medium, "dead" sample, and "living" sample or as mixture. One "mixture" sample was mistakenly classified as a living sample (Figure 4.6).

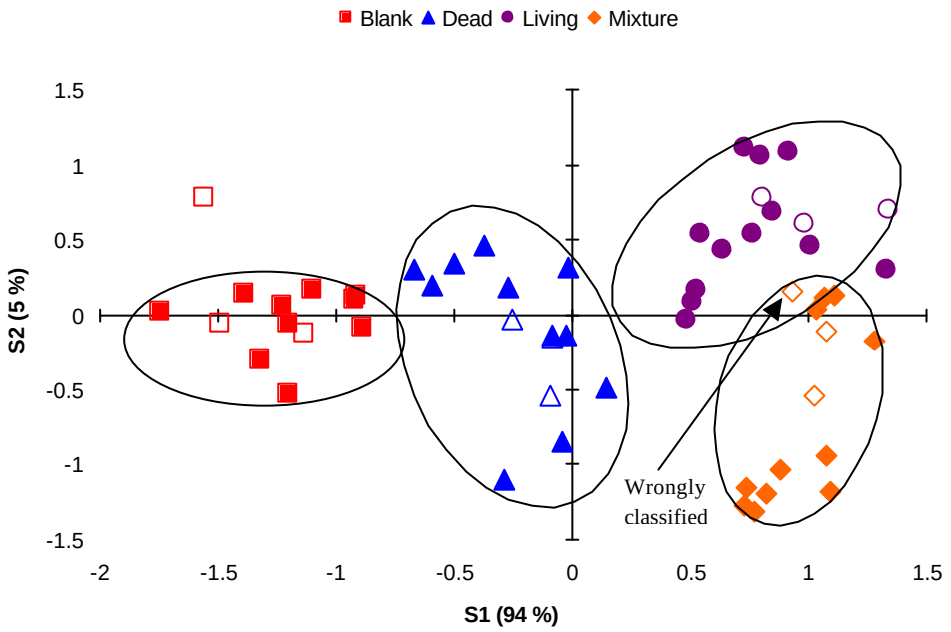

Figure 4.6: Discriminant function analysis of a living *M. tuberculosis* suspension (circles, 15 samples), a dead *M. tuberculosis* suspension (triangles, 15 samples) and a mixture of it (diamonds, 15 samples) compared to blank medium (squares, 15 samples). Cross-validation: 12 samples (three of each group) (open symbols).

4.3.2 ANALYSIS OF SPIKED SPUTUM SAMPLES

Analysis of Mycobacterium spp. and Pseudomonas aeruginosa

The collected sputum samples were pooled and spiked with *M. tuberculosis*, *M. avium*, *P. aeruginosa* and a mixture of *M. tuberculosis* and *P. aeruginosa*. All samples were spiked to obtain a final concentration of 1 x 10^8 bacteria ml^{-1}. The normalised raw data were analysed by PCA followed by DFA. It was possible to distinguish between "unspiked" sputum and "spiked" sputum samples. Within the "spiked" sputum samples, a difference in smell was observable for the different bacteria classes (Figure 4.7).

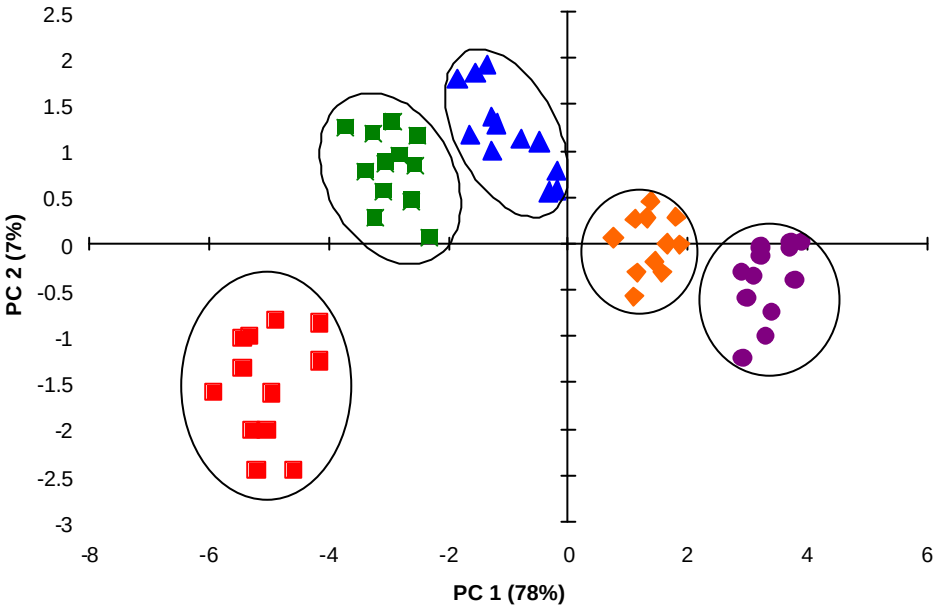

Figure 4.7: Principal component analysis showing the distinguished clusters of sputum samples spiked with *M. tuberculosis* (triangles, 12 samples), *M. avium* (green squares, 12 samples), *P. aeruginosa* (circles, 12 samples), and a mixture of *M. tuberculosis* and *P. aeruginosa* (diamonds, 12 samples) and blank medium (red squares, 12 samples).

Based on the PCA, a classification model was built using 50 samples (10 of each class). The result of the DFA is shown in Figure 4.8. The model was validated by the analysis of 10 unknown samples. All unknown samples were correctly identified as unspiked sputum or spiked sputum. Within the spiked sputum samples all unknown samples were correctly assigned to one of the four "sub-clusters" representing the different bacteria classes (Figure 4.8).

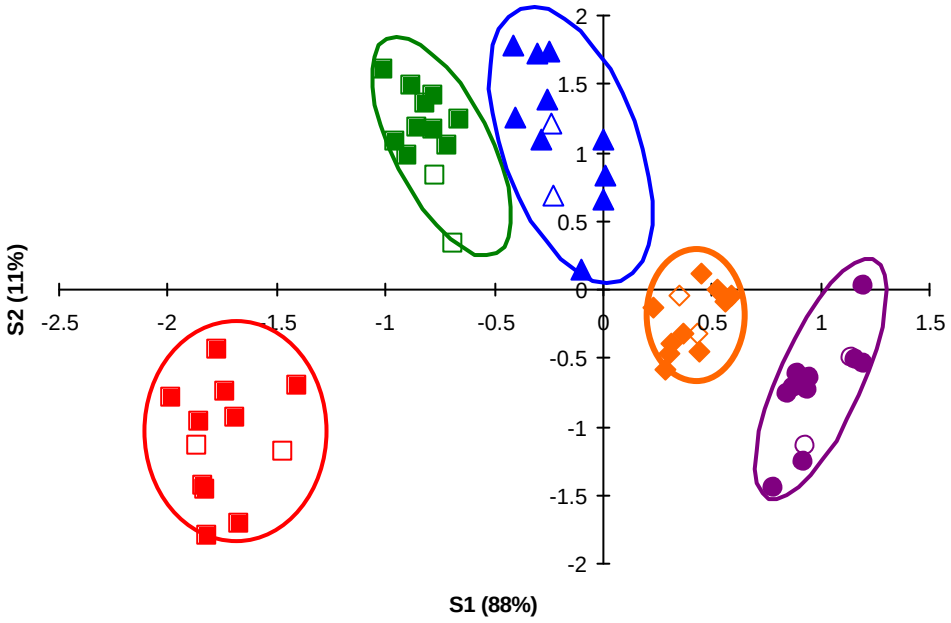

Figure 4.8: DFA analysis of sputum samples spiked with *M. tuberculosis* (triangles, 12 samples), *M. avium* (green squares, 12 samples), *P. aeruginosa* (circles, 12 samples), mixed infection (diamonds, 12 samples) and blank sputum (squares, 12 samples). Cross-validation: 10 samples (two from each group) were withheld from building the DFA model but subsequently assigned correctly once the model was built (open symbols).

Determination of the detection limit for M. tuberculosis

The detection limit of *M. tuberculosis* in spiked sputum samples was determined. This was done, since sputum is the usual source of diagnosis TB in high-burden countries. A sputum pool was divided into two parts. One part was spiked with a *M. tuberculosis* suspension containing 1 x 10^4 mycobacteria ml^{-1} (compare Figures 4.3 and 4.4), the other part was used as control sputum. The EN raw data were analysed by PCA followed by DFA.

The result of the principal component analysis is shown in Figure 4.9. This demonstrates the ability of the EN to discriminate spiked sputum (1 x 10^4 mycobacteria ml^{-1}) from control sputum and control medium (Middlebrook 7H9).

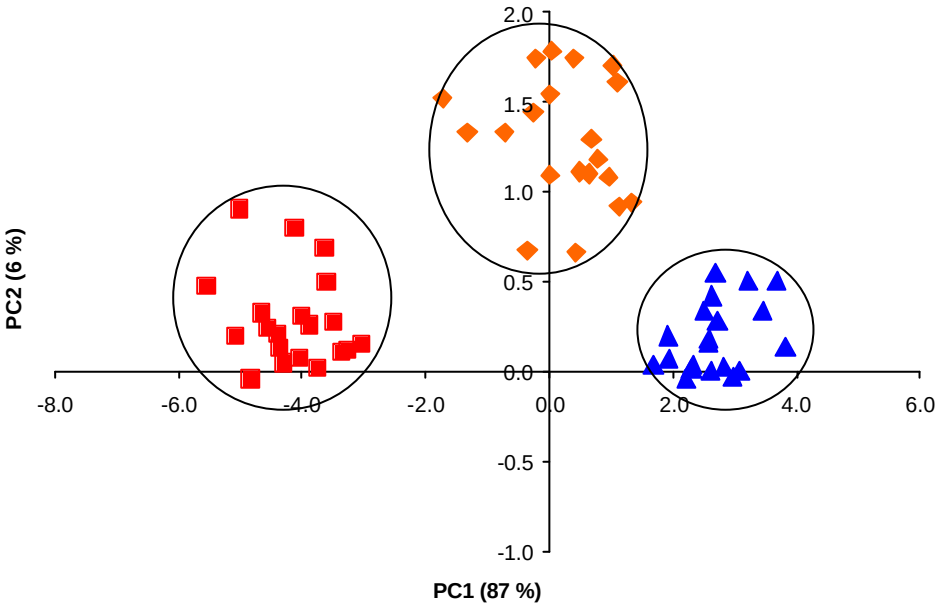

Figure 4.9: Principal component analysis showing the separate clusters of spiked sputum (20 samples, triangles), control sputum (20 samples, diamonds) and control medium (20 samples, squares). The sputum was spiked with 1 x 10^4 mycobacteria ml^{-1}.

The DFA classification model was build using 48 samples. Figure 4.10 shows that it was possible to distinguish between spiked, unspiked samples and control medium. The DFA model was validated by the analysis of 12 "unknown" samples. All "unknown" samples (open symbols) were correctly classified (Figure 4.10). The variability within the unspiked samples is higher than within the spiked samples.

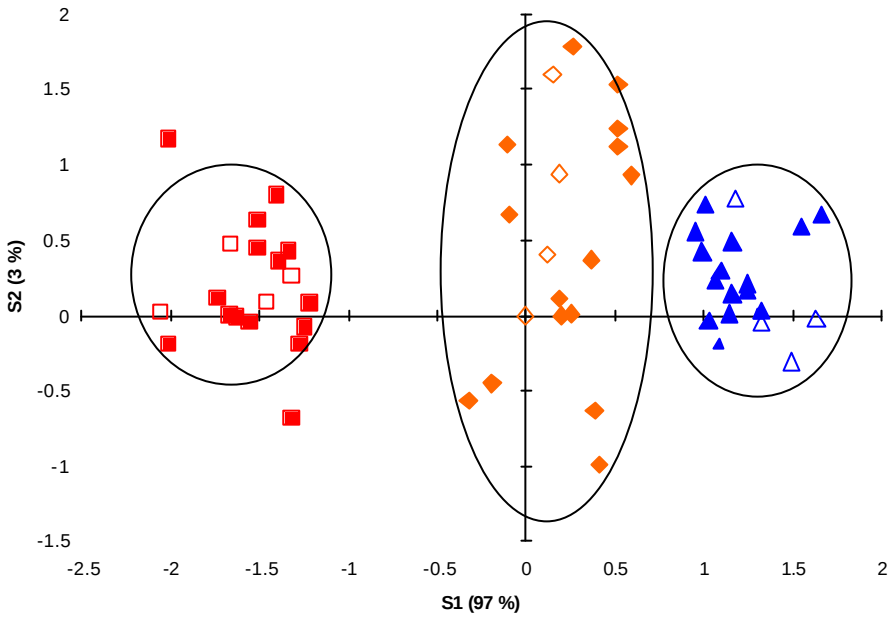

Figure 4.10: Discriminant function analysis showing the separate clusters of spiked sputum (triangles), control sputum (diamonds) and control medium (squares). The sputum was spiked with 1 x 10^4 mycobacteria ml^{-1}. Cross-validation: 12 samples (four samples of each group) were withheld from building the DFA model but subsequently assigned correctly once the model was built (open symbols).

4.3.3 ANALYSIS OF CLINICAL SPECIMENS

The PCA analysis of 50 positive control samples (spiked sputum), 50 negative control samples (non-TB sputum) and 280 clinical samples (see Table 1 for details) is shown in Figure 4.11. It was possible to obtain a good discrimination between negative control samples and positive control samples. It is, however, much more important to achieve this separation with real samples. As shown in Figure 4.11, TB negative samples can be found on the left hand side, whereas TB positive samples are on the right hand side. Nevertheless, no clear separation could be obtained as indicated by the overlapping circles in Figure 4.11. In both groups (TB positive and TB negative), a sub-cluster could be identified. These sub-clusters contained the samples of smoking patients. However, not all smokers were present in this sub-cluster (89 % present). Patients suffering from pneumonia formed a separate cluster (Figure 4.11).

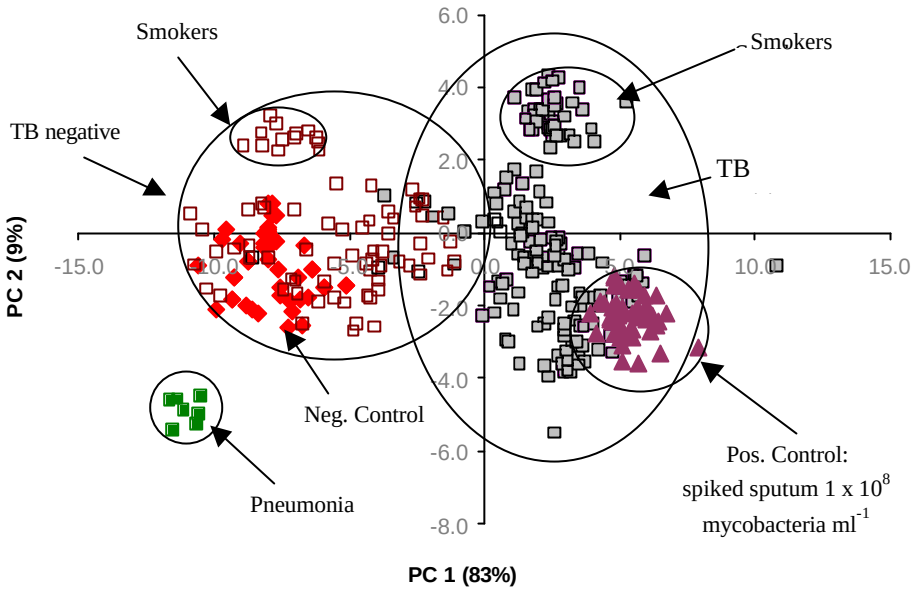

Figure 4.11: Principal component analysis showing the analysis of negative control samples (50 samples, red diamonds), positive control samples (50 samples, violet triangles), pneumonia samples (7 samples, green squares) and clinical samples (92 TB negatives samples, open red squares; 188 TB positive samples, squares with grey background).

After training the neural network with 70 % of the original samples, the remaining 30 % (84 samples) were used to validate the model. Among the 84 samples were 55 culture confirmed TB samples, of which 51 were ZN positive and 4 ZN negative. The result of the artificial neural network (ANN) is summarised in Table 4.5.

Table 4.5: Performance of the electronic nose – neural network system in comparison to culture.

	Culture confirmed TB	Culture TB negative	Total
EN positive	49	7	56
EN negative	6	72	78
Total	55	79	***134***

The neural network was able to predict 49 TB positive patients out of 55 correctly. Six TB positive suspects gave a false negative result. Among these six false negatives were four ZN negative and 2 ZN positive patients. All six false negatives were culture positive. Three of the four ZN negative false negatives were HIV positive and one was a smoker. Among the ZN positive false negatives were one HIV positive patients, who was also a smoker.

The neural network was also able to predict 72 TB negative suspects correctly. Seven TB negative patients gave a false positive result. One false positive was HIV positive and a smoker.

The sensitivity for the detection of culture proven TB was 89% (95% confidence interval [95%CI] 80-97%), the specificity was 91% (95%CI 85-97%) and the positive and negative predictive values were 88 % (95%CI 78-96) and 92% (95%CI 86-98), respectively.

4.4 SPECIFIC DISCUSSION

At present global tuberculosis (TB) control programs depend on the early detection of new cases followed by adequate treatment. However, current laboratory methods do not fully fulfil the requirements published by the WHO for high burden countries (Perkins *et al*, 2001). The detection of acid-fast bacilli in a sputum smear (Ziehl-Neelsen stain) is still the main mean of identifying new TB cases in low-income countries.

Here we showed that volatile detection through electronic nose technology is able to identify *M. tuberculosis* in culture and sputum. It is long established, that smell can be used to diagnose disease such as diabetes and uraemia (Ping *et al*, 1997; Lin *et al*, 2001). Pavlou and Turner (2000) were among the first who applied electronic noses in medical diagnostics. They showed that different bacteria such as *H. pylori, E. coli* and *P. mirabilis* generate a unique "smell" and can therefore be differentiated from each other allowing a diagnosis.

Electronic nose technology offers certain advantages such as low detection limit (5 – 0.1 ppm) (Schiffman *et al*, 1997), cost and time effectiveness, robustness, simplicity and operator independency in contrast to molecular or immunological based assays. Therefore, we investigated the ability of an electronic nose to detect *Mycobacterium spp*. and other lung pathogens in culture and sputum. In the past, the work of several groups revealed that "smell" could be used as an indicator for bacterial infections. Worthwhile is the work of Aathithan *et al* (2001) who used an Osmetech Microbial Analyser to diagnose bacteriuria. Analysing 534 clinical urine specimens, the sensitivity and specificity were 83.5% and 87.6%, respectively compared to culture. Among the first who used electronic nose technology to detect

M. tuberculosis in culture were Pavlou and Turner (2000). In this study, we could show that *Mycobacterium spp*. and *Pseudomonas aeruginosa* emit characteristic volatiles allowing discrimination between the different bacterial classes in both culture and sputum (Figures 4.1, 4.2, 4.7 and 4.8). The intra-group (classes) variability is bigger in sputum compared to culture (Figures 4.1 and 4.7). The reasons leading to this observation are not clear. The volatility of molecules is influenced by parameters such as sample viscosity, equilibrium temperature and concentration (Seto, 1994). Since the incubation parameters for liquid and sputum sample were similar, we assume that the higher viscosity, the heterogeneity and/or a stronger background "smell" of sputum might be responsible for it. As shown in Figures 4.7 and 4.8, by adding *M. tuberculosis* to sputum an additional "odor" was introduced into the sample headspace leading to a reduced intra-group variability. This indicates that *Mycobacteria* release enough volatiles into the headspace even in a complex matrix (sputum) allowing a diagnosis at low concentrations (1×10^4 mycobacteria ml^{-1}). This result is of extreme importance for clinical diagnostic, where sputum is the usual source for TB detection.

Electronic noses show a linear relationship between sensor response and concentration. This concentration dependency was exploited here to determine the detection limit (Figures 4.3 and 4.4) (Hudon *et al*, 2000). The detection limit was found to be as low as 1×10^4 mycobacteria ml^{-1} in both culture and sputum. Similar detection limits were found for other bacterium species. Canhoto *et al* (2003) reported that a *Pseudomonas aeruginosa* suspension as well as an *Enterobacter aerogenes* suspension both containing 10^2 CFU ml^{-1} could be discriminated from control samples. Similar results were found by Magan *et al* (2001) who reported that it was

possible to discriminate between milk spoilage bacteria and yeast using an initial inoculum of about $10^3 – 10^4$ CFU ml^{-1}. In contrast, McEntegart *et al* (2000) reported the detection of bacteria in liquid media, of about 5 x 10^8 cells ml^{-1} using a hybrid electronic nose. This relationship (concentration dependent sensor response) might also reveal relevant clinical information. For the treatment itself, it is not important how many bacteria are present in sputum, but the number of bacteria present largely influences the infectiousness of patients. This opens the possibility to predict not only the presence of TB but also the risk of patients to transmit the disease.

As illustrated in Figures 4.4 and 4.5, dead bacteria emit enough volatiles to cause a sensor response. However, the amount of volatiles emitted by dead mycobacteria seemed to be less than from living mycobacteria, as indicated in Figures 4.4 and 4.5. The difference between the "smell" of a mixture (dead and living bacteria) and living bacteria is not as distinctive as between dead bacteria and living bacteria. This observation could be of value for the assessment of the treatment, i.e. for the follow-up of patients during the treatment by analysing the odour shift from living to dead bacteria. This needs to be validated in a larger study with samples from patients under treatment which sputa are ZN positive but culture negative.

As mentioned above, the usual mean of case finding is the Ziehl-Neelsen staining followed by direct microscopic examination. The sensitivity of the ZN stain compared to culture is under field conditions at most 60 %-70 % using three consecutively sampled specimens (Lipsky *et al*, 1984; Perkins, 2000; Cleeff *et al*, 2003). We achieved with the method presented, a specificity of 93 % and a sensitivity of 89 % compared to culture employing a single sputum specimen per patient. The electronic nose was unable to detect the four ZN negative but culture positive specimens (false

negatives). The bacterial load in these four specimens was most likely below the detection limit of the electronic nose under the current set-up, but larger number of ZN negative specimens need to be tested. As shown above, the detection limit of the electronic nose for *M. tuberculosis* in spiked sputum was 10^4 mycobacteria ml^{-1}. However, the two remaining false negative specimens had a positive ZN stain (1+) and should therefore contain enough Mycobacteria to cause a sufficient sensor response. At present, we do not know the reasons for either the false-negatives or false-positives. It could well be due to the non-optimised system used here or due to sample degradation during storing.

Clinical specimens are more diverse than spiked samples (sputum pool) used in previous experiments (spiking). It is assumed that the viscosity, background smell and especially the heterogeneity of sputum influence the outcome of the analysis. Interestingly, smoking itself did not affect the analysis in terms of diagnosis TB. However, not all smokers were grouped in the sub-clusters shown in Figure 4.11. The individual smoking habits (number of cigarettes per day, last cigarette before sample taking) could not be established. We assume that certain smoke ingredients give rise to a slightly different sensor response allowing a separation.

Seven cases of pneumonia were among the clinical specimens. As shown in Figure 4.11, they formed a separate cluster. This indicates that the causative agent for pneumonia generates a different volatile profile (smell) to Mycobacteria. This is of clinical importance showing the potential to differentiate between TB cases and other respiratory disease.

To date, it is unknown which volatile compounds are responsible for the sensor response. We assume that the sensor response is caused by the combined effect

of a) microbial metabolites and b) volatile cellular compounds. In the past, many research groups tried to identify volatile substances emitted from microorganism using gas chromatography (GC) or gas chromatography – mass spectroscopy (GC-MS). Jantzen *et al* (1989) utilized a gas chromatograph to identify mycobacteria based on their cellular fatty acids and alcohols present in the headspace. They studied 165 mycobacteria isolates (other than *M. tuberculosis*) and 24 *M. tuberculosis* isolates. Twelve characteristic lipid constituents allowed discrimination between the different *Mycobacterium spp*. All isolates belonging to the *M. tuberculosis* complex were characterized by a high level of hexacosanic acid (1 – 13 %), low concentrations of tetracosanoic acid (0.1 –3 %), lack of fatty alcohol and the presence of tuberculostearic acid. *M. avium*, *M. intracellulare* and *M. scrofulaceum* (MAIS complex) had generally high levels of fatty alcohols including 2-octadecanol (0.1 – 5%) and 2-eicosanol (2 –21 %) and high concentrations of tetracosanoic acid (1 – 15%) and the presence of tuberculostearic acid. *M. gordonae* was easily identified by their lack of tuberculostearic acid and the presence of 2-methyl-tetradecanoic acid (2 –12 %). The fatty alcohol 2-docosanol (2-13 %) was only found in *M. xenopi* isolates. *M. malmoense* strains contained the two unique compounds 2-methyl eicosanoic acid (1-4 %) and 2,4,6-trimethyl tetracosanoic acid (2-4 %), whereas *M. kansasii* were characterized by 2.4 dimethyl tetradecanoic acid (0.2 –1.2 %). In contrast, *Pseudomonas aeruginosa* emit sulphur compounds and esters (Gibson *et al*, 1997).

The presented method is not yet fully optimised and is open to further improvement. The volatility of molecules is affected by many parameters including equilibrium temperature, concentration and viscosity (Seto, 1994). At the moment, only sodium chloride was added to the specimens to increase the concentration of

volatiles in the sample headspace due to the "salting out" effect of salts (Banat *et al*, 2003). Banat investigated the vapour-liquid equilibrium of an aqueous system. They found an increased amount of volatiles in the vapour phase as the salt concentration increases, whereas the equilibrium temperature had little or no effect.

Alternatively, Pavlou *et al* (2004) used an enzymatic cocktail contain porcine pancreas lipase and *Aspergillus niger* lipase to digest the mycobacterial cell wall, necrotic tissue and other metabolic products present in sputum. Using this sample pre-treatment they were able to discriminate between *M. tuberculosis* and related *M. avium M. scrofulaceum, P. aeruginosa* and negative controls using a neural network. The trained neural network had a prediction rate 96% in sputum. A similar prediction rate was achieved with liquid culture of the same bacterial classes. However, no enzymatic pre-treatment was performed on liquid cultures. They assumed that enzymes such as lipases interact with fatty acids and create a unique volatile signature of the samples. A recent publication, however, reported the presence of protease especially serine and metallo proteases in human sputum. If this is true, it would make the enzymatic pre-treatment inefficient due to the degradation of the lipases by the proteases (Simpson *et al*, 2004).

The application of sophisticated data analysis software is absolutely necessary in electronic nose applications. For culture and spiked sputum samples it was sufficient to use discriminant function analysis to discriminate between the different bacterial classes. However, for the clinical samples it was inevitable to apply artificial neural networks due to the high variability between the individual samples (variation) (Figure 4.12). Freeman *et al* (1994) applied an artificial neural network to distinguish between *M. tuberculosis* and *M. bovis* based on pyrolysis mass spectra. In contrast,

Veropoulos *et al* (1999) used neural networks in conjunction with fluorescence microscopy of stained sputum smears. The images were captures with a digital camera and via image processing software and neural network, they were able to identify *M. tuberculosis* in the smear sample. This preliminary study achieved a sensitivity of 94 %.

The described method is not fully optimized yet. Nevertheless, it potentially fulfils all requirements for a new diagnostic tool for TB (Perkins, 2000) including robustness, simplicity, sensitivity and cost-effectiveness. Among many advantages are the simple sample preparation and its amenability to automation. Together with an appropriate classification model, this method has the potential to become rapid and automated system for the early diagnosis of respiratory diseases through sputum or even breath analysis. It might also be possible to improve or modify currently available sensors towards specific *M. tuberculosis* markers, which would simplify the optimisation of such as system.

Chapter 5

General Discussion

5.1 INTRODUCTION

The aim of the project was to investigate the possibility of using a gas sensor as a point-of-care medical device. In particular, two applications were examined. The first application was aimed to use the electronic nose as a new monitoring device for haemodialysis to replace current tools, which are based on urea monitoring. In the second application the gas sensor array was utilised to diagnose tuberculosis and therefore replace the Ziehl-Neelsen stain followed by direct microscopy.

Clinical chemistry and immunoassays make up the largest proportion of the diagnostic market (Table 5.1). The world clinical diagnostics market is approximately $19 billion in sales. The annual growth rate is approximately 5% worldwide. For the last decade, improving technology has led to the availability of a wide variety of rapid diagnostics for use in GP surgeries, emergency rooms and bedside testing in hospital wards. Technology now allows the health professionals to accurately obtain many results without waiting for blood or urine specimens to be analysed in centralised laboratories. However, point-of-care (POC) testing is still not fully implemented in routine practice. Famous examples of POC testing are diabetes monitoring and pregnancy testing. A summary of the worldwide diagnostic market is given in Table 5.1. The worldwide POC market is estimated to be growing at an annual rate of 10 to 11% (Pavlou, 2002).

In the industrialised world, hospital laboratories are usually well equipped with modern automated instruments performing the routine tests. However, some tests are still time and labour consuming and therefore are still expensive, e.g. many microbiological tests. In contrast, in less developed countries, the situation looks different. Most people are only able to attend remote field clinics, which are in most

cases poorly equipped and the staff is not well trained. There is an urgent need in both industrialised and developing countries for new point-of-care devices that are not only cheap and robust but also simple to operate. In this research project, a novel approach based on gas-sensing technology was taken to investigate the suitability of such as system as a point-of-care device.

Table 5.1: Worldwide Diagnostics Market by Discipline (adapted from Pavlou, 2002).

Type of test	**Sales ($ millions)**	**Annual growth rate (%)**
Immunoassays	7,200	4
Clinical Chemistry	3,100	0
Blood gas/Electrolytes	600	2
Haematology/Flow cytometry	1.800	4
Coagulation	700	6
Nucleic acid tests	500	25
Microbiology	1,300	2
Diabetes	2,800	3
Urinalysis	500	0
Histology/Cytology	500	8
Total	***19,000***	***5***

5.2 GAS SENSING BASED DIAGNOSTICS

The association of specific odours with distinct pathological conditions has been recognised for centuries, and odour recognition has played an important part in clinical diagnosis (Mitruka, 1975). The level of human olfactory sophistication however has remained relatively poor compared to many mammals, but the

development of the electronic nose however has broadened our olfactory horizons.

Pavlou and Turner (2000) identified three key parameters for gas-sensing based diagnostics:

- A generating mechanism for generating volatiles
- Gas injection system and sensorial detection system
- Complex pattern recognition system

5.2.1 VOLATILE GENERATING MECHANISM

In every gas-sensing based diagnostic test, there is an inevitable need to generate a unique set of volatiles, which in turn represent the samples of interest. This unique volatile pattern (for each sample group) is subsequently detected by an array of gas sensors. The main target specimens, which can be used as potential odour pools are urine, blood, sputum, sweat and gastric fluids.

The simplest way of obtaining volatiles is to utilise the naturally present volatile organic compounds (VOCs) in a specimen. As we have shown in this report, there are enough volatile compounds naturally present in clinical specimens. For instance, it was possible to discriminate "uraemic" blood from control blood and more importantly pre- from post-dialysis blood purely based on volatiles accumulated in blood. In a similar way, volatiles generated by bacteria were released by incubating the samples in the presence of salt. Sodium chloride was added to a complex matrix such as sputum to enhance the concentration of volatiles in the headspace (salting-out effect). Using this methodology, it was possible to discriminate between different *Mycobacterium spp.* and other lung pathogens (e.g. *Pseudomonas aeruginosa*). Most other investigators used similar methodologies to analyse the headspace (gaseous

phase) of samples. Among the many groups using electronic nose technology are Aathithan *et al* (2001), and Di Natale *et al* (1999). Aathithan and his group (2001) utilised the natural produced volatiles by bacteria such as *E. coli* and *Proteus spp.* to diagnose bacteriuria. One possible indication of kidney disease is the presence of blood in urine. This circumstance was exploited by Di Natale *et al* (1999) who used an electronic nose to detect the natural occurring volatiles in urine. They were able to distinguish between urine samples of healthy subjects and urine sample containing blood purely on the basis of volatile detection emitted by the different specimens.

In contrast, other investigators suggested the chemical or enzymatic degradation of a sample to generate volatiles. For instance, gas chromatographic determination of fatty acids requires a pre-column derivatisation step to convert the fatty acids into volatile derivates (Pauschmann, 1990). Chandiok *et al* (1997) treated human vaginal tissue with KOH to generate amino compounds, which in turn are specific for bacterial vaginosis. In contrast, Pavlou *et al* (2004) suggested the enzymatic treatment of bacteria. They treated *M. tuberculosis* bacteria with lipases to utilise the unique set of mycolic acids synthesised by *Mycobacterium spp*. A number of proteases, lipases and lipooxygenases have been reported to liberate volatile esters, fatty acids and convert unsaturated fatty acids to certain flavours (Berger, 1997). In addition, natural pills or solutions could be taken orally before each test in order to interact specifically with pathogens or infected tissues. For instance, radioactive labelled urea is used as a biochemical *in vitro* substrate to enable *Helicobacter pylori* infection diagnosis (Urea Breath Test) (Phillips, 2002).

5.2.2 GAS INJECTION SYSTEM AND SENSORIAL DETECTION SYSTEM

Another crucial factor during the development of a novel gas sensing based diagnostic tool is the complete reproduction and safe delivery of the headspace sample into the sensory unit. Several workers dealing with clinical specimens have used standardised conditions, by using a water bath or gas carrier atmospheres (Distelheim, 1973). To date numerous artificial nose systems have used models of static headspace analysis in laboratory bags (Chandiok *et al*, 1997) or sealable sample vials (Di Natale *et al*, 1999). However, such a common technique is considered as a quick method of analysis but bears little relationship to mammalian odour delivery, and if not performed with consistency it may adversely influence pattern recognition reproducibility. On the contrary, automatic control systems such as flow injection analysis (FIA) are more efficient in terms of delivering repetitive volatile patterns to the sensor panel due to their higher similarity to the biological olfactory system (Pearce, 1997b).

The current system is based on the static headspace sample procedure due to its simplicity in terms of automation. The samples were incubated in headspace vials and the sample headspace was delivered to the gas sensor by placing a needle into the sample headspace. A second needle has to be placed in the liquid phase of the sample to drive the volatiles into the headspace by a carrier gas (Pavlou *et al*, 2000). On one hand, the composition of the samples used herein, hampered the utilisation of a carrier gas system due to the blockage of the gauge of the second needle (e.g. blood cells or sputum). On the other hand, in terms of point-of-care testing especially for TB diagnosis in remote field clinics, it was considered as impractical to develop a gas injection system based on FIA. Nevertheless, the sampling point, the headspace, and

liquid volumes were kept constant in addition to a continuous monitoring of environmental conditions at the sampling point. Although a prototype system, it managed to derive relatively reproducible patterns, being fast, cheap and yielding rapid results

As mentioned previously, the main sensor types used in electronic noses are either conducting polymers or metal oxide sensors. The precise physico-chemical properties of the sensor surface of conducting polymers and the mechanism of volatile interactions remain unknown. Specific doping materials can make each sensor response unique to a certain volatile mixture, whereas a sensor array can employ a much broader overlapping selectivity and functions at room temperature (Gardner and Bartlett, 1994). Conducting polymers are now being used in many commercial applications ranging from food monitoring to medical diagnostics. As shown in this report, conducting polymers were responding to different volatiles derived from either blood samples or bacteria. The sensor array was selective enough to enable discrimination between the different sample types (pre- and post-dialysis blood or different bacteria classes) independent of the source from which the volatiles were derived. In the past, conducting polymers were applied to diagnose urinary tract infections (Pavlou *et al*, 2002) or *H. pylori* infection (Pavlou *et al*, 2000) to detect milk spoilage (Magan *et al*, 2001), and for the characterisation of coffee (Pardo *et al*, 2000) or virgin olive oil (Guadarrama *et al*, 2001), and thus makes conducting polymers an attractive solution for point-of-care devices due to their low power consumption, but long-term drift and humidity sensitivity remain some of the major drawbacks (Persaud *et al*, 1996). In contrast, metal oxide sensors are not as sensitive and are operated at around 400 °C (Dickinson *et al*, 1998) and thus require a larger

sample volume and much more power, which in turn makes metal oxide sensors less attractive for point-of-care devices.

5.2.3 COMPLEX PATTERN RECOGNITION

A typical gas sensor array comprises up to 32 gas sensors, which each provides five parameters describing the sensor response. However, not all parameters provided by the sensor are reliable and therefore only two were used in this report, namely the maximum step response and the area under the curve. The electronic nose responses can only be expressed as a pattern (sample signature) unique to a sample class. The majority of groups used principal component analysis (PCA) as the initial data analysis technique. As shown in this report, PCA was able to reveal hidden relationships within sample groups as well as between different sample classes. A clear separation could be obtained between the different samples using PCA. McEntegart *et al* (2000) found distinctive clusters of *Enterobacter aerogenes* and *E. coli* in a two-dimensional PCA plot. In addition, the same group showed that it was possible to trace the growth of bacteria. They presented a two dimensional PCA chart with clearly discriminated clusters where each cluster represented a different incubation time ranging from two to six hours. The first principal component showed a qualitative correlation to the incubation time. This finding is in agreement with the results presented in the report. As shown in Figures 3.33 and 4.3 the first principal component was able to separate the samples according to time (pre- and post-dialysis, shift observed during HD session, see section 3.3.4) and concentration (different concentrated *M. tuberculosis* suspensions, see section 4.3.1). Hierarchical cluster analysis (HCA) is as PCA an exploratory data analysis technique aimed to visualise

data. In the work presented, it was mainly used to visualise the difference, expressed as the Euclidean distance, between samples, which allowed a visual assessment of the difference.

After having confirmed that the electronic nose is providing sufficient information to distinguish between the samples of interest either by PCA or HCA, it was possible to build a classification model. Two well established methods used in this report are discriminant function analysis and artificial neural networks (ANN). These methods use training data to build a mathematical definition for each class of odour (Saini *et al*, 2001). Unknown samples can then be classified according to the definition which the match most closely (Saini *et al*, 2001). Artificial Neural Networks (ANN) are a useful classification tool, as they can model more complex relationships than Discriminant Function Analysis. On the other hand, they are more difficult and time consuming to train and optimise (Bartlett and Hines, 1997; Saini *et al*, 2001).

As demonstrated in this report, discriminant function analysis (DFA) is a useful tool to classify samples such as spiked samples, liquid culture samples or even "uraemic" blood samples. However, DFA is not useful for more complex patterns derived from clinical sputum samples (see section 4.3.3) or from samples taken over a long period of time (see section 3.3.4). Due to the huge variability within individual patients it was necessary to apply more sophisticated methods such as ANN. As shown in Chapter 3 and 4, ANNs are able to cope with more variability (Tables 3.4 and 4.5). Selecting and constructing the right learning data (input variables) is crucial in pattern recognition methods. Each class must be composed of representative and reproducible samples. The quantity of these samples does not increase the

discrimination-confidence instead it is the "quality" of representation carried in each input sample that determines pattern recognition performance (Otto, 1999). Aathithan *et al* (2001) confirmed the power of ANN when analysing 534 clinical urine specimens of patients suspected for bacteriuria achieving a specificity of 87.6 % and a sensitivity of 83.5 %, respectively. Once the ANN is trained, it can be easily implemented into a point-of-care device providing the operator with the result directly displayed on the screen.

5.3 ELECTRONIC NOSES AS POINT OF CARE DEVICE

Effective clinical care requires decision making based upon multiple data inputs e.g. gross symptoms, previous history, and biochemical tests. Rather surprisingly, such a broad approach has been the main approach for the development of point of care testing, which generally rely on a "one target – one result" approach. Under certain circumstances, it is possible to use single marker molecules to monitor a disease. Famous examples are blood glucose monitoring in diabetic patients and home pregnancy testing.

Microbiology, clinical chemistry and immunoassays are still the traditional means of diagnosing diseases. However, the facilities to perform these tests are normally only available at centralised hospital laboratories and not where they are most required. These methods are absolutely necessary in medical diagnostics as in many cases act as the "gold standard". Nevertheless, they are time and labour consuming, expensive, and require skilled personnel, which makes them unattractive for point-of-care testing. In contrast, electronic noses are simple to perform, robust, cheap and amendable to automation. The applications of electronic noses are widely spread

ranging from monitoring the quality of food packaging (Forgren *et al*, 1999) and dairy products (Schaller *et al*, 1999), sausage fermentation (Eklov *et al*, 1998), wastewater treatment (Bourgeois *et al*, 2001) to medicine (Aathithan *et al*, 2001; Di Natale *et al*, 2003; Pavlou *et al*, 2004) Yet, no medical applications have been implemented in routine practice, but as outlined in this report, there is potential in revolutionising point-of-care testing using gas-sensors. Chronic renal failure and tuberculosis are two diseases, where people could benefit from new point-of-care devices.

As mentioned previously, chronic renal failure patients have to undergo intermittent haemodialysis to counter loss of kidney function. Currently the assessment of the treatment adequacy is based on the marker substance urea and expressed either as the urea reduction ratio (URR) or the normalised dialysis dose Kt/V. None of these two parameters is satisfactory, since the uraemic syndrome is not attributable to the retention of a single molecule. The electronic nose offers the possibility to assess the treatment adequacy based on a wide range of molecules (see chapter 3). The information provided by the gas sensor array can be gained on-line and in real-time as demonstrated by Bourgeois *et al* (2001) for waste-water treatment. Together with an appropriate mathematical classification model, it could provide the health professions in a dialysis unit with the relevant information necessary to ensure optimal treatment. Nevertheless, one of the biggest challenges will be to correlate a certain sample profile (pattern) to a clinical outcome (morbidity or mortality). In addition, the classification model can be fed with other relevant clinical information such as urea concentration or weight as long as the parameters are available on-line and thus might reflect a better clinical picture compared to a single parameter.

Gas sensor arrays are able to detect multiple pathogens as shown in Figure 4.1 (e.g. *M. tuberculosis*, *M. avium*, *M. scrofulaceum*, *P. aeruginosa*) compared to immunoassays, which can only detect one specific target or automated instruments which are only able to detect bacterial growth without the ability to determine the species (Thorpe *et al*, 1990). In this respect, the electronic nose offers a powerful alternative to the current available techniques. The electronic nose as presented in this report, yet not fully optimised, cannot compete with molecular techniques (e.g. PCR, *in situ* hybridisation) in terms of sensitivity and specificity. However, the current method is still open to further improvements, which will hopefully increase both sensitivity and specificity. Recently, Kivihya-Ndugga *et al* (2004) compared PCR with the Ziehl-Neelsen staining procedure for diagnosing pulmonary tuberculosis (TB). They concluded that PCR is a powerful tool to diagnose TB but its limitation include high maintenance of equipment, water supply, short shelf life of PCR kits and high costs. This makes PCR unattractive for implementation as a routine test for TB in high-prevalence countries. Currently, the electronic nose is able to detect *M. tuberculosis* and other respiratory pathogens in culture and sputum. However, recent findings suggest that patients suffering from TB emit volatiles with their breath which are associated with the diseases. Currently, a group in Africa utilises the extraordinary olfactory system of giant rats to diagnose TB (New Scientist, Dec. 2003). The electronic nose could be used to replace the giant rats, which in turn would be a more patient friendly technique. This technology will hopefully be available in the future as a diagnostic tool.

The company, Osmetech plc, followed a different route for point-of-care testing. Osmetech has received 510(k) approval from the FDA for the use of its microbial

analyser as a UTI sensor device. Offering both a centralised laboratory based instrument and a smaller "point-of-care" option, Osmetech's view is that the device should enable negative samples to be screened out within minutes enabling the number of cultured samples to be greatly reduced, resulting in cost savings (Woodman and Fend, 2004). However, the results presented in this report and by others, indicate that the electronic nose is not only able to detect negative samples but also detect the causative agent of an infectious disease.

In terms of point-of-care testing, electronic noses have also potential as a non-invasive screening tool for cancer based on breath analysis. Phillips *et al* (2003 a, b) investigated marker molecules of oxidative stress as possible indicators for breast and lung cancer using GC-MS. Both cancers are accompanied by increased oxidative stress. Among elevated breath VOC were nonane, tridecane, octane, and dodecane. In contrast, Di Natale *et al* (2003) used an electronic nose to identify patients with lung cancer. They found distinctive groups for patients with lung cancer and healthy volunteers. A simple point-of-care test based on electronic nose technology could replace current screening procedures and thus reducing the risk due to reduced exposure to X-rays.

Chapter 6

Conclusions and Future Work

6.1 CONCLUSIONS

The overall aim of this study was to evaluate the potential of an electronic nose as a point-of-care device for renal medicine and pulmonary tuberculosis. As demonstrated in this thesis, the aim and hence, the individual objectives were achieved. The conclusions are as follows:

6.1.1 ELECTRONIC NOSE IN RENAL MEDICINE

- The electronic nose is able to distinguish between control blood and "uraemic" blood. Furthermore, the gas sensor array is not only capable of discriminating pre- from post-dialysis blood but also can follow the volatile shift occurring during a single haemodialysis session.

- The electronic nose can be used for both dialysate side and blood-side monitoring of haemodialysis.

- The sensor response showed a slight day-to-day variation (except sensor 11 and 14) with a maximum of 15% deviation and thus the sensor drift was considered as negligible.

- To date it is unknown which exact compounds are responsible for the sensor response, but as demonstrated in this report, urea and creatinine do not contribute to the sensor response

- The volatile shift occurring during haemodialysis was not correlated with the urea reduction ratio.

- The pattern observed for post- and pre-dialysis blood might reflect the health status of the patients and can therefore be related to the long-term outcome (morbidity and mortality risk).

- To follow haemodialysis patients over a longer period of time, traditional chemometric tools such as principal component analysis or discriminant function analysis are not sophisticated enough. In contrast, artificial neural networks are capable to distinguish between pre- and post-dialysis blood with high accuracy (97 % correct classified).

6.1.2 ELECTRONIC NOSE FOR THE EARLY DETECTION OF PULMONARY TB

- The electronic nose was able to discriminate between *Mycobacterium spp.* and other lung pathogens such as *Pseudomonas aeruginosa*. More importantly the gas sensor array was capable of resolving different *Mycobacterium tuberculosis*, *M. scrofulaceum*, and *M. avium* in both liquid culture and spiked sputum samples.

- The detection limit for *M. tuberculosis* in both sputum and liquid culture is 1×10^4 mycobacteria ml^{-1} and therefore partially fulfils the requirement set by the WHO.

- The electronic nose has the potential to follow up patients during treatment to assess the efficiency of the treatment as indicated by the different smell of "dead" bacteria and living bacteria suspension (Figures 4.6 and 4.7)

- The sensitivity for the detection of culture proven TB was 89% (95% confidence interval [95%CI] 80-97%), the specificity was 91% (95%CI 85-97%) and the positive and negative predictive values were 88 % (95%CI 78-96) and 92% (9%CI 86-98), respectively.

- The analysis time (incl. preparation time) for detecting *M. tuberculosis* in liquid culture is approximately 60 minutes, and in sputum approximately five hours. However, most of the time is used for incubation and thus does not require labour.

- The exact compounds, which cause the sensor response, could not be established.

The promising studies presented herein indicate that there is a real potential for electronic noses at point of medical delivery, where they could be used as a rapid screen for specific diseases or disorders. However it is the combination of the "point-of-care" environment with the opportunity to gather data remotely and use advanced information-technology approaches, mobile communication and web-based knowledge systems to transfer them back to centralised facilities either for processing or disease management which add another dimension to this technology.

6.2 FUTURE WORK

6.2.1 ELECTRONIC NOSE IN RENAL MEDICINE

- GC-MS studies to identify the key volatiles responsible for causing the sensor response.
- Use the knowledge gained from the GC-MS studies to customise the sensor array towards these key volatiles.
- Identify a volatile pattern, which correlates with a better clinical outcome, i.e. a lower morbidity and mortality risk.
- Correlate key volatiles (potential uraemic toxins) to the volatile shift observed in HD.
- Develop a flow-cell and associated parts, which allows the on-line monitoring of HD sessions.
- Develop a model which is able to predict the "optimal" end point for each treatment session
- Develop a protocol and device for monitoring haemodialysis based on breath analysis.

6.2.2 ELECTRONIC NOSE FOR THE EARLY DETECTION OF PULMONARY TB

- GC-MS studies to identify the key volatiles responsible for causing the sensor response.
- Use the knowledge gained from the GC-MS studies to customise the sensor array towards these key volatiles.

- Increase the sensitivity and specificity of the electronic nose by altering the sample pre-treatment and sensor panel.
- Try to identify *Mycobacterium spp*. other than *M. tuberculosis* in clinical specimens and other relevant respiratory pathogens.
- Evaluate the performance of the electronic nose in Ziehl-Neelsen negative samples (e.g. in HIV co-infected patients).
- Investigate the potential of an electronic nose as a monitoring tool for treatment success.
- Develop a protocol, so that the electronic nose is able to identify multiple drug resistance strains.
- Develop a protocol and device for breath sampling and subsequent breath analysis for diagnosing pulmonary tuberculosis.

References

Aathithan S, Plant JC, Chaudry AN, French GL. (2001), Diagnosis of bacteriuria by detection of volatile organic compounds in urine using an automated headspace analyser with multiple conducting polymer sensors. *J Clin Microbiol* 39: 2590 – 2593

Abuja PM, Albertini R. (2001), Methods for monitoring oxidative stress, lipid peroxidation and oxidation resistance of lipoproteins, *Clin Chim Acta* 306:1-17

Adams F. (1994), Hippocratic writings: Aphorisms IV, V. In: Stevenson DC ed. *The internet classic archive.* New York: Web Atomics

Ampuero S, Bosset JO. (2003), The electronic nose applied to dairy products: a review, *Sens Actuators B*, 94:1-12

Arloing S. (1898), Agglutination du bacilli de la tuberculose vraie, *Comptes Rendues de l'Academie de Scienses* 126:1398-1400

Armoni A. (1998), Use of neural networks in medical diagnosis, *MD Computing* 15:100-104

Asaka M, Iida H, Izumino K, Sasayama S. (1988), Depressed natural killer cell activity in uremia, *Nephron* 49:291-295

Baba S, Watanabe Y, Gejyo F, Arakawa M. (1984), High-performance liquid chromatographic determination of serum aliphatic amines in chronic renal failure, *Clin Chim Acta* 136:49-56

Badak FZ, Goksel S, Sertoz R, Nafile B, Ermertcan S, Cavusoglu C, Bilgic A. (1999), Use of nucleic acid probes for identification of *Mycobacterium tuberculosis* directly from MB/BactT bottles, *J Clin Microbiol* 37:1602-1605

Baldacci S, Matsuno T, Toko K, Stella R, De Rossi D. (1998), Discrimination of wine using taste and smell sensors, *Sensors Materials* 10:185-200

Baltruschat H, Kamphausen I, Oelgeklaus R, Rose J, Wahlkamp M. (1997), Detection of volatile organic solvents using potentiodynamic gas sensors, *Anal Chem*, 69:743-748

Banat F, Al-Asheh S, Simandl J. (2003), Vapour-liquid equilibria of propionic acid-water system in the presence of different types of inorganic salts: effect of temperature and salt concentration, *Chem Eng Proc*, 42:917-923

Bartlett PN, Elliott JM, Gardner JW. (1997), Application of, and Developments in, Machine Olfaction, *Annali di Chimica*, 87:33-44

Bartlett PN, Ling-Chung SK. (1989), Conducting polymer gas sensors part III: Results for four different polymers and five different vapours. *Sens Actuators B*, 20: 287-292

Bazilinski N, Shaykh M, Dunea G. (1985), Inhibition of platelet function by uremic middle molecules, *Nephron*, 40:423-428

Berger RG. (1997), Biotechnology of Aroma compounds in: *Advances in Biochemical Engineering and Biotechnology 55*, Springer Verlag, Berlin

Bergström J. (1997), Uremic Toxicity in *Nutritional Management of Renal Disease* edited by Kopple D., Massry S. G., Williams and Wilkins, Baltimore, 1997, pp 97-190

Bernard P, Crest M, Rinaudo JB, Gallice P, Fournier N, Crevat A, Murisasco A, Saingra S, Frayssinet R. (1982), A study of the cardiotoxicity of uremic middle molecules on embryonic chick hearts, *Nephron*, 31:135-140

Bothamley GH, Rudd R, Festenstein F, Ivanyi I. (1992), Clinical value of the measurement of *Mycobacterium tuberculosis* specific antibody in pulmonary tuberculosis, *Thorax*, 47:270-275

Bothamley GH. (1995), Serological diagnosis of tuberculosis, *Eur Respir J Suppl*, 20:676s-688s

Bowen D, Cowburn D, Rennekamp M, Sullivan J. (1975), Benzyl alcohol: high levels found in plasma of uremic patients on hemodialysis, *Clin Chim Acta*, 61:399-401

Brauger D, Chauvet-Monges AM, Sari JC. (1983), Inhibition in vitro of the polymerisation of tubulin by uremic middle molecules. Corrective effect of isaxonine. *Clin Nephrol*, 20:149-154

Brooks JB, Daneshvar M1, Haberberger RL Mikhail IA. (1990), Rapid diagnosis of meningitis by frequency-pulsed electron-capture gas-liquid chromatography detection of carboxylic aid in cerebrospinal fluid, *J Clin Microbiol*, 28:989-997

Brudzewski K, Osowski S, Markiewicz T. (2004), Classification of milk by means of an electronic nose and SVM neural network, *Sens Actuators B*, 98:291-298

Brunello F, Favari F, Fontana R. (1999). Comparison of the MB/BacT and BACTEC 460 TB systems for recovery of mycobacteria from various clinical specimens, *J Clin Microbiol*, 37:1206-1209

Campanella L, Sammortino MP, Tomassetti M. (1990), Suitable potentiometric enzyme sensors for urea and creatinine, *Analyst*, 115:827-830

Canaud B, Bosc JY, Carrol L, Learay-Moragues H, Naviono C, Verzetti G, Thomaseth K. (2000), Urea as a marker of adequacy in hemodialysis: Lessons from in vivo urea dynamics monitoring, *Kidney Int*, 58:28-40

Canaud B, Cristol JP, Morena M, Leray-Moragues H, Bosc J, Vaussenat F. (1999), Imbalance of Oxidants and Antioxidants in Haemodialysis Patients, *Blood Purif*, 17:99-106

Canhoto OF, Magan N. (2003), Potential for detection of microorganisms and heavy metals in potable water using electronic nose technology, *Biosens Bioelectron*, 18:751-175

Capodicasa E, Trovarelli G, De Medio G, Pelli M, Lippi G, Verdura C, Timio M. (1999), Volatile Alkanes and Increased Concentrations of Isoprene in Exhaled Air during Hemodialysis, *Nephron*, 82:331-337

Ceballos-Picot I., Witko-Sarat V., Merad-Boudia M., Nguyen AT, Thevenin M, Jaudon MC, Zingraff J, Verger C, Jungers P, Descamps-Latscha B. (1996), Glutathione antioxidant system as a marker of oxidative stress in chronic renal failure, *Free Radical Biology & medicine* 21:845-853

Cernacek P, Spustova V, Dzurik R. (1982), Inhibitor(s) of protein synthesis in uremic serum and urine: Partial purification and relationship to amino acid transport, *Biochem Med*, 27:305-316

Chandiok S, Crawley BA, Oppenheim BA, Chadwick PR, Higgins S, Persaud KC. (1997), Screening for bacterial vaginosis: a novel application of artificial nose technology, *Journal of Clinical Pathology*, 50:790-795

Chandramuki A, Allen PR, Kenn M, Ivanyi I. (1985), Detection of mycobacterial antigen and antibodies in the cerebrospinal fluid of patients with tuberculous meningitis, *J Med Microbiol*, 20:239-247

Chang BW, Hsu YM, Chang HC. (2000), An improving method for determination for Escherichia coli population based on multi-channel series piezoelectric quartz crystal systems, *Sens Actuators B*, 65:105-107

Chanteau S, Rasolofo V, Rasolonavalona T, Ramarokoto H, Horn C, Auregan G, Marchal G. (2000), 45/47 kDA (APA) antigen capture and antibody detection assay for the diagnosis of tuberculosis, *Int J Tuberc Lung Dis***,** 4:377-383

Clancy J, Mc Vicar AJ. (1995), Physiology and Anatomy: A Homeostatic Approach, Springer, New York, pp. 165-196

Cleeff MR van, Kivihya-Ndugga L, Githui WA, Nganga L, Odhiambo JA, Klatser PR. (2003) A comprehensive study of the efficiency of the routine pulmonary tuberculosis diagnostic process in Nairobi. *Int Journal Tuberc Lung Dis*, 7:186-189.

Cloix HF, Cueille G, Funck-Brentano JL. (1976), Inhibition of bovine renal adenylate cyclase by urinary products, *Biomedicine* 25:215-218

Colasanti G, Arrigo G, Santoro S, Mandolfo S, Tetta C, Bucci R, Spongano M, Imbasciati E, Rizza V, Cianciavicchia D. (1995), Biochemical aspects and clinical perspectives of continuous urea monitoring in plasma ultrafiltrate. Preliminary results of a multicenter study, *Int J Artif Organs*, 18:544-547

Craven MA, Gardner JW, Bartlett PN. (1996), Electronic noses – development and future prospects, *Trends in analytical chemistry*, 16:486-493

D'Amico A, Di Natale C, Verona E. (1997), Acoustic Devices in: *Handbook of Biosensors and Electronic Noses Medicine, Food and the Environment*, edited by E. Kress-Rogers, CRC press, New York, pp 197-223

Daugirdas JT, Smye S. (1997), Effect of a two compartment distribution on apparent urea distribution volume, *Kidney Int*, 51:1270-1273

Davies T, Hayward NJ. (1984), Volatile products from acetylcholine as markers in the rapid urine test using head-space gas-liquid chromatography, *J Chromat*, 307:11-21

De Palma JR., Pittard JD. (2001), Dialysis dose, www.hemodialysis-inc.com

Del Vecchio L, Di Filippo S, Andrulli S, Manzoni C, Corti M, Barbisoni F, Locatelli F. (1998), Conductivity: on-line monitoring of dialysis adequacy, *Int J Artif Organs*, 21:521-525

Depner TA, Keshaviah PR, Ebben JP, Emerson PF, Collins AJ, Jindal KK, Nissenson AR, Lazarus JM, Pu K. (1996), Multicenter clinical validation of an on-line monitor of dialysis adequacy, *J Am Soc Nephrol*, 7:4640471

Despagne F. Massart DL. (1998), Neural networks in multivariate calibration, *Analyst*, 123:157R-178R

Dhondt A, Vanholder R, Van Biesen W, Lameire N. (2000), The removal of uremic toxins, *Kidney Int*, 58:47-59

Di Filippo S, Manzoni C, Andrulli S, Pontoriero G, Dell'Oro C, La Milia V, Bacchini G, Crepaldi M, Bigi MC, Locatelli F. (2001), How to determine ionic dialysance for the online assessment of delivered dialysis dose, *Kidney Int*, 59:774-782

Di Natale C, Macagnano A, Martinelli E, Paolesse R, D'Arcangelo, Roscioni C, Finazzi-Agro A, D'Amico A. (2003), Lung cancer identification by the analysis of breath by means of an array of non-selective gas sensors. *Biosens Bioelectron*, 18: 1209-1218

Di Natale C, Mantini A, MacagnanoA, Antuzzi D, Paolasse R, D'Amico A. (1999), Electronic nose analysis of urine samples containing blood. *Physiological Measurements*, 20: 377-384

Dickinson TA, White J, Kauer JS, Walt DR. (1998), Current trends in artificial-nose technology, *Tibtech*, 16:250-258

Dieterle F, Strathmann S. (2000), Introduction to data evaluation for sensor systems, *In Nose Lectures Series Vol 1*, eds Strathmann S, Harbeck M, Weimar U, Tuebingen, Germany

Distelheim IH. (1973), A method for separating characteristics of odours in detection in disease processes, *Int J Dermatol*, 12:241-244

Doern GV. (1996), Diagnostic mycobacteriology: where are we today? *J Clin Microbiol*, 34:1873-1876

Doleman BJ, Lewis NS. (2001), Comparison of odor detection thresholds and odor discriminabilities of a conducting polymer composite electronic nose versus mammalian olfaction, *Sens Actuators B*, 72:41-50

Dolin PJ, Raviglione MC, Kochi A. (1994), Global Tuberculosis incidence and mortality during 1990 – 2000, *Bull. World Health Organ*, 72:213-220

Dowty B, Charlisle D, Laseter J, Gonzalez F. (1975), Gas chromatographic mass spectrometric computer analysis of volatile compounds in blood plasma from hemodialysis patients, *Biomed. Mass. Spectrometry*, 2:142-147

Drukker W. (1983), History of Hemodialysis, in *Replacement of the renal function by Dialysis*, edited by Drukker W., Parsons M., Maher J. F., Martinus Nijhoff Publishers Boston, pp. 3-52

Dutta R, Hines EL, Gardner JW, Bollot P. (2002), Bacteria classification using Cyranose 320 electronic nose. *BioMedical Engineering Online*, 1: 1-7

Eklov T, Johansson G, Winquist F, Lundstrom I. (1998), Monitoring sausage fermentation using an electronic nose, *J Sci Food Agric*, 76: 525 – 532

Erdogan C, Unlucerci Y, Tuerkmen A, Kuru A, Cetin O, Bekpinar S. (2002), The evaluation of oxidative stress in patients with chronic renal failure, *Clin Chim Acta*, 332:157-161

Everitt BS, Dunn G. (2001), *Applied Multivariate Data Analysis*, Arnold Publishers, London

Flynn JL, Goldstein MM, Chan J, Triebold KJ, Pfeffer K, Lowenstein CJ, Schreiber R, Mak TW, Bloom BR.. (1995), Tumor necrosis factor-alpha is required in the protective immune response against *Mycobacterium tuberculosis* in mice. *Immunity*, 2:561-572

Forgren G, Frisell H, Ericsson B. (1999), Taint and odour related quality monitoring of two food packaging board products using gas chromatography, gas sensors, and sensing analysis, *Journal of Nordic Pulp Paper Research*, 14:5-16

Frank M, Hermle T, Ulmer H, Mitrovics J, Weimar U, Goepel W. (2000), Qualitiy tests of electronic noses: the influence of sample dilution and sensor drift on the pattern recognition for selected case studies, *Sens Actuators B*, 65:88-90

Freeman R, Goodacre R, Sisson PR, Magee JG, Ward AC, Lightfoot NF. (1994), Rapid identification of species within the Mycobacterium tuberculosis complex by artificial neural network analysis of pyrolysis mass spectra, *J Med Microbiol*, 40:170-173

French GL, Chan CY, Cheung SW, Oo KT. (1987), Diagnosis of pulmonary tuberculosis by detection of tuberculostearic acid in sputum by using gas chromatography-mass spectrometry with selected ion monitoring, *J Infect Dis*, 156:356-362

Fridolin I, Magnusson M. Lindberg LG. (2002), On-line monitoring of solutes in dialysate using absorption of ultraviolet radiation: technique description, *Int J Art Org*, 25:748-761

Frieden TR, Sterling TR, Munsiff SS, Watt CJ, Dye C. (2003), Tuberculosis, *The Lancet*, 362:887-899

Gardner JW, Bartlett PN. (1994), A brief history of electronic noses, *Sensor Act B*, 18-19:211-220

Gardner JW, Bartlett PN. (1999), *Electronic Noses: Principles and Applications*, Oxford University Press, Oxford

Gardner JW, Hines EL. (1997), Pattern Analysis Techniques, in *Handbook of Biosensors and Electronic Noses Medicine, Food and the Environment*, edited by E. Kress-Rogers, CRC press, New York, pp 633-652

Gardner JW, Shin HW, Hines EL. (2000), An electronic nose system to diagnose illness, *Sens Actuators B*, 70: 19-24

Garg SK, Tiwari RP, Tiwari T, Singh R, Malhotra D, Ramnani VK, Prasad GB, Chandra R, Fraziano M, Colizzi V, Bisen PS. (2003), Diagnosis of Tuberculosis: Available Technologies, Limitations, and Possibilities, *J Clin Lab Anal*, 17:155-163

Gibson T, Prosser O, Hulbert J. (2000), Electronic noses: an inspired idea?, Chemistry and Industry, 17th April 2000, 287-289

Gibson TD, Prosser O, Hulbert JN, Marshall RW, Corcoran P, Lowery P., Ruck-Keeni EA, Heron S. (1997), Detection and simultaneous identification of microorganism from headspace samples using an electronic nose, *Sens Actuators B,* 44:413-422

Gibson TD, Puttick P, Hulbert JN, Marshall RW, Li Z. (1999), Odour sensor, *US patent:* 5,928,609

Gonzales-Martin Y, Concepcion-Cerrato-Oliveros M, Pavon JLP, Garcia Pinto C, Cordero BM. (2001), Electronic nose based on metal oxide semiconductor sensors and pattern recognition techniques: characterisation of vegetable oils, *Anal Chim Acta,* 449:69-80

Gotch FA, Sargent JA. (1985), Mechanistic analysis of the National Cooperative Study (NCDS). *Kidney Int*, 28:56-534

Grametbauer P, Kartusek S, Hausuer O. (1988), Diagnosis of aerobic gram-negative bacteria by the detection of volatile metabolites using gas-chromatography, *Ceskoslovenska Epidemiologie Microbiologi Immunologie*, 37:216-223

Guadarrama A, Rodriguez-Mendez ML, de Saja JA. (2002), Conducting polymer-based array for the discrimination of odours from trim plastic materials used in automobiles, *Anal Chim Acta,* 455:41-47

Guadarrama A, Rodriguez-Mendez ML, Sanz C, Rios JL, de Saja JA. (2001), Electronic nose based on conducting polymers for the quality control of the olive oil aroma. Discrimination of quality, variety of olive and geographic origin, *Anal Chim Acta,* 342:283-292

Hageman J, Bast A, Vermulen N. (1992), Monitoring of oxidative free radical damage in vivo: analytical aspects, *Chem Biol Interactions*, 82:243-293

Harper WJ. (2001), The Strengths and Weaknesses of the Electronic Nose, *Headspace Analysis of Food and Flavors: Theory and Practice,* edited by Rouseff and Cadwallader, Kluwer Academic/Plenum Publishers, New York, 2001, pp 59 – 71

Haslett C, Chilvers ER, Hunter J, Boon N. (1999), Davidson's Principle and Practice of Medicine, 18th edition, Churchill Livingstone, UK, pp. 458-470

Hasper HJ, Brink HS, Brouwer RMS. (1997), In adequately treated hemodialysis patients, dialysis efficiency measured using either a urea monitor or the Daugirdas equation is not related to Protein Catabolic Rate, protein intake or serum albumin, *Netherlands Journal of Medicine*, A1-A44

Hay P, Tummon A, Ogunfile M, Adebiyi A, Adefowora A. (2003), Evaluation of a novel diagnostic test for bacterial vaginosis: 'the electronic nose', *Int J STD AIDS*, 14:114-118

Hayden GF. (1980), Olfactory diagnosis in medicine, *Postgrad Med*, 67:110-116

Haywood NJ, Jeavons TH. (1977), Assessment of technique for rapid detection of *E. Coli* and *Proteus sp* in urine by headspace gas liquid chromatography. *J Clin Microbiol*, 6: 202 – 208

Hegebrant J, Hultkvist-Bengtsson U. (1999), Vitamin C and E as antioxidants in hemodialysis patients, *Int J Artif Organs* 22:69-73

Held PJ, Port FK, Wolfe RA, Stannard DC, Carroll CE, Daugirdas CA, Bloembergen WE, Greer JW, Hakim RM. (1996), The dose of dialysis and patient mortality, *Kidney Int*, 50:550-556

Henderson LW, Clark WR, Cheung AK. (2001), Quantification of Middle Molecular Weight Solute Removal in Dialysis, *Seminars in Dialysis* 14:294-299

Hillier SL, Martius J, Krohn M, Kiviat N, Holmes KK, Eschenbach DA. (1988), A case-control study of chorioamnionic infection and histologic chorioamnionitis in prematurity. *N Engl J Med*, 319:972-978

Honkinen O, Lehtonen OP, Ruuskanen O, Huovinen P, Mertsola J. (1999), Cohort study of bacterial species causing urinary tract infection and urinary tract abnormalities in children. *BMJ*, 318:770-771

Hörl WH. (1998), Genesis of the uraemic syndrome: Role of uraemic toxins, *Wien Klin Wochenschr*, 110:511-520

Hudon G, Guy C, Hermia J (2000). Measurement of Odor Intensity by an Electronic Nose, *Air Waste Manag Assoc*, 50:1750-1758

Ichiyama S, Iinuma Y, Yamori, Hasegawa Y, Shimokata K, Nakashima N. (1997), *Mycobacterium* Growth Indicator Tube testing in conjunction with the AccuProbe or the Amplicor-PCR assay for detecting and identifying mycobacteria from sputum samples, *J Clin Microbiol*, 35:2022-2025

Jacket P, Bothamley GH, Batra V, Mistry A, Young DB, Ivanyi J. (1988), Specificity of antibodies to immunodominant mycobacterial antigens in pulmonary tuberculosis, *J Clin Microbiol*, 26:2313-2318

Jackson JE (1991), *A User's guide to Principal Components*, Wiley, New York, p. 569

Jacobs WR, Barletta RG, Udani R, Chan J, Kalkut G, Sosne G, Kieser T, Sarkis GJ, Hatfull GF, Bloom BR. (1993), Rapid assessment of drug susceptibilities of *Mycobacterium tuberculosis* by means of luciferase reporter phages, *Science*, 260:819-822

Jantzen E, Tangen T, Eng J. (1989), Gas chromatography of mycobacterial fatty acids and alcohols: diagnostic applications, *APMIS*, 97:1037-1045

Jurs PC, Bakken GA, McClelland HE. (2000), Computational methods for the analysis of chemical sensor array data from volatile analytes, *Chem Rev*, 100:2649-2678.

Kahn GF, Wernet W (1997), A highly sensitive amperometric creatinine sensor, *Anal Chim Acta*, 351:151-158

Katopodis KP, Hoenich NA. (2002), Accuracy and clinical utility of dialysis dose measurement using online ionic dialysance, *Clin Nephrol*, 57:215-220

Kemp HJ, Parnham A, Tomson CR. (2001), Urea kinetic modelling: a measure of dialysis adequacy, *Ann Clin Biochem*, 38:20-27

Keshaviah P. (2002), Adequacy of dialysis: Comparison of hemodialysis (HD) to CAPD, *Indian Journal of Nephrology*, 16:51-55

Kharitonov S, Barnes PJ. (1997), Biomarkers of some pulmonary diseases in exhaled breath, *Biomarkers*, 7:1-32

Kharitonov S. (2004), Exhaled markers of inflammatory lung disease, ready for routine monitoring, *Swiss Med Wkly*, 134:175-192

Kivihya-Ndugga L, Cleeff M van, Juma E, Kimwomi J, Githui W, Oskam L, Schuitema A, van Soolingen D, Nganga L, Kibuga D, Odhiambo J, Klatser P. (2004), Comparison of PCR with the routine diagnostic procedure of tuberculosis in a population of high tuberculosis and HIV prevalence. *J Clin Microbiol*, 42:1012-1015

Knocki R, Radomska A, Glab S. (2000a), Potentiometric determination of dialysate urea nitrogen, *Talanta*, 52:13-17

Knocki R, Radomska A, Glab S. (2000b), Bioanalytical flow-injection system for control of hemodialysis adequacy, *Analytica Chimica Acta*, 418:213-224

Kohonen T (1988), An introduction to neural computing, *Neural Networks*, 1:3-16

Kolk AJH, Schuitema ARJ, Kuijper S, van Leeuwen J, Hermans PW, van Embden JD, Hartskeerl RA. (1992), Detection of *Mycobacterium tuberculosis* in clinical samples using polymerase chain reaction and a nonradioactive detection system. *J Clin Microbiol*, 30:567-575

Kopple JD. (1997), Nutritional status as a predictor of morbidity and mortality in maintenance dialysis patients, *ASAIO*, 43:246-250

Kox LFF, Rhienthong D, Medo-Miranda A, Udomsantisuk N, Ellis K, van Leeuwen J, van Heusden S, Kuijper S, Kolk AH. (1994), A more reliable PcR for detection of *Mycobacterium tuberculosis* in clinical samples, *J Clin Microbiol*, 32:672-678

Krcmery S, Dubrava M, Kcrmery V Jr. (1983), Fungal urinary infections in patients at risk. *Int J Antimicro. Agents*, 11: 289 – 291

Kumegawa M, Hiramatsu M, Yamada T, Yajima T. (1980), Effects of intermediate-sized molecular compounds in uremic sera on nerve tissue in vitro, *Brain Res*, 1198:234-238

Kuroyanagi T, Saito M. (1966), Presence of toxic substances which inhibit erythropoiesis in serum of uremic nephrectomized rabbits. *Tohoku J Exp Med*, 88:117

Laird BN, Berkey CS, Lowrie EG. (1983), Modelling success or failure of dialysis therapy: the National Cooperative Dialysis Study, *Kidney Int*, 23:101-106

Larrson L, Mardh PA, Odham G. (1978), Analysis of amines and other bacterial products by head-space gas-chromatography, *Acta Scandinavian Pathology Microbiology*, 86:207-213

Le Febvre JMJ, Spanner E, Heidenheim AP, Lindsay RM. (1991), Kt/V (urea): patients do not get what the physician prescribes, *ASAIO Trans*, 37:132-133

Le Moel G, Strecker G, Troupel S, Dolegeal M, Jacobs C, Galli A, Agneray J (1980), Carbohydrate content of middle molecular weight substances in uremic patients: preliminary results, *Artif Organs*, 4:37-40

Leber HW, Debus E, Grulich U, Schuetterl G. (1980), Potential role of middle molecules compounds in the development of uremic anemia, *Artif Organs*, 4:63-67

Levy J, Morgan J, Brown E. (2001), Oxford Handbook of Dialysis, Oxford University Press, Oxford

Lichtenberger L, Gardner J, Barreto J, Dial E, Weinman E. (1993), Accumulation of Aliphatic Amines in Gastric Juice of Acute Renal Failure Patients, *Digestive Diseases and Sciences*, 38:1885-1888

Lidell K, Withe J. (1975), The smell of cancer, *Brit J of Dermat*, 92:215-217

Lidell K. (1976) Smell as diagnostic marker, *J of Postgrad Med*, 53:136-138

Liebig J, Woehler F. (1837), Ueber die bildung des bittermandeloels, *Annals in Pharmacy*, 22:1

Lieblich H, Pickert A, Tetschner B. (1984), Gas chromatographic and gas chromatographic-mass spectrometric analysis of organic acids in plasma of patients with chronic renal failure, *J Chromat*, 289:259-266

Lieblich H, Woell J. (1977), Volatile substances in blood serum: profile analysis and quantitative determination, *J Chromat*, 142:505-516

Lin YJ, Guo H, Chang Y. (2001), Application of the electronic nose for uremia diagnosis. *Sens Actuators B*, 76: 177 – 180

Lindsay RM, Sternby J. (2001), Future Directions in Dialysis Quantification, *Sem Dial*, 14:300-307

Lipsky BA, Gates JA, Tenover FC, Plorde JJ (1984), Factors affecting the clinical value of microscopy for acid-fast bacilli. *Rev. Infect. Des*, 6:214-222

Lipsky BA. (1999), Prostatitis and urinary tract infection in men: whats new; whats true? *Am J Med*, 106: 327 – 334

Lirk P, Bodrogi F, Raifer H, Greiner K, Ulmer H, Rieder J (2003), Elective haemodialysis increases exhaled isoprene, *Neph Dial Trans*, 18:937-941

Louden RG, Roberts RM. (1966), Droplet expulsion from the respiratory tract, *Am Rev Respir Dis*, 95:435-42

Lowrie EG. (2000), The Normalised Treatment Ratio (Kt/V) Is Not the Best Dialysis Dose Parameter, *Blood Purification*, 18:286-294

Lutz W, Markiewicx K, Klyszeijo-Stefanowicz I. (1974), Investigation on the activity of lactic dehydrogenase and its inhibitors in the serum of uremic patients during hemodialysis, *Acta Med Pol*, 15:97-104

Magan N, Pavlou A, Chrysanthakis I. (2001), Milk sense: a volatile sensing system recognises spoilage bacteria and yeasts in milk, *Sens Actuators B*, 72:28-34

Manolis A. (1983), The diagnositic potential of breath analysis, *Clin Chem*, 29:5-15

Manzoni C., Di Filippo S., Corti M, Locatelli F. (1996), Ionic dialysance as a method for the on-line monitoring of delivered dialysis without blood sampling, *Nephrol Dial Transplant*, 11:2023-2030

Martin YG, Pavon JLP, Cordero BM, Pinto CG. (1999), Classification of vegetable oils by linear discriminant analysis of electronic nose data, *Anal Chim Acta*, 384:83-94

Massart DL, Vandeginste BGM., Demign SN, Michotte Y, Kaufman L. (1988), *Chemometrics: A Textbook*. Elsevier Science Publishers, Amsterdam, The Netherlands, pp.325-330, 339-368

Mayakova TI, Kuznetsova EE, Lazareva MV, Dolgushina GS. (1989), Quantitative estimantion of volatile fatty acids by means of gas chromatography in rapid diagnosis of non-clostridial anaerobic infection, *Voprosy Meditsinskoi Khimii*, 35:71-75

Mc Cusker FX, Teehan BP, Thorpe KE, Keshaviah PR, Churchill DN. (1996). How much peritoneal dialysis is required for the maintenance of a good nutritional state. *Kidney Int*, 50:56-61

Mc Dermott FT. (1971), The effect of 10 % human uremic serum upon human fibroblastic cell cultures, *J Surg Res*, 11:119-122

McEntegart CM, Penrose WR, Strathmann S, Stetter JR (2000), Detection and discrimination of coliform bacteria with gas senor arrays, *Sens Actuators B*, 70:170-176

McGregor JA, French JI. (2000), Bacterial vaginosis in pregnancy. *Obstet Gynecol Surv*, 55:S1-19

Mercadel L, Petitclerc T, Jaudon MC, Bene B, Goux N, Jacobs C. (1998), Is ionic dialysance a valid parameter for quantification of dialysis efficiency?, *Artif Organs*, 22:1005-1009

Middlebrook G, Reggiardo Z, Tigertt WD. (1977), Automatable radiometric detection of growth of Mycobacterium tuberculosis in selective media. *Am Rev Respir Dis*, 115:1066-1069

Mitruka BM. (1975). Presumptive diagnosis of infectious diseases. In: Mitruka BM (ed) *Gas chromatographic applications in microbiology and medicine*. John Wiley and Sons, New York, pp 349-374

Mohamed EI, Linder R, Perriello G, Di Daniele N, Popple SJ, De Loren A. (2002), Predicting type 2 diabetes using an electronic nose-based artificial neural network analysis. *Diabetes Nutr Metab*, 15: 215- 221

Moret-Bonillo V. (1998), Integration of data information and knowledge in intelligent patient monitoring, *Expert Systems with Applications*, 15:155-163

Movilli E. (1999), Adequacy, Nutrition, and Biocompatibility: Their Relevance on Clinical Outcome in Haemdialysis Patients, *Blood Purif*, 17:159-165

Mullis KB, Faloona FA. (1987), Specific synthesis of DNA in vitro via a polymerase-catalysed chain reaction. *Methods Enzymol*, 155:335-350

Narinesingh D, Mungal R, Ngo TT. (1991), Urease coupled to poly(vinyl alcohol) activated by 2-fluoro-1-methylpyridinium salt: preparation of a urease potentiometric electrode and application to the determination of urea in serum, *Anal Chim Acta*, 249:387

Nephrologychannel: www.nephrologychannel.com, March 22, 2004

Nguyen LN, Kox LFF, Pham LD, Kuijper S, Kolk AH. (1996), The potential contribution of the polymerase chain reaction to the diagnosis of tuberculous meningitis. *Arch Neurol*, 53:771-776

NIH-Publication (1999), no: 99-4556, www.niddk.nih.gov, July 1999

Niwa T, Maeda K, Ohki T (1981), A gas chromatographic-mass spectrometric analysis for phenols in uremic serum, *Clin Chim Acta*, 110:51-57

Nourooz-Zadeh J. (1999), Effect of dialysis on oxidative stress in uraemia. *Redox Rep*, 4:17-22.

Nylander C, Liedberg B, Lind T (1982), Gas detection by means of surface plasmon resonance, *Sens and Act*, 3:79-83

Olesberg JT, Armitage B, Arnold MA, Flanigan MJ. (2002), Online measurement of urea concentration in spent dialysate during hemodialysis, www.ostc.physics.uiowa.edu (accessed, June 2004)

Omelianski VL. (1923), Aroma producing microorganisms, *J Bacteriol* 8:393-419

Orenstein R, Wong ES. (1999), Urinary tract infections in adults. *Am Fam Physician*, 59: 1225–1234

Osmetech plc - http://www.osmetech.com/products/laboratory.html (accessed March 2004)

Otto M. (1999), *Chemometrics*: Statistics and Computer Application in Analytical Chemistry, Wiley-VCH, pp. 119-174

Palacios JJ, Ferro J, Palma R, Garcia JM, Villar H, Rodriguez J, Macias MD, Prendes P. (1999), Fully automated liquid culture systems compared with Löwenstein-Jensen solid medium for rapid recovery of mycobacteria from clinical samples. *Eur J Clin Microbiol Infect Dis*, 18:265-273

Pardo M, Niederjaufner G, Benussi G, Comini E, Faglia G, Sberveglieri G, Holmberg M, Lundstrom I (2000), Data preprocessing enhances the classfication of

different brands of Espresso coffee with an electronic nose, *Sens Actuators B*, 69:397-403

Parker TF, Husni L, Huang W, Lew N, Lowrie EG. (1994), Survival of hemodialysis patients in the United States is improved with a greater quantity of dialysis, *Am J Kidney Dis*, 23:670-80

Parry AD, **Oppenheim B**. (1995), Leg ulcer detection identifies beta-haemolytic streptococcal infection. *J Wound Care*, 4: 404-406

Patel SR, Ke HQ, Hsu Y. (1994), Regulation of calcitriol receptor and its mRNA in normal and renal failure rats, *Kidney Int*, 45:1020-1027

Patzer JF (2001), www.pitt.edu/~patzer/dialysis/dialysisprinciples.htm

Pauschmann H. (1990), Gaschromatographie in: *Untersuchungsmethoden in der Chemie*, eds Naumer H, Heller W, Thieme, Stuttgart, pp37-53

Pavlou A. (2002), Novel Intelligent Gas-Sensing in Diagnosis of Infectious Diseases, PhD thesis, Cranfield University at Silsoe

Pavlou AK and Turner APF. (2000), Sniffing out the Truth: Clinical Diagnosis Using the Electronic Nose. *Clin Chem Lab Med*, 38: 99-112

Pavlou AK, Magan N, McNulty C, Meedham-Jones J, Sharp D, Brown J, Turner APF. (2002), Use of an electronic-nose system for diagnoses of urinary tract infections. *Biosens Bioelectron*, 17: 893 – 899

Pavlou AK, Magan N, Meecham Jones J, Brown J, Klatser PR, Turner APF. (2004), Detection of *Mycobacterium tuberculosis* (TB) *in vitro* and *in situ* using an electronic nose in combination with a neural network system, *Biosens Bioelectron* ***(in press)***

Pavlou AK, Magan N, Sharp D, Brown J, Barr H, Turner APF. (2000), An intelligent rapid odour recognition model in discrimination of *Helicobacter pylori* and other gastroesophageal isolates *in vitro*. *Biosens Bioelectron*, 15: 333 – 342

Pearce TC. (1997a), Computational parallels between the biological olfactory pathway and its analogue 'The electronic nose'. 1. Biological olfaction, *Biosystemes*, 41:43-67

Pearce TC. (1997b), Computational parallels between the biological olfactory pathway and its analogue 'The electronic nose'. 2 Sensor based machine olfaction. *Biosystems*, 41: 69-90

Perkins MD. (2000), New diagnostic tools for tuberculosis, *Int J Tuberc Lung Dis*, 4:182-188

Persaud K, Dodd G. (1982), Analysis of discrimination mechanisms in the mammalian olfactory system using a model nose, *Nature*, 299:352-355

Persaud KC, Khaffaf SM, Hobbs PJ, Sneath RW. (1996), Assessment of conducting polymer odour sensors for agricultural malodour measurements, *Chem Sens*, 21:495-505

Persaud KC, Travers PJ. (1997), Arrays of Broad Specificity Film for Sensing Volatile Chemicals, in *Handbook of Biosensors and Electronic Noses Medicine, Food and the Environment*, edited by E. Kress-Rogers, CRC press, New York, pp. 563-592

Persuad KC, Pisanelli AM, Evans P. (2002), *In Handbook of machine olfaction: electronic nose technology;* Chapter 18. pp 445 – 460. Wiley, London

Petitclerc T. (1999), Recent developments in conductivity monitoring of haemodialysis session, *Nephrol Dial Transplant*, 14:2607-2613

Phillips M, Erickson GA, Sabas M, Smith JP, Greenberg J. (1995), Volatile organic compounds in the breath of patiens with schizophrenia, *J Clin Path*, 48:466-469

Phillips M, Gleeson K, Huges JMB, Greenberg J, Cataneo RN, Baker L, Mc Yay WP. (1999), Volatile organic compounds in breath as markers of lung cancer: a cross-sectional study, *The Lancet*, 353:1930-1933

Phillips M. (1997), Method for the collection and assay of volatile organic compounds in breath. *Anal Biochem*, 247: 272-278

Phillips M, Cataneo RN, Cummin AR, Gagliardi AJ, Gleeson K, Greenberg J, Maxfield RA, Rom WN. (2003a), Detection of Lung Cancer With Volatile Markers in the Breath, *Chest*, 123:2115-2123

Phillips M, Cataneo RN, Ditkoff BA, Fisher P, Greenberg J, Gunawardena R, Kwon CS, Rahbari-Oskoui F, Wong C. (2003b), Volatiles Markers of Breast Cancer in the Breath, *The Breast Journal*, 9:184-191

Phillips M. (2002), Detection of volatile organic compounds in breath, In *"Disease markers in exhaled breath"* pp 219-231, eds Markczin N, Kharitonov SA, Yacoub MH, and Barnes PJ, Marcel Dekker, NY

Ping W, Yi T, Haibao X, Farong S. (1997), A novel method for diabetes diagnosis based on electronic nose. *Biosens Bioelectron*, 12: 1031-1036

Ping W, Yi T, Haibao X, Farong S. (1997), A novel method for diabetes diagnosis based on electronic nose. *Biosens Bioelectron*, 12:1031-1036

Polaschegg HD. (1993), Automatic, non-invasive intradialytic clearance measurement, *Int J Artif Organs*, 16:185-191

Porter R. (1997), The early years. In Porter R ed. *The greatest benefit to mankind: a medical history of humanity from antiquity to the present*. London: Harper Collins, pp 147-62

Qureshi AR, Alvestrand A, Danielsson A, Divino-Filho JC, Gutierrez A, Lindholm B, Bergstrom J. (1998), Factors predicting malnutrition in hemodialysis patients: a cross-sectional study, *Kidney Int*, 53:773-782

Radhakrishnan VV, Mathai A, Sundaram P. (1992), Diagnostic significance of circulation immune complexes in patients with pulmonary tuberculosis, *J Med Microbiol*, 36:128-131

Radhakrishnan VV, Mathai A. (1991), Detection of Mycobacterium tuberculosis antigen 5 in cerebrospinal fluid by inhibition ELISA and its diagnostic potential in tuberculosis meningitis, *J Infect Dis*, 163:650-652

Radler F, Gerwarth B. (1971), On the formation of volatile by-products of fermentation by lactic acid bacteria, *Archives of Microbiology*, 76:299-307

Raja A, Baughman RP, Daniel TM. (1988), the detection by immunoassay of antibody to mycobacterial antigens and mycobacterial antigens in bronchoalveolar lavage fluid from patients with tuberculosis and control subjects, *Chest*, 94:133-137

Raviglione MC, Narain JP, Kochi A. (1992), HIV-associated tuberculosis in developing countries: clinical features, diagnosis and treatment. *Bull. World Health Organ*, 70:515-526

Raviglione MC, Snider D, Kochi A. (1995), Global epidemiology of tuberculosis. Morbidity and mortality of a worldwide epidemic. *JAMA*, 273:220-226

Rieder HL, Zellweger JP, Raviglione MC, Keizer ST, Migliori GB. (1994), Tuberculosis control in Europe and international migration. *Eur Respir. J,* 7:1545-1553

Riley RL, Mills CC, Nyka W, Weinstock N, Storey PB, Sultan LU, Riley MC, Wells WF. (1995), Aerial dissemination of pulmonary tuberculosis: a two-year study of contagion in a tuberculosis ward. *Am J. Hygiene*, 70:185-96

Roggenkamp A, Hornef MW, Masch A, Aigner B, Autenrieth IB, Heesemann J. (1999), Comparison of MB/BacT and BACTEC 460 TB systems for recovery of mycobacteria in a routine diagnostic laboratory. *J Clin Microbiol*, 37:3711-3712

Roussel S, Forsberg G, Grenier P, Bellon-Maurel V. (1999), Optimisation of electronic nose measurements. Part II: Influence of experimental parameters, *Journal of Food Engineering*, 39:9-15

Sada E, Aguilar D, Torres M, Herrera T. (1992), Detection of lipoarabinomannan as a diagnostic test for tuberculosis, *J Clin Microbiol*, 30:2415-2418

Sada E, Ruiz-Palacios GM, Lopez-Vidal Y, Ponce de Leon S. (1983), Detection of mycobacterial antigens in cerebrospinal fluid of patients with tuberculous meningitis by enzyme-linked immunosorbent assay, *Lancet ii*:651-652

Saini S, Barr H, Bessant C (2001) Sniffing out disease using the artificial nose. *Biologist*, 48:229- 233

Santoro A, Mancini E, Zucchelli P. (2000) The impact of hemofiltration on the systemic cardiovascular response. *Nephrol Dial Transplant*, 15:49-54

Santoro A, Tetta C, Mandolfo S, Arrigo S, Berti M, Colasanti G, D'Amico G, Imbasciati E, Mazzocchi C, Pacini G, Spongano M, Thomaseth K, Wratten ML, Zucchelli P. (1996), On-line urea kinetics in haemodiafiltration. *Nephrol Dial Transplant*, 11:1084-1092

Sargent JA, Gotch FA. (1983), Principles and Biophysics of Dialysis *in Replacement of the renal function by Dialysis*, edited by Drukker W., Parsons M., Maher J. F., Martinus Nijhoff Publishers Boston, pp. 53-96

Schaecter M, Medoff G, Eisenstein BL, eds. (1993), Mechanisms of Microbial Disease, 2nd edn, Williams & Wilkins, Baltimore, USA, pp

Schaller E, Bosset JO, Escher F. (1998), "Electronic nose" and their application to food (review), *Lebensm Wiss Techn*, 31:305-316

Schaller E, Bosset JO, Escher F. (1999), Practical experience with electronic nose systems for monitoring the qulaity of dairy products, *CHIMIA*, 53:98-102

Schiffman S., Kermani B. Nagle H (1997), Analysis of Medication Off-odors Using an Electronic Nose, *Chem Sens*, 22:119-128

Schleger HG. (1992), Allgemeine Mikrobiologie, 7th ed, Thieme Verlag, Stuttgart

Schluger NW, Rom WN. (1998), The host immune response to tuberculosis. *Adv Tuberc Res*, 19:1-63

Schneider J, Grundig B, Renneberg R, Cammann K, Madaras MB, Buck RP, Vorlop KD. (1996), Hydrogel matrix for three enzyme entrapment in creatine/creatinine amperometric biosensing, *Anal Chim Acta*, 325:161-167

Seto Y. (1994) Determination of volatile substances in biological samples by headspace gas chromatography, *J Chromatography A*, 674:25-62

Shafer RW, Edlin BR. (1996), Tuberculosis in patients infected with human immunodeficiency virus: perspective on the past decade. *Clin Infect Dis*, 22:683-704

Shak CG. (1999), The role of Urea Kinetic Modelling in Determining Adequacy of Hemodialysis, *Nephrology News & Issues*, 13:14-16

Shih Y (1994), Neuralyst – Users Guide, Cheshire Engineering Cooperation, Pasadena, CA, USA

Shilova MV, Dye C. (2001), The resurgence of tuberculosis in Russia, *Philos Trans R Soc Lond Biol Sci*, 356:1069-1075

Shinzato T, Nakai S, Fujita Y, Takai I, Morita H, Nakane K, Maeda K. (1994), Determination of Kt/V and Protein Catabolic Rate Using Pre- and Postdialysis Blood Urea Nitrogen Concentrations, *Nephron*, 67:280-290

Shurmer HV, Gardner JW. (1992), Odour discrimination with an electronic nose, *Sens Actuators B*, 8:1-11

Simpson JL, Gibson PG, Wark PAB. (2002), Optimization of sputum-processing methods for the measurement of Interleukin-5: Effects of protease inhibition, *Respirology*, 7:111-116

Smith M. (1982), The use of smell in differential diagnosis, *The Lancet*, 2:1452-1453

Smogorzewski M, Massry SG. (1997), Uremic cardiomyopathy: Role of parathyroid hormone, *Kidney Int*, 52:S12-S14.

Smolentski O, Tabarowski Z, Miszta H, Dabrowski Z. (1993), Effect of haemodialysate and its peptide fractions on acetylcholinesterase activity in erythrocytes from healthy subjects and patients with terminal renal failure. *Int Urol Nephrol*, 25:503-508

Soldatkin AP, Montoriol J, Sant W, Martelet C, Jaffrezic-Renault N. (2002), Creatinine sensitive biosensor based on ISFETs and creatinine deiminase immobilised in BSA membrane, *Talanta*, 58:351-357

Srinivasa-Rao P, Dakshinamurty K, Saibaba K, Sheela RB, Venkataramana G, Sreekrishna V, Ambekar JG, Jayaseelan L. (2001), Oxidative stress in haemodialysis: immediate changes caused by passage of blood through the dialyser, *Ann Clin Biochem* 38:401-405

Sternby J. (1999), Urea Sensors – A world of Possibilities, *Advances in Renal Replacement Therapy*, 6:265-272

Stetter JR, Strathmann S, McEntegart C, Decastro M, Penrose WR. (2000), New sensor arrays and sampling systems for a modular electronic nose, *Sens Actuators B*, 69:410-419

Stevens A., Lowe J. (2000), Pathology, 2nd edition, Mosby, Edingborough, pp.350-375

Sutter JM, Jurs PC. (1997), Neural network classification and quantification of organic vapors based on fluorescence data from a fiber-optic sensor array, *Anal Chem*, 69:856-862

Teruel JL, Fernandez L, Marcen R, Rodriguez JR, Rivera M, Liano F, Ortuno J. (2001), Estimate of the dialysis dose using ionic dialysance, *Sem Dial*, 13:305-317

Tetta C, Biasioli S, Schiavon R, Inguaggiato P, David S, Panichi V, Wratten ML. (1999), An overview of Haemodialysis and Oxidant stress, *Blood Purif*, 17:118-126

Thorpe TC, Wilson ML, Turner JE, Di Guiseppi JL, Willert M, Mirrett S. *et al.* (1990), BactT/Alert: an automated colorimetric microbial detection system, *J Clin Microbiol*, 28:1608-1612

Tortora GJ, Grabowski SR. (2000), Principles of Anatomy and Physiology, 9th edition, John Wiley & Sons, New York, pp. 914-954

Turner APF, Magan N (2004), Electronic noses and disease diagnostics. *Nature Reviews – Microbiology*, 2: 1–7

UK Renal Registry Report (2003), UK Renal Registry, Bristol, UK, eds: Ansell D, Feest T

Vanholder R, De Smet R, Chen H, Vogeleere P, Ringoir S. (1994), Uremic Toxicity: The middle molecule hypothesis revisited, *Seminars in Nephrology*, 14:205-218

Vanholder R, De Smet R, Glorieux G. Argiles A, Baurmeister U, Brunet P, Clark W, Cohen G, De Deyn PP, Deppisch R, Descamps-Latscha B, Henle T, Jorres A, Lemke HD, Massy ZA, Passlick-Deetjen J, Rodriguez M, Stegmayr B, Stenvinkel P, Tetta C, Wanner C, Zidek W. (2003) Review on uremic toxins: Classification, concentration, and interindividual variability, *Kidney Int*, 63:1934-1943

Vanholder R, De Smet R, Lesaffer G. (2002), Dissociation Between Dialysis Adequacy and Kt/V, *Sem Dial*, 15:3-7

Vanneste M. (1997), Arylenne alkenylenes as chemoresistors in electronic nose. *Seminars in Food Analysis: Proc. Of 4th Symposium on Olfaction and the Electronic Nose*, Nice, France

Verbon A, Kuijper S, Jansen HM, Speelman P, Kolk AH. (1990), Antigens in culture supernatant of *Mycobacterium tuberculosis*: epitops defined by monoclonal and human antibodies. *J Gen Microbiol*, 136:955-964

Veropoulos K, Learmonth G, Campbell C, Knight b, Simpson J. (1999), Automated identification of tubercle bacilli in sputum. A preliminary investigation, *Analysis Quantitation in Cytology and Histology*, 21:277-282

Walker GT, Little MC, Nadeau JD, Shank DD. (1992), Isothermal *in-vitro* amplification of DNA by a restriction enzyme/DNA polymerase system. *Proc Natl Acad Sci USA*, 89:392-396

Walt DR. (2002), Imaging optical sensor arrays, *Current Opinion in Chem Biol*, 6:689-695

Wessel-Aas T. (1981), The effect of serum and plasma from hemodialysis patients on human mononuclear phagocytes cultered in vitro. *Acta Pathol Microbiol Scand*, 89:345-351

Wilkinson RJ, Haslov K, Rappuoli R, Giovannoni F, Narayanan PR, Desai CR, Vordermeier HM, Paulsen J, Pasvol G, Ivanyi J, Singh M. (1997), Evaluation of the recombinant 38-kilodalton antigen of Mycobacterium tuberculosis as a potential immunodiagnostic reagent, *J Clin Microbiol*, 35:553-557

Wolfson M, Strong C. (1996), Assessment of nutritional status in dialysis patients, *Advances in Renal Replacement Therapy*, 3:174-179

Woodman AC and Fend R. (2004), Electronic-Nose Technology, Potential Applications in Point-of-Care Clinical Diagnosis and Management, in *Point-of-Care testing 2nd edition,* Eds: Price CP, John AS, Hicks JM (eds) *Point of Care Testing*, 2nd ed. AACC Press, Washington, DC

Woolf N. (2000), Cell, Tissue and Disease: The basis of pathology, 3rd edition, W.B Saunders, London, pp. 251-265

Zimmerman L, Jörnvall J, Bergström J. (1980), Characterisation of Middle Molecule Compounds, *Artif Organs*, 4:33-36

Appendices

APPENDIX A

A.1 CONSENT FORM FOR VOLUNTEERS

Consent Form

Donation of blood for the analysis of volatile compounds

using an electronic nose

- I give my consent for the Medical Centre at Cranfield University to take 10 ml of my blood and for it to be used in medical research.
- I consent for the blood to be analyzed by an electronic nose for volatile compounds as well as the preparation of a biochemical profile.
- I understand that I will not be informed of any results from this research.

_____ _____

Name of Donor: Date: Signature of Donor:

_____

Signature of Medical Centre Representative

_____

Signature of Scientist receiving the blood

A.2 CONSENT FORM FOR PATIENTS

Gloucestershire Royal NHS
NHS Trust

Gloucestershire Royal Hospital
Great Western Road
Gloucester
GL1 3NN

Tel: 01452 528555

CONSENT FORM

Title of Project: **Towards interactive dialysis: electronic nose analysis of volatile compounds generated and removed during dialysis treatment**

Name of Researchers: Dr. A.J. Williams Mr R Fend

1. I confirm that I have read and understand the information sheet dated..... for the above study ☐
2. I understand that my participation is voluntary and that I am free to withdraw at any time without my medical care or legal rights being affected. ☐
3. I am willing to allow access to my medical records by the researchers for the duration of the study but understand that strict confidentiality will be maintained. The purpose of this is to check that the study is being carried out correctly ☐
4. I agree to take part in the above study. ☐

Name of patient	Date	Signature
Name of person taking consent (if different from researcher)	Date	Signature
Researcher	Date	Signature

1 for patient; 1 for researcher; 1 to be kept with hospital notes

1

Chair: Margaret Greenwood, Chief Executive: Mariella Dexter

GRH066

APPENDIX B

B.1 GAS SENSORS USED IN THIS STUDY

The gas-sensing unit was developed in the Department of Biochemistry and Molecular Biology at Leeds University (UK) and is being commercialised by Bloodhound Sensors Ltd. (UK).

Gibson *et al* (1997) and Bloodhound's US Patent 5,928,609 report that the company's sensors were prepared by electro-polymerising the different monomers (Table B.1) onto interdigitated gold electrodes. The resulting polymer structures were electrically conducting and show different sensitivities to volatile odour compounds. The interaction between odour compounds and polymer structure is indirectly measured by the alteration of the applied potential or current due to changes in resistance, impedance or capacitance of the polymer film. To obtain overlapping specificities toward volatile compounds, the individual polymers were doped with different chemicals (Table B.1).

***Table B.1*:** Monomers and dopants used in the Bloodhound BH114 system (adapted from Gibson *et al*, 1999).

Sensor	Polymer monomer	Dopant
1	Ethylaniline	Sulphate
2	Aniline	Sulphate
3	Aniline	Sulphate
4	Tryptophan	Sulphate
5	Tryptophan	Sulphate
6	2-methoxy-5- nitroaniline	Sulphate
7	Thiophene and thiophene-3-tetrabutyl-ammonium carboxylic acid	Perchlorate
8	Aniline	Ethanol sulphate
9	Pyrrole	Octanoic acid ethyl ester
10	Pyrrole	CO_4
11	1, 4-phenlene diamine	Chloride
12	1, 4-phenlene diamine	Chloride
13	Pyrrole	Chloride
14	Pyrrole	Tetrabutyl-ammonium perchlorate

Note:
Sensor 7: co-polymer
Sensor 10: with upper Octanoic acid ethyl layer of poly-tryptophan ester dopant

APPENDIX C

C.1 DIALYSATE COMPOSITION

Table C.1: Usual composition of dialysis fluid (Levy *et al*, 2001).

Sodium	132 – 155 mmol/L
Potassium	0 – 4 mmol/L
Calcium	1.25 – 2 mmol/L
Magnesium	0.25 – 0.75 mmol/L
Chloride	90 – 120 mmol/L
Bicarbonate	27 – 40 mmol/L
Dextrose	0 – 5.5 mmol/L
pH	7.1 – 7.3

At Gloucester Royal Hospital the following two bicarbonate concentrations are in use: 35 mmol/L or 40 mmol/L

C.2 HAEMODIALYSIS AT GLOUCESTSHIRE ROYAL HOSPTIAL

At Gloucestershire Royal Hospital (GRH) two Fresenius dialysers are in use, namely F6 and F8 dialysers. The difference is the surface area of the polysulfone membrane; the F6 dialyser has a surface area of 1.3 m^2, whereas the F8 has a surface area of 1.8 m^2.

The blood flow rate varies between 200 and 350 ml/min, depending on the patient. The dialysate flow rates are the same for all patients at 500 ml/min. The majority of the patients at GRH are dialysed for 4 hours three times a week.

The routine monitoring includes:

- Monthly blood samples (pre- and post-dialysis blood) ➔ dialysis dose, adequacy
- Measurement of blood pressure as well as weight. Both parameters are determined before and after the treatment session ➔ they are used to determine the excessive body fluid, which has to be removed from the patients body by Haemodialysis (HD).

APPENDIX D

D.1 LONG-TERM PERFORMANCE (STABILITY)

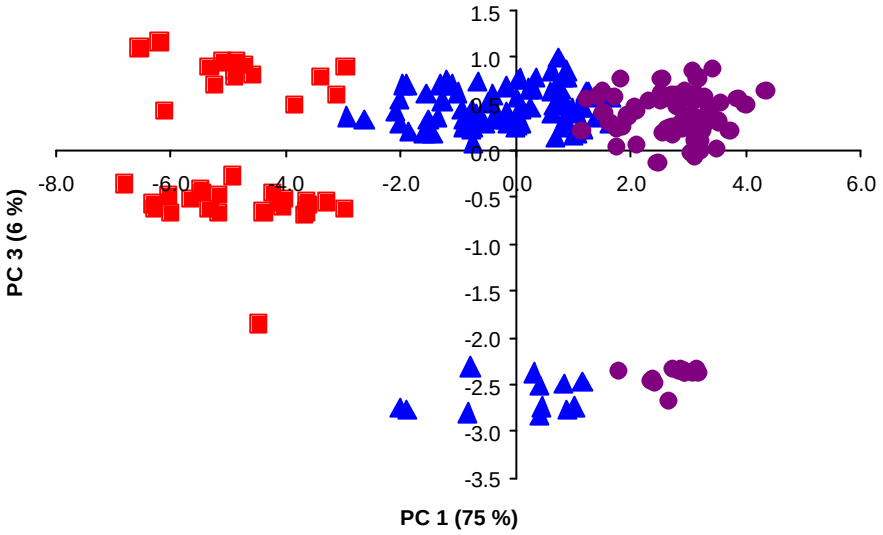

Figure D.1: Principal component analysis (1st and 3rd principal component) of control blood (45 volunteers, squares), post – dialysis (99 samples, triangles) and pre-dialysis blood (99 samples, circles). The blood samples of 11 HD patients were taken at nine consecutive dialysis sessions.

D.2 COMPARISON OF TRADITIONAL BIOCHEMICAL MARKERS WITH ELECTRONIC NOSE DATA

Table D.1: Biochemical data of the three patients with similar pre- and post-dialysis biochemical profile (see page 133).

		Post-dialysis	Pre-dialysis
Patient 9	*Urea (mmol l^{-1})*	9.3	12.0
	Creatinine (mmol l^{-1})	434	549
	CO_2 (mmol l^{-1})	31	29
	Phosphate (mmol l^{-1})	0.88	0.9
	Ca^{2+} PO_4^{2-} (mmol l^{-1})	2.2	2.1
Patient 15	*Urea (mmol l^{-1})*	11.4	7.2
	Creatinine (mmol l^{-1})	659	887
	CO_2 (mmol l^{-1})	28	28
	Phosphate (mmol l^{-1})	1.46	1.66
	Ca^{2+} PO_4^{2-} (mmol l^{-1})	3.9	4.1
Patient 25	*Urea (mmol l^{-1})*	9.2	11.8
	Creatinine (mmol l^{-1})	489	548
	CO_2 (mmol l^{-1})	28	26
	Phosphate (mmol l^{-1})	0.81	0.79
	Ca^{2+} PO_4^{2-} (mmol l^{-1})	1.95	1.90

APPENDIX E

E.1 COMPOSITION OF THE MIDDLEBROOK 7H9 MEDIUM WITH OADC ENRICHMENT

Middlebrook 7H9	4.7 g
Tween 80	0.5 g
Water	900 ml

OADC enrichment

Oleic Acid	50 mg
Albumin, Fraction V, bovine	5 g
Dextrose	2 g
Catalase (Beef)	3 mg
Sodium chloride	0.85 g
WR 1339, Triton	0.25 g
Water	100 ml

Sterilisation: Autoclave at 121 ^{o}C for 10 min, cool to 45 ^{o}C and add aseptically 100 ml of Middlebrook OADC enrichment solution.

E.2 FORMULA FOR CALCULATING SENSITIVITY, SPECIFICITY, PPV AND NPV

Table E.1: Table for calculating sensitivity, specificity, PPV and NPV.

	Disease positive	Disease negative	Total
Test positive	a	b	a + b
Test negative	c	d	c + d
Total	a + c	b + d	a+b+c+d

$$Sensitivity = \frac{a}{a+c} * 100$$

$$Specificity = \frac{b}{b+d} * 100$$

$$PPV = \frac{a}{a+b} * 100$$

$$NPV = \frac{d}{c+d} * 100$$

APPENDIX F - PUBLICATIONS

F.1 PEER REVIEWED JOURNALS

1. **Reinhard FEND**, Conrad Bessant, Anthony J Williams, and Anthony C Woodman, (2004), Monitoring Haemodialysis using an Electronic Nose and Chemometrics, *Biosensors and Bioelectronics,* 19:1581-1589

2. **Reinhard FEND**, Conrad Bessant, Anthony J Williams, and Anthony C Woodman, An Electronic Nose to Monitor Haemodialysis, (submitted Nephrol Dial Transplant)

3. **Reinhard FEND**, Arend HJ Kolk, Conrad Bessant, Paul R Klatser, and Anthony C Woodman, Early detection of *M. tuberculosis* infections in culture and sputum using electronic nose technology, (submitted J Clin Microbiol)

4. **Reinhard FEND**, Arend HJ Kolk, Conrad Bessant, Paul R Klatser, and Anthony C Woodman, Electronic nose technology for the diagnosis of tuberculosis, (submitted J Clin Microbiol)

5. **R. FEND**, R Geddes, S Lesellier, HM Vordermeier, LAL Corner, E Gormley, R G Hewinson, AC Woodman, and MA Chambers, The Use of an Electronic Nose to Detect *Mycobacterium bovis* Infection in Badgers and Cattle, (submitted J Clin Microbiol).

F.2 BOOK CHAPTERS

1. Woodman AC**,** **Fend R** (2004) Electronic-Nose Technology: Potential Applications in Point-of-Care Clinical Diagnosis and Management. In: Price CP, St John A, Hicks JM (eds) *Point of Care Testing*, 2nd ed. AACC Press, Washington, DC

F.3 PRESENTATIONS AND POSTERS

1. The use of an electronic nose for the management of haemodialysis, Reinhard Fend, Conrad Bessant, Anthony J. Williams, Anthony C. Woodman, presented at the House of Common, Feb 2003, London, UK

2. The use of an electronic nose for the management of haemodialysis, Reinhard Fend, Conrad Bessant, Anthony J. Williams, Anthony C. Woodman, presented at the 10th international symposium on Olfaction and Electronic Noses, June 2003, Riga, Latvia

3. Electronic nose for the detection of *M. tuberculosis in vitro* and *in vivo,* Fend R, Kolk A, Klatser P, Woodman AC, to be presented at 2004 UNION conference, Paris, France, November 2004